Chapter 4

Nickel-Catalyzed Asymmetric Reductive Cross-Coupling of N-Hydroxyphthalimide Esters and Alkenyl Bromides◊

4.1 INTRODUCTION

As part of our efforts to develop asymmetric cross-coupling reactions that employ a variety of C(sp^3) electrophiles, we became interested in the coupling of redox-active *N*-hydroxyphthalimide (NHP) esters.[1,2] These electrophiles are prepared from the corresponding carboxylic acids, and have been recently demonstrated as C(sp^3) substrates for Ni-catalyzed Negishi,[3,4] Suzuki,[5] and reductive cross-coupling[6] reactions to generate racemic products (Scheme 4.1).[7,8] However, NHP esters have not been demonstrated as competent coupling partners in Ni-catalyzed *enantioselective* cross-coupling reactions. We recognized that the use of NHP esters might be advantageous for substrates in which

◊ Portions of this chapter have been reproduced from published studies (see reference **30**) and the supporting information found therein. The research presented in this chapter was completed in collaboration with Dr. Naoyuki Suzuki, then a postdoctoral scholar in the Reisman group, and Julie Hofstra, a graduate student in the Reisman group.

the corresponding alkyl chlorides are unstable or challenging to prepare. We recognize that many feedstock chemicals contain carboxylic acids, and finding a straightforward means of engaging carboxylic acid derivatives in asymmetric cross-coupling reactions would be of great use to the synthetic community.

Scheme 4.1. *NHP esters in cross-coupling reactions.*

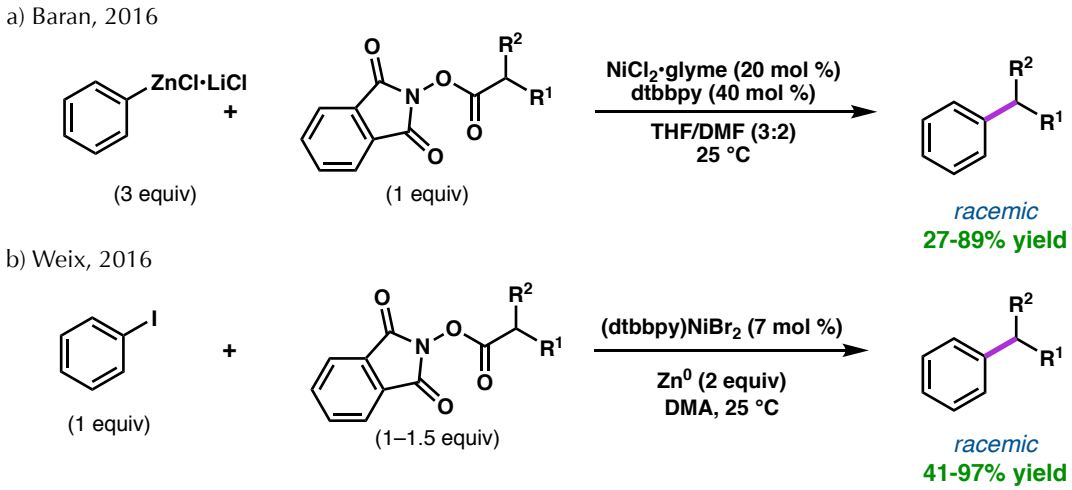

4.2 REACTION DEVELOPMENT

Our efforts began with NHP ester **31**, which is prepared in one step from commercially available 2-phenylpropanoic acid. Subjection of **31** and **27** to our optimal conditions developed for the reductive cross-coupling of alkenyl bromides and benzyl chlorides[9] provided only trace quantities of product (Table 4.1, entry 1), highlighting the challenges presented by this new C(sp^3)-electrophile. Slightly improved results could be obtained under the same conditions by adding 1.0 equiv TMSCl (Table 4.1, entry 2). An investigation of alternative reductants revealed that tetrakis(*N*,*N*-dimethylamino)ethylene (TDAE) substantially increased the reactivity, delivering **28** in 61% yield and 95% ee (Table 4.1, entries 2–4).[10]

Table 4.1. *Reductant investigation.*

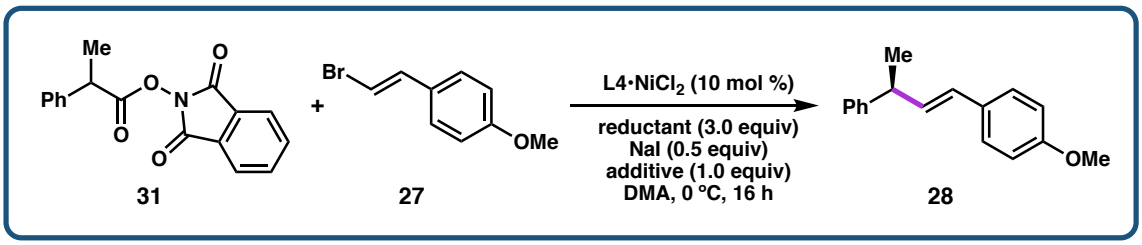

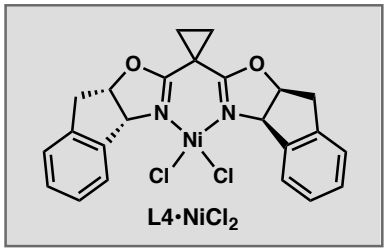

Entry	Reductant	Additive	% Yield 28	% ee 28
1	Mn^0	none	trace	—
2	Mn^0	TMSCl	27	90
3	Zn^0	TMSCl	38	64
4	TDAE	TMSCl	61	95

Monitoring the reaction progress at room temperature indicated that (*E*)-1-(2-chlorovinyl)-4-methoxybenzene was forming and accumulating under the reaction conditions, presumably through a Ni-catalyzed halide exchange process.[11,12] Since the alkenyl chloride does not readily engage in the cross-coupling reaction, we hypothesized that the yield of **28** could be improved by removing chloride from the reaction, thus preventing formation of this unproductive side product. Indeed, the use of TMSBr instead of TMSCl, and the use of **L4·NiBr$_2$** as the catalyst, furnished product **28** in 75% yield and 92% ee (Table 4.2, entry 2). By decreasing the reaction temperature to –7 °C, and using only 1.5 equivalents of TDAE, **28** could be obtained in 80% yield and 96% ee (Table 4.2, entry 4). Unfortunately, the reaction mixture freezes at temperatures lower than –7 ºC. Interestingly, in the coupling of (1-chloroethyl)benzene (**24**), TDAE provides the cross-coupled product in only 23% yield and 94% ee. Running the reaction under the optimal conditions, but omitting TMSBr, confirms that this additive is critical for obtaining high yields of **28** (Table 4.2, entry 3). The role of TMSBr under the optimal

conditions, which do not employ a metal reductant, is unclear. TMSCl has been proposed to activate Mn^0 or Zn^0.[13,14] We note that these optimal reaction conditions employ a 1:1 stoichiometry of the two electrophiles and only 10 mol % catalyst loading.

Table 4.2. *Additive and temperature investigation.*

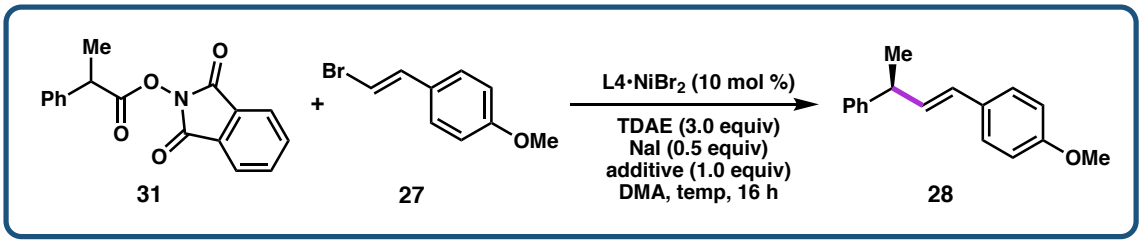

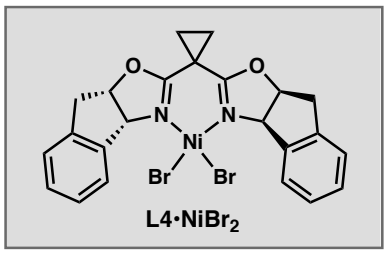

Entry	Additive	temp (°C)	% Yield 28	% ee 28
1	TMSCl	0	61	95
2	TMSBr	0	75	92
3	none	0	19	88
4	TMSBr	–7	80	96

4.3 SUBSTRATE SCOPE

To demonstrate the scope of the reaction, a series of (*E*)-alkenyl bromides was cross-coupled with NHP ester **31**, providing the corresponding products in uniformly good yield and high ee (Table 4.3). The reaction exhibits good tolerance of Lewis basic functional groups: for example, anilines (**181**), nitriles (**183**), and esters (**184**, **188**) can be incorporated into the substrate without detriment to the yield or enantioselectivity. A pyridine-containing alkenyl bromide also performs well, providing **187** in 67% yield and 95% ee. In addition, alkyl-substituted alkenyl bromides react smoothly, providing the corresponding products in good yield and ee (**188**–**191**). An alkenyl bromide possessing a free alcohol couples efficiently, although silylation occurs under the reaction conditions to give silyl ether **191**. The silyl ether can easily be cleaved with a mild acid workup; in

this case it was preserved in order to facilitate purification. It is notable that alkenyl MIDA-boronate **192** and alkenyl silane **193** can be prepared in 97% ee from commercially available vinyl bromides and could be used in further cross-couplings. To demonstrate that this method can be used preparatively, the coupling between **31** and **27** was conducted on 5.0 mmol scale, which delivered 918 mg (77% yield) of **28** in 91% ee.

Table 4.3. *Alkenyl bromide substrate scope.*[a]

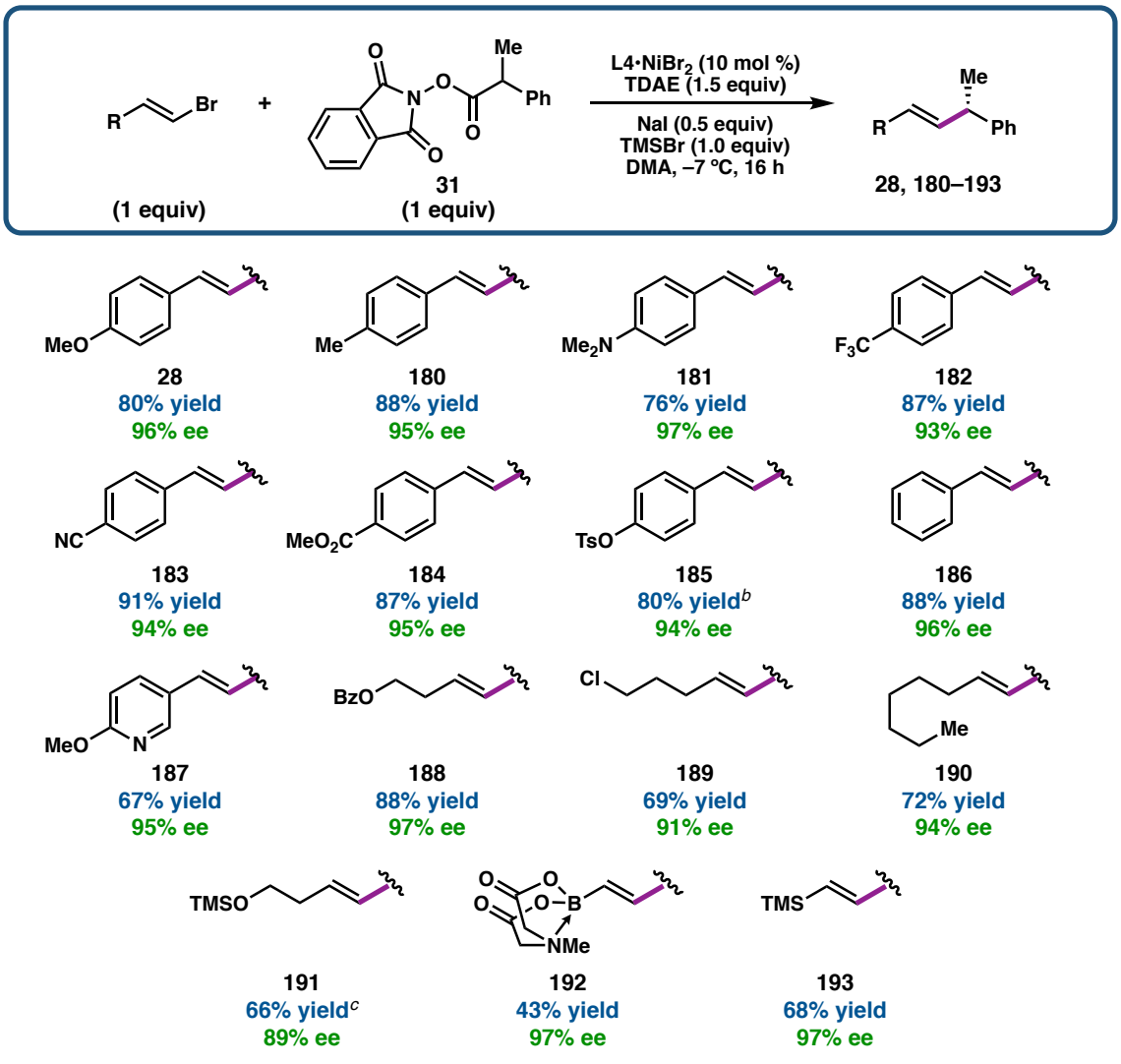

[a] Isolated yields, reactions conducted on 0.2 mmol scale under an N_2 atmosphere in a glovebox. % ee determined by SFC using a chiral stationary phase. [b] 1.5 equiv NHP ester used. [c] 2.0 equiv TMSBr used; the alcohol silylated under reaction conditions.

***Table 4.4**. NHP ester substrate scope.* [a]

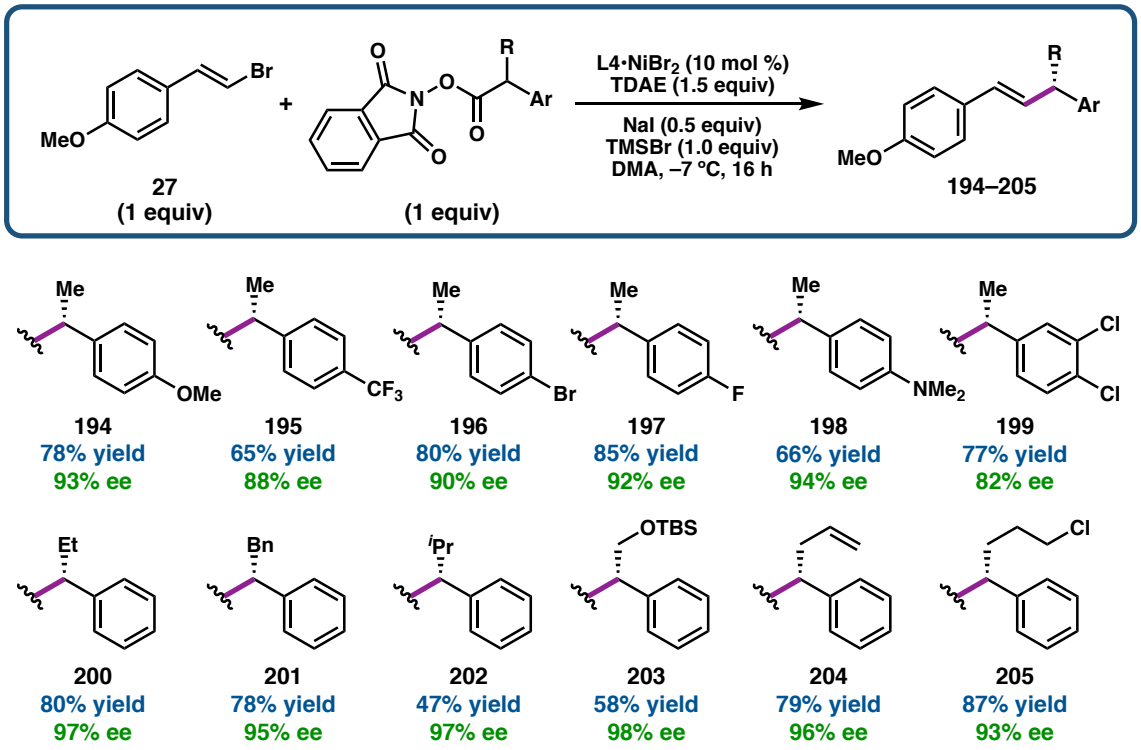

[a] Isolated yields, reactions conducted on 0.2 mmol scale under an N_2 atmosphere in a glovebox. % ee determined by SFC using a chiral stationary phase.

The reaction also exhibits broad scope for the NHP ester coupling partner, delivering good yields and high enantioselectivities for a range substrates bearing substitution on the arene or at the benzylic position (Table 4.4). In certain cases (e.g. **194**–**196**), the NHP esters cross-couple with improved yield relative to the corresponding benzyl chlorides (under the previously reported conditions).[9] Moreover, aniline **198** can be prepared in 66% yield and 94% ee; this compound could not be accessed via our previously reported benzylic chloride coupling due challenges in preparing and handling 4-(chloro(phenyl)methyl)-*N*,*N*-dimethylaniline under standard conditions. Higher substitution at the benzylic position is also tolerated (**200**–**205**), although the yield begins to decrease with larger groups (e.g. ^{i}Pr, **202**). Notable products include **203**, which

incorporates a siloxy group, **204**, containing an alkene, and **205**, which has an alkyl chloride. Perfect chemoselectivity for cross-coupling of the NHP ester over the primary alkyl chloride is observed.

Although the primary focus of this study was the cross-coupling of NHP esters with alkyl substituents at the benzylic position, we have also have begun to investigate substrates containing heteroatom substitution (Scheme 4.2). Reaction of α-methoxy ester **207** proceeds smoothly, furnishing allylic ether **208** in good yield and ee. This highlights an advantage of the NHP ester for certain C(sp^3) electrophiles, as the corresponding α-chloroether substrate is unstable and difficult to work with.

Scheme 4.2. *Reaction of α-methoxy NHP ester.*

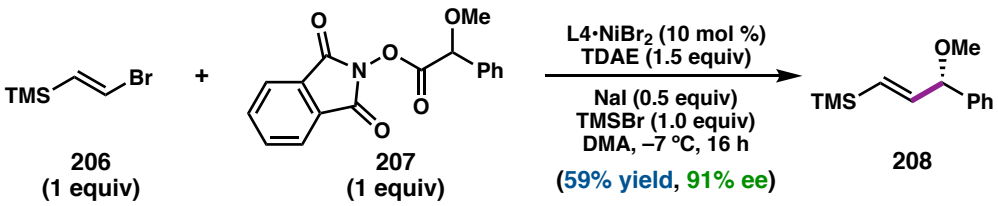

4.4 MECHANISTIC INVESTIGATIONS

We propose a catalytic cycle similar to the radical chain reaction mechanism described in **Chapter 2** for the cross-coupling of NHP esters and alkenyl bromides (Figure 4.1). Starting from a Ni(0) species (**14**), oxidative addition with alkenyl bromide **209** produces Ni(II)-alkenyl complex **210**. This can undergo radical addition with a benzylic radical (**214**) generated from single electron transfer (SET) with a Ni(I)-halide species (**21**), to form Ni(III) **211**. This Ni(III) complex can undergo reductive elimination to form the desired product **212** and a Ni(I) species, which can then undergo single-electron transfer (SET) with NHP ester substrate **213** to form Ni(II)-dihalide **22**. We hypothesize that this SET event results in the oxidation of Ni(I) species **21** to cationic

Ni(II) (**216**) and the reduction of phthalimide **213**. The resultant radical anionic species **215** could then decarboxylate to give the alkyl radical (**214**) and an equivalent of anionic phthalimide (**217**). We believe a role of TMSBr in the reaction could be to trap this stoichiometric phthalimide species to prevent reaction inhibition. Reduction of **22** regenerates **14** and closes the cycle.

Figure 4.1. *Proposed catalytic cycle for reductive alkenylation of NHP esters.*

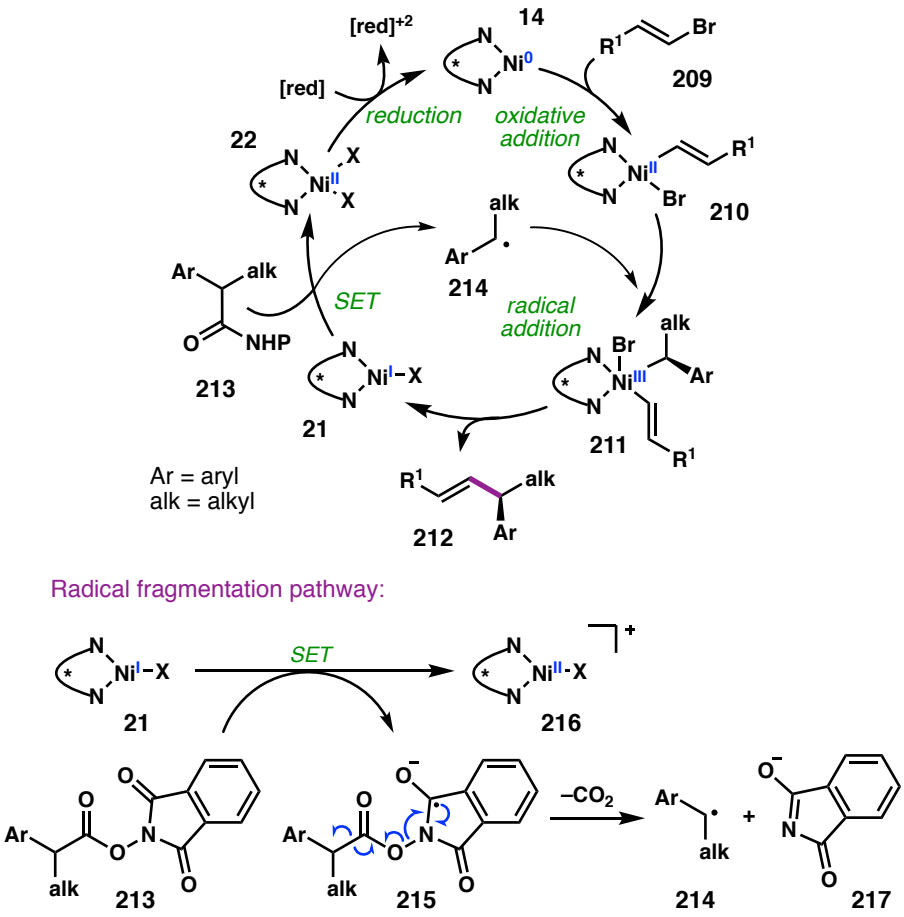

To probe for the intermediacy of a radical species, NHP ester **218** was prepared and subjected to the standard cross-coupling conditions (Scheme 4.3, 10 mol % **L4•NiBr$_2$**). A 42% combined yield of the coupled products **219a–c** was obtained. It has been shown that for phenyl substituted cyclopropyl carbonyl radicals, the ring opening is

reversible and that the cyclopropane species is favored at lower temperatures.[15,16] The fact that **219b** and **219c** predominate, even though they derive from the minor equilibrium species, perhaps indicates that the rate of radical recombination with nickel is sensitive to the steric profile of the radical. When the catalyst loading of **L4•NiBr$_2$** was varied, the ratio of **219a** to total ring opened product (**219b** + **219c**) was found to increase at higher nickel concentrations. This Ni-dependent behavior suggests that the mechanism proceeds through a cage-escaped radical, which at higher concentrations of **L4•NiBr$_2$**, can competitively recombine with nickel before undergoing ring scission.[17]

Scheme 4.3. *Radical clock study.*

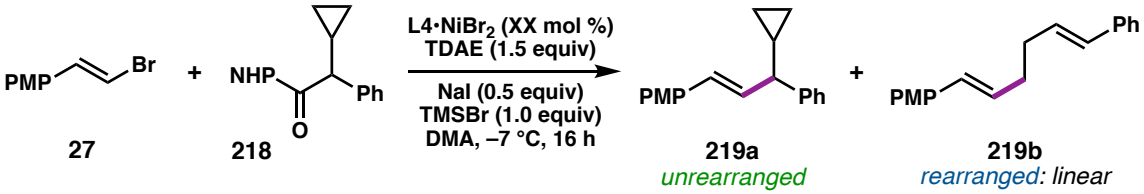

27 218 **219a** *unrearranged* **219b** *rearranged: linear*

Entry	L4•NiBr$_2$ mol %	Total Yield 219 (%)	Ratio 219a : [219b + 219c]
1	5	44	12 : 88
2	10	42	16 : 84
3	20	49	20 : 80

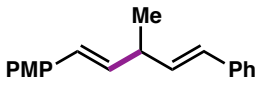

219c *rearranged: branched*

Mechanistic Hypothesis:

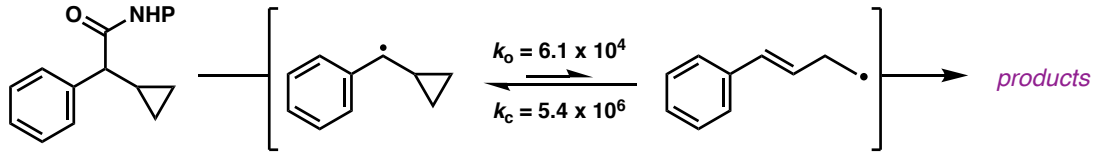

Further studies of the mechanism are ongoing; it is unclear at this time whether the absolute stereochemistry is set during the oxidative addition or reductive elimination[18] steps. We do note, however, that the products are formed in similar ee when using either the NHP esters under the conditions reported here or the benzyl chloride

using the conditions reported previously,[9] which suggests that the reactions proceed through the same stereochemistry-determining step.

4.5 CYLINDROCYCLOPHANE NATURAL PRODUCTS

4.5.1 Background and significance

The cylindrocyclophanes are a family of cytotoxic natural products isolated from the photosynthetic cyanobacteria *Cylindrospermum licheniforme* Kützing (ATTC 29204).[19–21] Many of these natural products are C_2-symmetric, featuring a unique 22-membered, [7,7]-paracyclophane skeleton (Figure 4.2). Isotopic sodium acetate labeling studies revealed the polyketide origin of these paracyclophane natural products and the highly symmetric nature of the observed isotope patterns suggested a head-to-tail dimerization of a monomer unit.[19,20] Recently, Balskus and coworkers elucidated details of the biosynthesis through the use of genome-sequencing and *in vivo* and *in vitro* experiments.[22,23] The enzymatic reactions involved in the paracyclophane formation include an enantioselective chlorination of an unactivated C(sp^3)–H bond, followed by first an intermolecular stereospecific aromatic ring alkylation, then a second, intramolecular alkylation to complete the macrocyclization.[24]

Figure 4.2. *Cylindrocyclophanes A–F.*

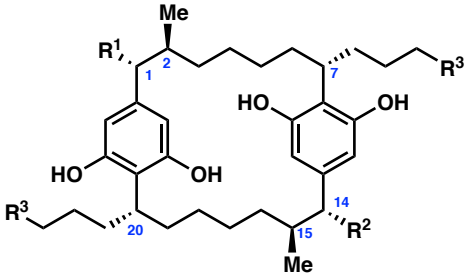

220A-F

	R^1	R^2	R^3
A	OH	OH	Me
B	OH	OAc	Me
C	OH	H	Me
D	OAc	OAc	Me
E	OAc	H	Me
F	H	H	Me
A_4	OH	OH	$CHCl_2$

Initial reports found that several cylindrocyclophanes are cytotoxic against KB and LoVo tumor cells lines (IC_{50} = 2-10 μg/mL).[20] Orjala and coworkers determined that chlorinated cylindrocyclophanes inhibit the 20S proteasome, an important protein in the control of apoptosis, differentiation and proliferation in healthy and cancer cells.[25] It is believed the chloroalkyl moiety is important for inhibition of the proteasome, and that the presence of the hydroxyl groups at C1 and C14 contribute to binding.

Scheme 4.4. *Prior syntheses of the cylindrocyclophanes that employ head-to-tail cyclodimerization approaches.*

a) Smith (2000)

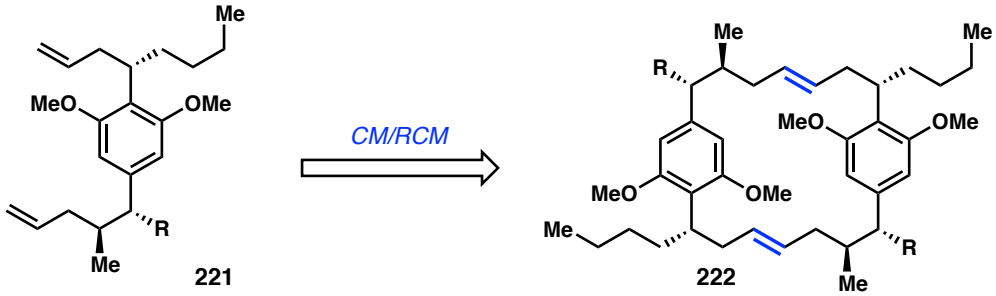

b) Hoye (2000)

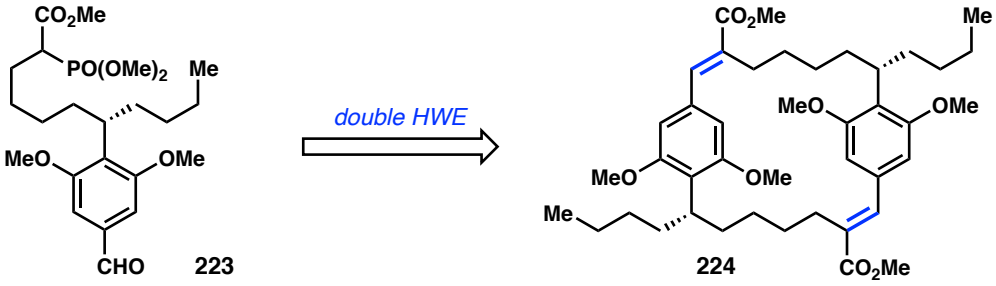

c) Nicolaou (2010)

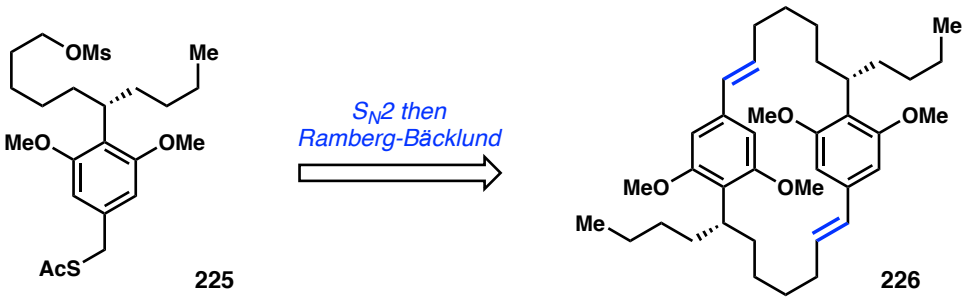

Leveraging the C_2-symmetry of these molecules, previous synthetic approaches have employed head-to-tail cyclodimerization strategies (Scheme 4.4). In 2000, Smith and coworkers prepared cylindrocyclophane A and F by using a cross-metathesis/ring-closing metathesis (CM/RCM) reaction of diolefin **221** to form macrocycle **222** (Scheme 4.4a), which could be elaborated to either cylindrocyclophane A or F, depending on the oxidation pattern.[26,27] The same year, Hoye reported a synthesis of cylindrocyclophane A in which Masamune-Roush conditions for a double Horner-Wadsworth-Emmons dimerization were used to construct macrocycle **224** (Scheme 4.4b).[28] More recently, Nicolaou and coworkers reported the use of a Ramberg-Bäcklund olefination reaction to construct **226**, possessing the cylindrocyclophane core (Scheme 4.4c).[29]

Scheme 4.5. *Macrocyclization by a Ni-catalyzed reductive cross-coupling.*

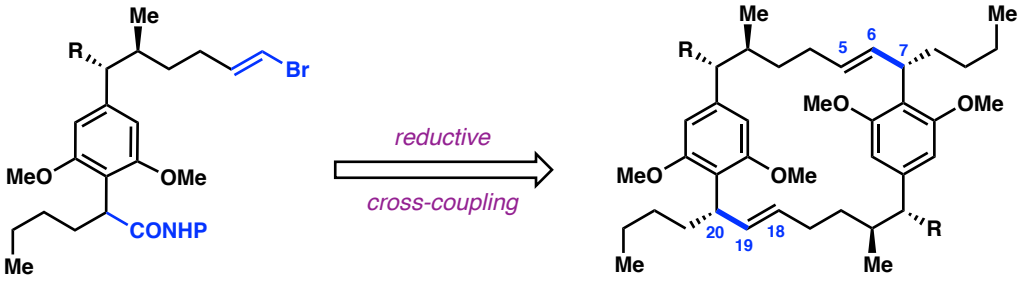

R=H (227), R=OTMS (228) **R=H (229), R=OTMS (230)**

In considering an approach to the cylindrocyclophanes, we envisioned that the target compounds could be prepared from macrocycle **229** or **230**, possessing C5–C6 and C18–C19 unsaturation (Scheme 4.5). Macrocycle **229** would arise from a Ni-catalyzed double asymmetric reductive cross-coupling of the bis-electrophile **227**, in which the key C6–C7 and C19–C20 bonds would be formed while also setting the C7/C20 stereogenic centers. This strategic application of an asymmetric reductive cross-coupling is particularly well-suited for the preparation of the macrocyclic cylindrocyclophanes, since

it obviates the need to prepare a dimerization substrate containing both an electrophile and a reactive organometallic functionality—as would be required for a conventional cross-coupling. Moreover, investigation of the key reductive alkenylation will advance the scope and deepen our understanding of these new and underexploited reductive cross-coupling transformations.

4.5.2 Preliminary studies

In 2014, our laboratory reported a Ni-catalyzed asymmetric reductive cross-coupling between alkenyl bromides and benzyl chlorides, which employ chiral BOX ligand **L4** and use Mn^0 as a stoichiometric reductant (Scheme 4.6a).[9] In 2017, the scope of this transformation was expanded through the use of *N*-hydroxyphthalimide (NHP) esters as the C(sp^3) electrophile, allowing for the incorporation of electron-rich functional groups on the arene (this chapter, Scheme 4.6b).[30] In the case of the NHP esters, the optimal conditions used tetrakisdimethylaminoethylene (TDAE) as the stoichiometric reductant and TMSBr as an activating agent.

Scheme 4.6. *Asymmetric reductive cross-coupling reactions with alkenyl bromides.*

a) Reisman, 2014

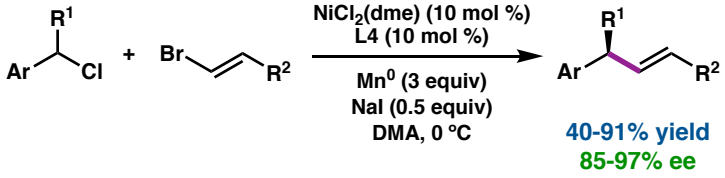

40-91% yield
85-97% ee

b) Reisman, 2017 (this chapter)

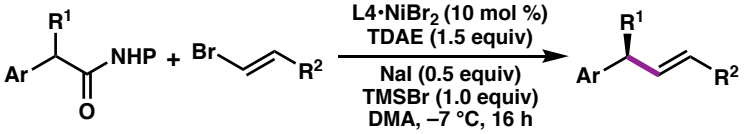

43-91% yield
82-98% ee

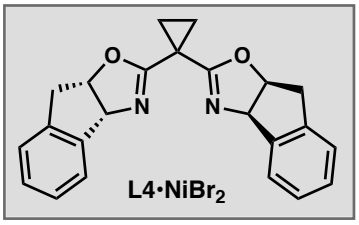

Based on this prior work, we envisioned preparing the cylindrocyclophane F macrocycle by a Ni-catalyzed asymmetric reductive dimerization/macrocyclization of NHP ester **227** (Scheme 4.5). Although the asymmetric reductive coupling of NHP esters tolerates electron-rich substrates, the *o*,*o*-disubstitution on the arene of the required substrate was expected to present a challenge to the established conditions and would require further reaction development.

To first probe the feasibility of the intermolecular reductive cross-coupling, model substrates **231** and **232** were synthesized (Scheme 4.7). The benzylic NHP ester substrate **231** was selected over the corresponding benzylic chloride due to its improved stability; the corresponding benzylic chloride readily eliminates to give the styrene during isolation and purification. A mixture of **231** and **232** were subjected to conditions previously developed for asymmetric reductive alkenylation of NHP esters: $NiBr_2$(diglyme) as catalyst, ^{c}Pro-indaBOX (**L4**) as ligand, TDAE as the stoichiometric reductant, and TMSBr as an activating agent; however, no product formation was observed under these conditions. In contrast, when Mn^0 was used as the stoichiometric reductant, the product was formed in 15% yield. At this time, it is unclear why TDAE does not work, even though it was found to be optimal in our original report; we will continue to investigate the use of TDAE and related organic reductants in our future work.

Scheme 4.7. *Cross-coupling between model NHP ester and alkenyl bromide.*

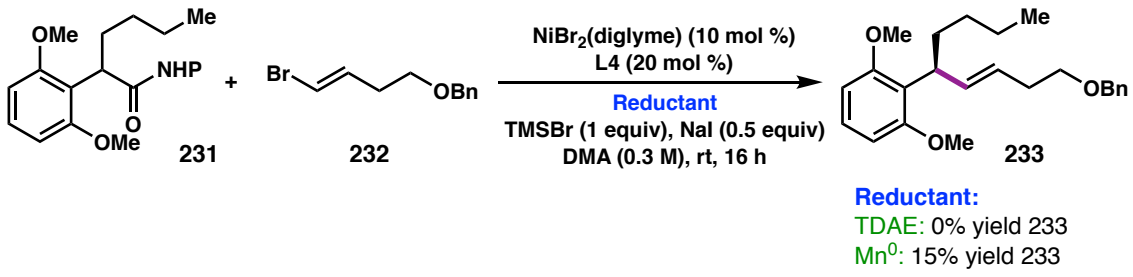

Following a survey of solvents including DMA, THF, and NMP, and several bis(oxazoline) (BOX) and bi(oxazoline) (BiOX) chiral ligands,[31] it was determined that DMA provided the most productive reactivity and **L6**, a new chiral ligand developed in our laboratory for diarylalkane formation (**Chapter 2**),[32] furnished the most promising enantioselectivity (Table 4.5). It is possible that the improved reactivity observed with the BiOX ligands results from the increased *N–N* distance, which provides better access to the nickel center for more sterically demanding coupling partners.

Table 4.5. *Ligand optimization of model cross-coupling.*

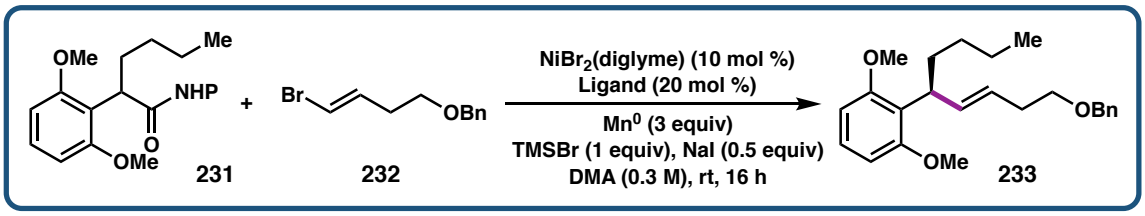

Bi(oxazoline) Ligand Scaffold

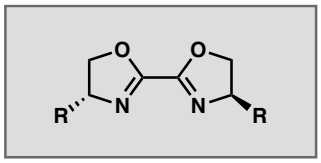

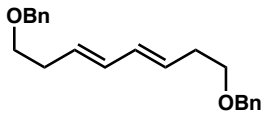

234

Ligand	R	Yield HC 234 (%)	Yield 233 (%)	ee 233 (%)
L21	Ph	59	8	7
L2	Bn	39	22	46
L8	^{i}Bu	70	28	65
L35	$CH_2{}^{t}$Bu	50	31	69
L19	^{i}Pr	51	30	63
L20	^{t}Bu	52	15	16
L22	CyHexyl	54	11	67
L6	4-Heptyl	35	24	86

The major side product in the reaction is diene **234**, resulting from homo-coupling of **232**. Although the homo-dimer derived from **231** was not isolated, NHP ester **231** was consumed under the conditions. While **L6** provides the most promising enantioselectivity, the initial screening of reaction parameters was conducted with **L35**, since it was more readily available at the time the screen was performed. The ee of **233**

improved slightly when the temperature was lowered to 0 °C, and the ratio of product **233** to dimer **234** improved (Table 4.6, entry 3). Use of Zn^0 as a reductant instead of Mn^0 gave comparable results. Interestingly, when 2.0 equivalents NHP ester **231** were employed, the yield almost doubled, giving **233** in 52% yield in 73% ee (Table 4.6, entry 6). This suggests that increasing the concentration of carbon-centered radical increases the productive cross-coupling.

***Table 4.6**. Optimization of model cross-coupling.*

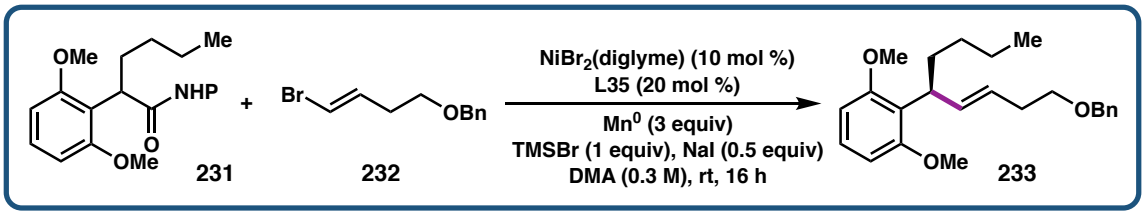

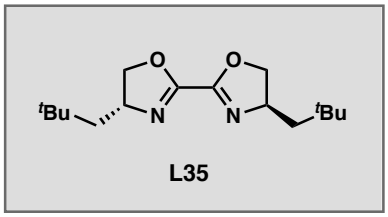

Entry	Deviation	Yield HC 234 (%)	Yield 233 (%)	ee 233 (%)
1	none	50	31	69
2	60 °C	16	12	76
3	0 °C	29	26	78
4	Zn	49	31	66
5	TDAE	0	0	—
6	2 equiv 231	21	52	73
7	2 equiv 232	36	26	67

4.5.3 Further development of substrate scope

Our efforts toward the cylindrocyclophanes will first focus on further improving the yield of the reductive alkenylation NHP ester **231**. Moving forward, we will reinvestigate chiral ligands, reductants, and additives while running the reaction at 0 °C, which showed improved ratios of product **233** to homo-dimer **234**. Our preliminary

studies determined that the yield increases when excess NHP ester is used, which could indicate that there is degradation of **231** through off-cycle non-productive pathways (see Figure 4.1 for proposed catalytic cycle). It is possible that tuning of the redox potential of the ester could improve the yield; thus, we will also investigate whether other redox-active esters (**235**, **236**, **237**) provide improved reactivity (Figure 4.3). In addition to tuning the redox potential of the ester, we will investigate whether substitution at the *para* position of the arene (e.g. **238**, X substituent) can be used to tune the stability of the radical; having a handle at the *para* position would also be helpful as we ultimately need to functionalize the arene here for elaboration to **227** (Figure 4.3). Similarly, different protecting groups at the *ortho* position will be evaluated for their effect on yield and selectivity (e.g. **239**, Y substituent).

Figure 4.3. *Electronic tuning of NHP ester substrate.*

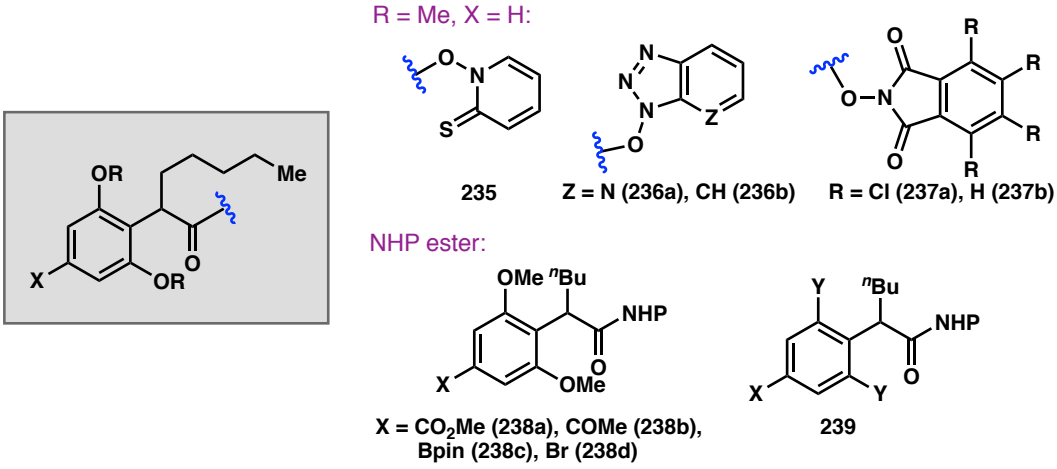

Given the promising levels of enantioselectivity obtained when using 4-HeptylBiOX (**L6**) under the initial screening conditions, we feel confident that appropriate conditions to deliver the product in high yield and enantioselectivity can be identified. Moreover, once optimal conditions have been identified for the cross-coupling

between **231** and **232**, we will investigate whether these conditions broaden the scope of the reductive alkenylation with respect to other challenging substrates. Of particular interest is improved reactivity with other NHP (or related) esters bearing *o*-substitution (**240**), or bulky substituents at the benzylic position (**241**) (Figure 4.4). In addition, we will investigate whether the newly identified conditions enable the cross-coupling of *Z*- and trisubstituted alkenyl bromides (**242** and **243**), substrates that fail to cross-couple under our first-generation conditions. Thus, in addition to solving the specific synthetic challenge presented by the cylindrocyclophanes, these studies will also serve to improve the generality of these asymmetric reductive alkenylation reactions.

Figure 4.4. *Expansion of substrate scope.*

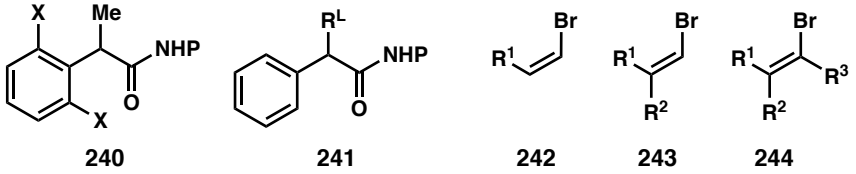

4.5.4 Synthesis of cylindrocyclophane F

Having identified conditions for the Ni-catalyzed enantioselective cross-coupling between **231** and **232**, attention will turn to the synthesis of a bifunctional dimerization/macrocyclization substrate for the synthesis of cylindrocylophane F (Scheme 4.8). As part of our strategy design, we envisioned using aryl bromide **245** as a lynchpin unit, wherein cross-coupling chemistry could be employed to modularly join the fragments containing the NHP ester and alkenyl bromide functionalities. This approach would ultimately provide a flexible route that could be used to prepare additional cylindrocyclophane natural products. To this end, commercially available aryl bromide **245** was coupled to *tert*-butyl acetate (**246)** under Pd-catalyzed enolate arylation

conditions in 88% yield.[33] Ester **247** can be smoothly alkylated with 1-bromobutane to give **248** in 78% yield. Ester **248** is then submitted to Ir-catalyzed C–H borylation conditions,[34–36] and the resulting aryl pinacol boronate is formed in 87% yield. This pinacol boronate will then be coupled with alkyl iodide **250** using the Ni-catalyzed conditions developed by Fu and coworkers.[37,38] Preliminary experiments demonstrate we can cross-couple a simple alkyl iodide with **249** in good yield (not shown), demonstrating the feasibility of this transformation. Alkyne **250** can be prepared from commercially available hex-5-ynoic acid following a protocol developed by Paquette.[39] Finally, alkyne **251** will be converted to the alkenyl bromide, and the ester will be transesterified to give bis-electrophile **227**.

Scheme 4.8. *Synthesis of dimerization substrate* ***227***.[40]

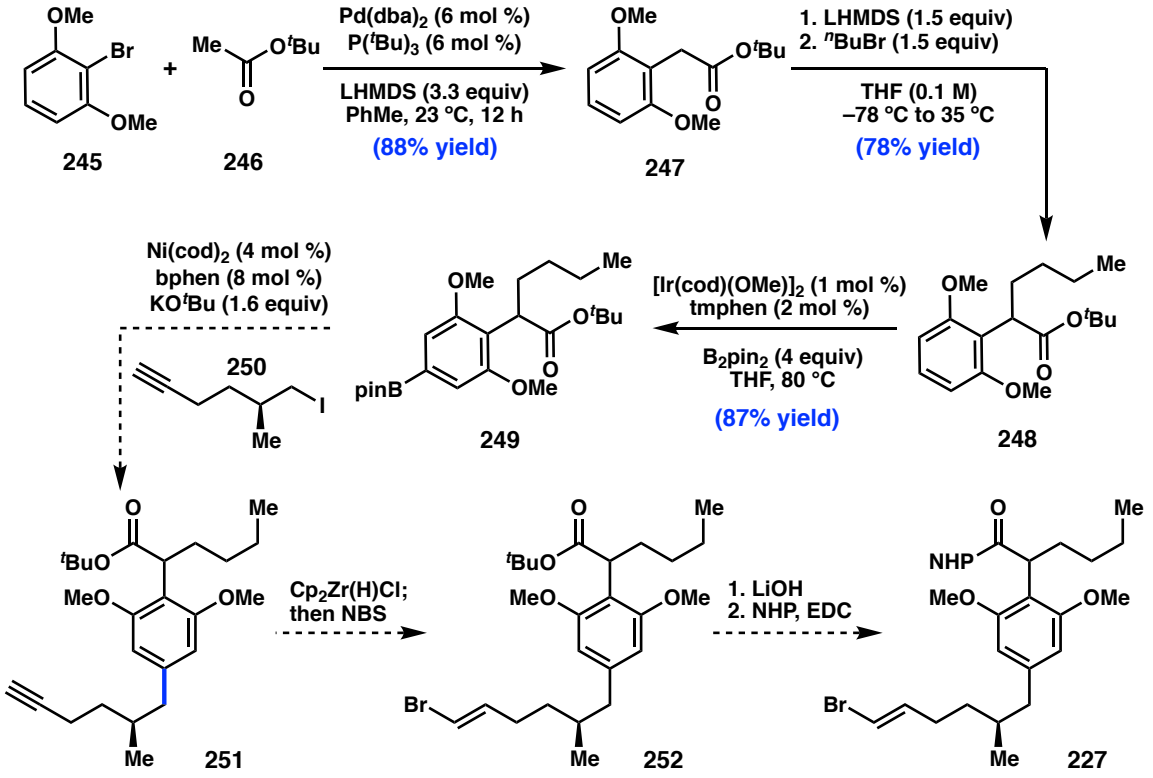

Scheme 4.9. *Ni-catalyzed dimerization to give cylindrocyclophane F (**220F**).*

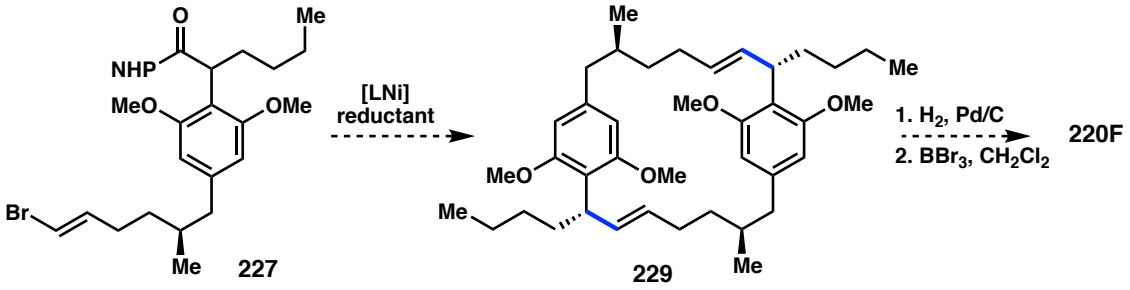

Bis-electrophile **227** will be subjected to the Ni-catalyzed reductive alkenylation conditions developed on the model system (Scheme 4.9). A range of reaction concentrations will be explored in order to favor the formation of macrocycle **229** over competing linear dimerization reactions. Hydrogenation of **229** and demethylation under standard conditions will provide cylindrocyclophane F (**220F**).

4.5.5 Alternative strategies

Scheme 4.10. *Sequential reductive coupling to access **229**.*

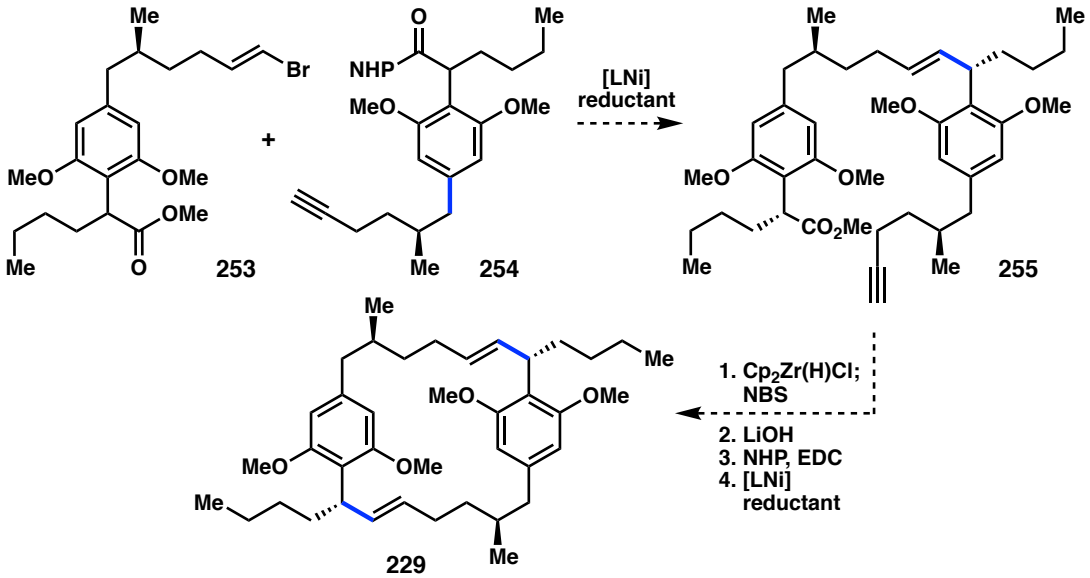

If the Ni-catalyzed asymmetric double reductive alkenylation strategy to form the cylindrocyclophanes proves problematic, two back-up strategies have been devised. The

first is a sequential coupling approach (Scheme 4.10), in which a Ni-catalyzed reductive coupling of vinyl bromide **253** with NHP ester **254** will provide **255**. Conversion of the alkyne to the alkenyl bromide, and conversion of the methyl ester to the NHP ester, will enable a second Ni-catalyzed reductive coupling to form the macrocycle and intercept diene **229**. Hydrogenation and demethylation would provide **220F**.

Scheme 4.11. *Macrocyclization through CM/RCM to access **229***.

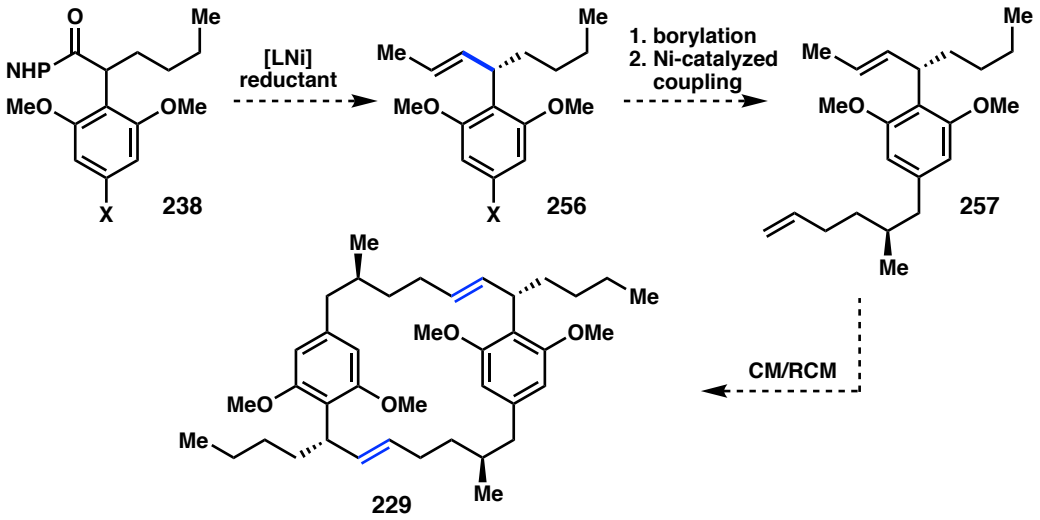

The second back-up strategy will prepare the key fragment, **229**, using a Ni-catalyzed asymmetric reductive alkenylation of NHP ester **238** (Scheme 4.11). Ir-catalyzed borylation of arene **256** followed by Ni-catalyzed cross-coupling will provide diene **257**. Exposure of **257** to the CM/RCM conditions developed by Smith and coworkers should result in macrocycle formation, and hydrogenation and demethylation would complete the synthesis of **220F**. This route could prove necessary if our optimization studies of the Ni-catalyzed alkenylation reveal that electronic modulation of the NHP ester through *p*-substitution is required.

4.6 CONCLUSION

In summary, these results demonstrate that Ni-catalyzed reductive cross-coupling reactions of NHP esters can be rendered highly enantioselective, thus broadening the scope of $C(sp^3)$ electrophiles available for asymmetric C–C bond formation. In contrast to the related reductive cross-couplings of benzyl chlorides, optimal results are obtained when TDAE is used as the terminal reductant in place of Mn^0 or Zn^0, which are typical in these reactions. A preliminary result demonstrates that these conditions can be used to cross-couple α-alkoxy NHP esters and other substrates for which the corresponding benzylic chloride could be difficult to prepare or unstable. The ability to use both NHP esters and benzylic chlorides in asymmetric reductive alkenylation reactions allows users to select from either electrophile depending on factors such as commercial availability of the corresponding carboxylic acid or benzylic chloride starting material, and improves the overall scope of this transformation. The expansion of this technology to more challenging $C(sp^3)$ and $C(sp^2)$ electrophiles is the focus of ongoing work in our laboratory. We aim to prove the synthetic utility of this strategic disconnection in the total synthesis of cylindrocyclophane natural products.

4.7 EXPERIMENTAL SECTION

4.7.1 *Materials and methods*

Unless otherwise stated, reactions were performed under a nitrogen atmosphere using freshly dried solvents. Methylene chloride (DCM), diethyl ether (Et_2O), tetrahydrofuran (THF), 1,4-dioxane and toluene (PhMe) were dried by passing through activated alumina columns. All other commercially obtained reagents were used as received unless specifically indicated. Aryl iodides were purchased from Sigma Aldrich, Combi-Blocks, or Astatech. Manganese powder (>99.9%) was purchased from Sigma Aldrich. $NiBr_2$(diglyme) was purchased from Strem. All reactions were monitored by thin-layer chromatography using EMD/Merck silica gel 60 F254 pre-coated plates (0.25 mm). Silica gel and basic alumina column chromatography was performed as described by Still et al. (W. C. Still, M. Kahn, A. Mitra, *J. Org. Chem*. **1978**, *43*, 2923.) using silica gel (particle size 0.032–0.063) purchased from Silicycle and aluminum oxide (activated, basic, Brockmann I, 58 Å pore size, powder) purchased from Sigma-Aldrich. ^1H and ^{13}C NMR were recorded on a Varian Inova 500 (at 500 MHz and 125 MHz respectively) or a Bruker Avance III HD with Prodigy cyroprobe (at 400 MHz and 101 MHz respectively). ^1H and ^{19}F NMR spectra were recorded on a Varian Inova 300 (at 300 MHz and 282 MHz, respectively). NMR data is reported relative to internal chloroform (^1H, δ = 7.26, ^{13}C, δ = 77.0) and C_6F_6 (^{19}F, δ = –164.9). Data for ^1H NMR spectra are reported as follows: chemical shift (δ ppm) (multiplicity, coupling constant (Hz), integration). Multiplicity and qualifier abbreviations are as follows: s = singlet, d = doublet, t = triplet, q = quartet, m = multiplet, br = broad. IR spectra were recorded on a Perkin Elmer Paragon 1000 spectrometer and are reported in frequency of absorption (cm^{-1}). Analytical

SFC was performed with a Mettler SFC supercritical CO_2 analytical chromatography system with Chiralcel AD-H, OD-H, AS-H, OB-H, and IA columns (4.6 mm x 25 cm). SFC analysis performed at 100.0 bar and 40 ºC. HRMS were acquired using either an Agilent 6200 Series TOF with an Agilent G1978A Multimode source in electrospray ionization (ESI), atmospheric pressure chemical ionization (APCI), or mixed (MM) ionization mode.

4.7.2 *Ligand Synthesis*

4.7.2.1 *Preparation of Ni(II) BOX Ligand Complex*

Bis((3a*R*,8a*S*)-3a,8a-dihydro-8*H*-indeno[1,2-*d*]oxazol-2-yl)methane (258)

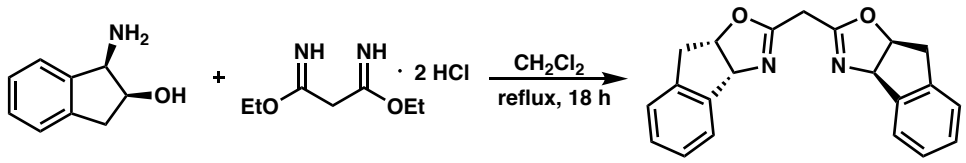

According to a procedure by Snyder and coworkers, the (1R,2S)-(+)-*cis*-1-amino-2-indanol (4.70 g, 31.5 mmol, 2.1 equiv) and diethyl malonimidate dihydrochloride (3.47 g, 15 mmol, 1 equiv) were added to a flame-dried 1 L round bottom flask fitted with a reflux condenser and a magnetic stirring rod, and put under an inert atmosphere (N_2). Then CH_2Cl_2 (360 mL) was added and the solution was heated at 45 °C for 18 hours. The reaction was cooled, then quenched with water (690 mL). The layers were separated, the aqueous layer was extracted with CH_2Cl_2 (4 x 180 mL), and the combined organic layers were dried with $MgSO_4$, filtered, and concentrated under reduced pressure. The crude material was purified by recrystallization from cooling hot ethanol to yield 3.30 g (67% yield) of **258** as a white solid. Spectral data matched those reported in literature.

(3a*R*,3a'*R*,8a*S*,8a'*S*)-2,2'-(Cyclopropane-1,1-diyl)bis(3a,8a-dihydro-8*H*-indeno[1,2-*d*]-oxazole) (L4)

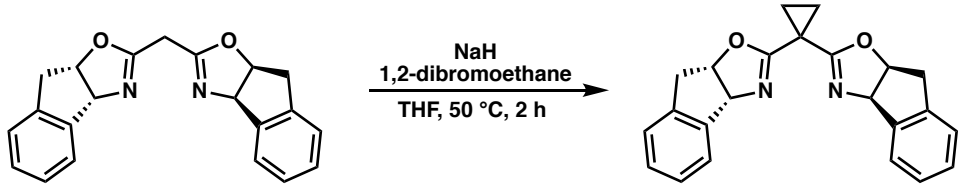

According to a procedure by Sibi and coworkers, the bis(oxazoline) ligand **L4** (1.65 g, 5 mmol, 1 equiv) was added to a flame-dried 200 mL round bottom flask with a magnetic stir bar and put under an inert atmosphere (N_2). The compound was dissolved in THF (25 mL) and cooled to 0 °C before *dry* sodium hydride (60 wt % in mineral oil, 601 mg, 15 mmol, 3 equiv) was added in portions. *Note: Wet NaH resulted in saponification of the oxazoline, which could be removed by column chromatography (silica, 10% MeOH/CH_2Cl_2).* The solution was allowed to stir for 30 minutes before 1,2-dibromoethane (517 mL, mmol, 1.2 equiv) was added dropwise over the course of 10 minutes. The reaction was warmed to 50 °C and stirred for 2 hours. *Note: Aliquots could be monitored by ^1H NMR to ensure complete conversion of the starting material.* The reaction was quenched with aqueous NH_4Cl (25 mL) and extracted with CH_2Cl_2 (2 x 85 mL). The combined organic layers were dried with Na_2SO_4, filtered, and concentrated under reduced pressure. The crude material was purified by recrystallization from cooling hot ethanol to yield 1.46 g (82% yield) of **L4** as a light tan solid. Spectral data matched those reported in literature.

Nickel(II) bis(bromide) (3a*R*,3a'*R*,8a*S*,8a'*S*)-2,2'-(cyclopropane-1,1-diyl)bis(3a,8a-dihydro-8*H*-indeno[1,2-*d*]oxazole) (L4•$NiBr_2$)

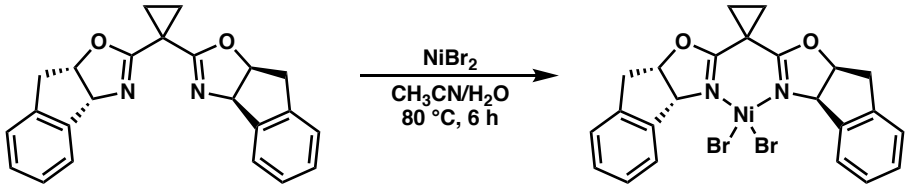

Similar to a procedure reported by Evans and coworkers, the bis(oxazoline) ligand **L4** (1.07 g, 3.0 mmol, 1 equiv) and anhydrous nickel(II) bromide (655 mg, 3.0 mmol, 1 equiv) were added to a round bottom flask equipped with a magnetic stir bar and dissolved in a mixture of acetonitrile (CH_3CN, 65 mL) and water (0.75 mL). The solution was heated to 80 °C for 6 hours to afford a dark purple solution. The reaction was concentrated under reduced pressure and the obtained solid was saturated in CH_2Cl_2, filtered through a plug of cotton, dispensed into four 20 mL scintillation vials, and recrystallized by vapor diffusion (CH_2Cl_2/pentane) to afford dark purple crystals suitable for X-ray diffraction. For the isolation of **L4•$NiBr_2$**, the crystals were washed with hexane, which was added by pipet and subsequently removed. The crystals were removed with a spatula, transferred to a new vial, and crushed to provide a powder. The resulting complex was dried under vacuum to yield 1.6 g (91% yield) of **L4•$NiBr_2$** as a purple solid.

m.p. = >300 °C

^{1}H NMR (400 MHz, $CDCl_3$): δ 96.48 (s, 2H), 46.46 (s, 2H), 20.16 (d, *J* = 17.1 Hz, 2H), 11.67 – 10.85 (m, 6H), 10.55 (d, *J* = 16.6 Hz, 2H), 6.96 (s, 2H), 5.40 (s, 2H), -0.65 (s, 2H).

FTIR (NaCl, thin film, cm^{-1}): 3333, 2222, 1660, 1479, 1461, 1444, 1427, 1312, 1247, 1227, 1214, 1120, 1010, 911, 859, 758, 728.

EA: Anal. Calc'd. for **L4•NiBr$_2$**, $C_{23}H_{20}Br_2N_2NiO_2$ (%): C, 48.05; H, 3.51; N, 4.87. Found: C, 48.38;

H, 3.54; N, 4.84

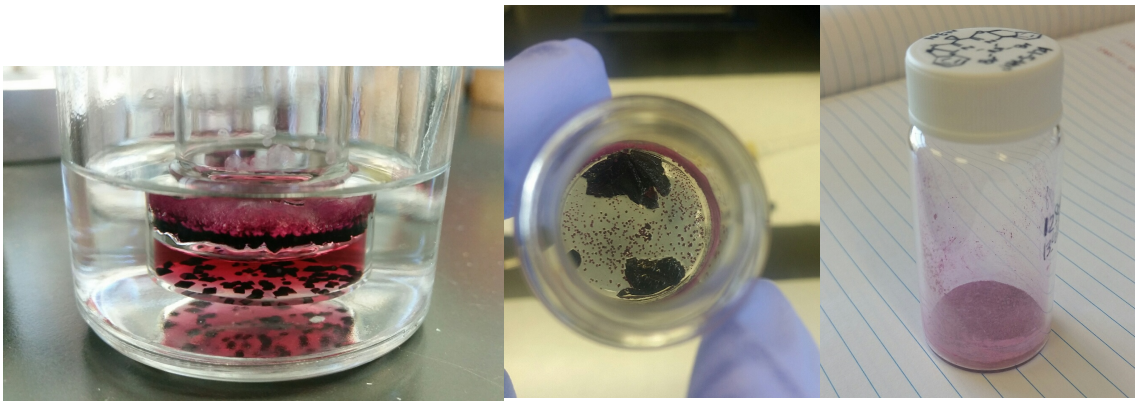

(Left) Crystallized **L4•NiBr$_2$** following vapor diffusion. **(Center)** Large crystals of **L4•NiBr$_2$**. **(Right)** The powdered form of **L4•NiBr$_2$** after crushing the crystals with a spatula and drying under vacuum.

4.7.2.2 *X-Ray Structure Determination*

Low-temperature diffraction data (ϕ- and ω-scans) were collected on a Bruker AXS KAPPA APEXII diffractometer coupled to a CCD detector with Mo-$K\alpha$ radiation (λ = 0.71073 Å) from a fine-focus sealed X-ray tube. All diffractometer manipulations, including data collection integration, and scaling were carried out using the Bruker APEXII software. Absorption corrections were applied using SADABS. The structure was solved by intrinsic phasing using SHELXT and refined against F^2 on all data by full-matrix least squares with SHELXL-2014 using established refinement techniques. All non-hydrogen atoms were refined anisotropically. All hydrogen atoms were included into

the model at geometrically calculated positions and refined using a riding model. Compound **L4•NiBr$_2$** crystallizes in the tetragonal space group $P4_1$ with one molecule in the asymmetric unit. The structure was solved as a merohedral twin with rotation around an axis 45° between a and b. The twin law was defined as the matrix (0.0, 1.0, 0.0, 1.0, 0.0, 0.0, 0.0, 0.0, -1.0). The BASF parameter [0.4980(14)] gave the twin ratio as 0.50:0.50. Absolute configuration was determined by anomalous dispersion (Flack = 0.011(2)). Crystallographic data for **L4•NiBr$_2$** can be obtained free of charge from The Cambridge Crystallographic Data Centre (CCDC) via www.ccdc.cam.ac.uk/data_request/cif under CCDC deposition number 1501744. Graphical representation of the structure with 50% probability thermal ellipsoids was generated using Mercury visualization software.

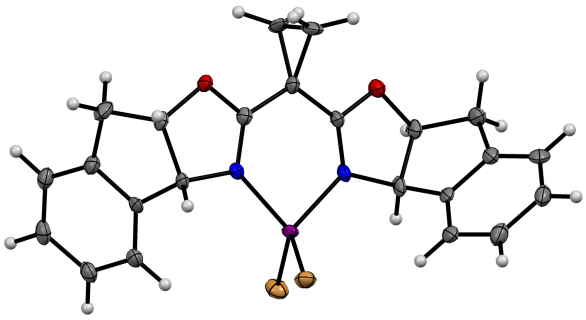

Table S4.1. Crystal data and structure refinement for L4•NiBr$_2$.

Identification code	JLH-3-168	
Empirical formula	$C_{23}H_{20}Br_2N_2NiO_2$	
Formula weight	574.94	
Temperature	100 K	
Wavelength	0.71073 Å	
Crystal system	Tetragonal	
Space group	$P4_1$	
Unit cell dimensions	a = 9.4823(6) Å	a= 90°.
	b = 9.4823(6) Å	b= 90°.
	c = 24.418(2) Å	g = 90°.
Volume	2195.5(3) Å^3	

Z	4
Density (calculated)	1.739 Mg/m^3
Absorption coefficient	4.546 mm^{-1}
F(000)	1144
Crystal size	0.31 x 0.27 x 0.14 mm^3
Theta range for data collection	0.834 to 38.918°.
Index ranges	-16<=h<=16, -16<=k<=16, -42<=l<=43
Reflections collected	113308
Independent reflections	12464 [R(int) = 0.0431]
Completeness to theta = 25.242°	100.0 %
Absorption correction	Semi-empirical from equivalents
Max. and min. transmission	0.7476 and 0.5466
Refinement method	Full-matrix least-squares on F^2
Data / restraints / parameters	12464 / 1 / 272
Goodness-of-fit on F^2	1.056
Final R indices [I>2sigma(I)]	R1 = 0.0470, wR2 = 0.1114
R indices (all data)	R1 = 0.0580, wR2 = 0.1168
Absolute structure parameter	0.011(2)
Extinction coefficient	n/a
Largest diff. peak and hole	2.381 and -1.019 $e.Å^{-3}$

4.7.3 *Substrate Preparation*

4.7.3.1 *NHP Ester Synthesis*

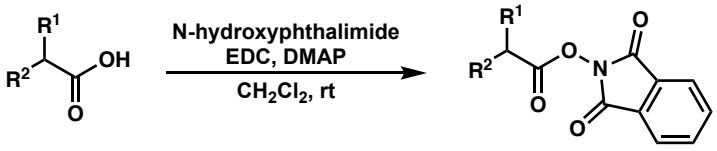

General Procedure 1: To a round bottom flask equipped with a magnetic stir bar was added the carboxylic acid (1.0 equiv), N-hydroxyphthalimide (1.0 equiv), and 4-dimethylaminopyridine (DMAP, 0.10 equiv). The reagents were dissolved in CH_2Cl_2 (0.2 M) and the N-(3-dimethylaminopropyl)-N-ethylcarbodiimide (EDC, 1.1 equiv) was added. The reaction continued to stir overnight at room temperature. The crude reaction was concentrated to afford a thick oil, which was purified by column chromatography (silica, EtOAc/hexane or CH_2Cl_2) to afford the desired product.

1,3-dioxoisoindolin-2-yl 2-phenylpropanoate (259)

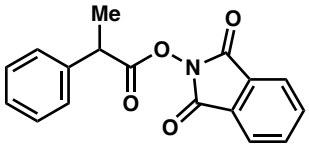

Prepared from 2-phenylpropanoic acid (5.0 g, 33.3 mmol) according to General Procedure 1. The crude residue was purified by filtering through a plug of silica with CH_2Cl_2 as the eluent to yield 8.7 g (88% yield) of **259** as a white solid.

R_f = 0.28 (silica gel, 20% EtOAc/hexane, UV).

m.p. = 62–64 °C

^{1}H NMR (400 MHz, $CDCl_3$): δ 7.85 (d, *J* = 5.5, 3.1 Hz, 2H), 7.76 (dd, *J* = 5.5, 3.1 Hz, 2H), 7.43 – 7.37 (m, 4H), 7.37 – 7.30 (m, 1H), 4.13 (q, *J* = 7.2 Hz, 1H), 1.68 (d, *J* = 7.2 Hz, 3H).

^{13}C NMR (101 MHz, $CDCl_3$): δ 170.9, 161.9, 138.5, 134.9, 129.02, 128.98, 127.9, 127.7, 124.0, 43.1, 19.1.

FTIR (NaCl, thin film, cm^{-1}): 1810, 1785, 1743, 1466, 1453, 1358, 1186, 1123, 1043, 1028, 877, 695.

HRMS (ESI-TOF, *m/z*): calc'd for $C_{17}H_{13}NO_4$ $[M+H]^+$: 296.0923; found: 296.0903.

1,3-dioxoisoindolin-2-yl 2-(4-methoxyphenyl)propanoate (260)

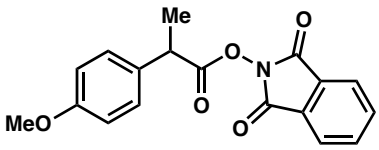

Prepared from 2-(4-methoxyphenyl)propanoic acid (500 mg, 2.77 mmol) according to General Procedure 1. The crude residue was purified by filtering through a plug of silica with 30% EtOAc/hexane as the eluent to yield 671 mg (74% yield) of **260** as a white solid.

R_f = 0.22 (silica gel, 20% EtOAc/hexane, UV).

m.p. = 91–92 °C

^{1}H NMR (400 MHz, $CDCl_3$): δ 7.86 (dd, *J* = 5.5, 3.1 Hz, 2H), 7.77 (dd, 2H), 7.33 (d, *J* = 8.7 Hz, 2H), 6.92 (d, *J* = 8.8 Hz, 2H), 4.08 (q, *J* = 7.2 Hz, 1H), 3.81 (s, 3H), 1.65 (d, *J* = 7.2 Hz, 3H).

^{13}C NMR (101 MHz, $CDCl_3$): δ 171.1, 162.0, 159.2, 134.9, 130.5, 129.0, 128.8, 124.0, 114.4, 55.4, 42.2, 19.2.

FTIR (NaCl, thin film, cm^{-1}): 1810, 1784, 1743, 1611, 1513, 1467, 1371, 1249, 1185, 1123, 1045, 1033, 878, 832, 696.

HRMS (ESI-TOF, *m/z*): calc'd for $C_{18}H_{15}NO_5$ $[M+H]^+$: 326.1028; found: 326.1022.

1,3-dioxoisoindolin-2-yl 2-(4-(trifluoromethyl)phenyl)propanoate (261)

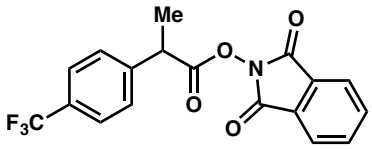

Prepared from 2-(4-(trifluoromethyl)phenyl)propanoic acid (200 mg, 0.92 mmol) according to General Procedure 1. The crude residue was purified by filtering through a plug of silica with 30% EtOAc/hexane as the eluent to yield 290 mg (87% yield) of **261** as a yellow solid.

R_f = 0.28 (silica gel, 20% EtOAc/hexane, UV).

m.p. = 76–77 °C

^{1}H NMR (400 MHz, $CDCl_3$): δ 7.87 (dd, *J* = 5.6, 3.2 Hz, 2H), 7.78 (dd, *J* = 5.5, 3.1 Hz, 2H), 7.66 (d, *J* = 7.8 Hz, 2H), 7.54 (d, *J* = 8.1 Hz, 2H), 4.19 (q, *J* = 7.2 Hz, 1H), 1.69 (d, *J* = 7.2 Hz, 3H).

^{13}C NMR (101 MHz, $CDCl_3$): δ 170.3, 161.9, 142.4 (q, J_{C-F} = 1 Hz), 135.0, 130.2 (q, J_{C-F} = 33 Hz), 128.9, 128.2, 126.1 (q, J_{C-F} = 4 Hz). 124.14, 124.11 (q, J_{C-F} = 272 Hz), 43.0, 19.1.

^{19}F NMR (282 MHz, $CDCl_3$): δ -65.8.

FTIR (NaCl, thin film, cm^{-1}): 1813, 1788, 1746, 1620, 1468, 1421, 1359, 1326, 1186, 1168, 1125, 1079, 1067, 1048, 1017, 878, 842, 697.

HRMS (ESI-TOF, *m/z*): calc'd for $C_{18}H_{12}F_3NO_4$ $[M+H]^+$: 364.0797; found: 364.0815.

1,3-dioxoisoindolin-2-yl 2-(4-bromophenyl)propanoate (262)

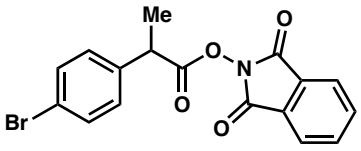

Prepared from 2-(4-bromophenyl)propanoic acid (1.0 g, 4.65 mmol) according to General Procedure 1. The crude residue was purified by filtering through a plug of silica with 20% EtOAc/hexane as the eluent to yield 511 mg (48% yield) of **262** as a light yellow solid.

R_f = 0.69 (silica gel, 20% EtOAc/hexane, UV).

m.p. = 77–78 °C

^{1}H NMR (400 MHz, $CDCl_3$): δ 7.86 (dd, *J* = 5.5, 3.0 Hz, 2H), 7.80 – 7.75 (m, 2H), 7.52 (d, *J* = 8.5 Hz, 2H), 7.29 (d, *J* = 8.4 Hz, 2H), 4.08 (q, *J* = 7.2 Hz, 1H), 1.65 (d, *J* = 7.2 Hz, 3H).

^{13}C NMR (101 MHz, $CDCl_3$): δ 170.5, 161.9, 137.4, 134.9, 132.2, 129.4, 129.0, 124.1, 122.0, 42.6, 19.0.

FTIR (NaCl, thin film, cm^{-1}): 1811, 1786, 1742, 1489, 1467, 1369, 1186, 1133, 1078, 1046, 1010, 877, 696.

LRMS (API-ES, *m/z*): calc'd for $C_{17}H_{12}BrNO_4$ $[M+H_2O]^+$: 391.0; found: 391.0.

1,3-dioxoisoindolin-2-yl 2-(4-fluorophenyl)propanoate (263)

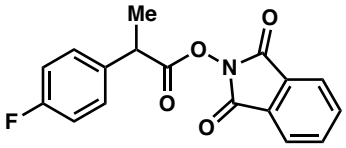

Prepared from 2-(4-fluorophenyl)propanoic acid (500 mg, 2.92 mmol) according to General Procedure 1. The crude residue was purified by filtering through a plug of silica with 20% EtOAc/hexane as the eluent to yield 590 mg (63% yield) of **263** as a white solid.

R_f = 0.35 (silica gel, 20% EtOAc/hexane, UV).

m.p. = 108–110 °C

^{1}H NMR (400 MHz, $CDCl_3$): δ 7.86 (dd, *J* = 5.6, 3.1 Hz, 2H), 7.77 (dd, *J* = 5.5, 3.1 Hz, 2H), 7.41 – 7.35 (m, 2H), 7.12 – 7.05 (m, 2H), 4.11 (q, *J* = 7.2 Hz, 1H), 1.66 (d, *J* = 7.2 Hz, 3H).

^{13}C NMR (101 MHz, $CDCl_3$): δ 170.78, 162.42 (d, $J_{C\text{-}F}$ = 246.4 Hz), 161.9, 134.9, 134.2 (d, $J_{C\text{-}F}$ = 3.3 Hz), 129.37 (d, $J_{C\text{-}F}$ = 8.3 Hz), 129.9, 124.1, 115.95 (d, $J_{C\text{-}F}$ = 21.5 Hz), 42.3, 19.2.

^{19}F NMR (282 MHz, $CDCl_3$): δ -117.64 (tt, $J_{F\text{-}H}$ = 8.4, 5.2 Hz).

FTIR (NaCl, thin film, cm^{-1}): 1811, 1785, 1739, 1605, 1509, 1467, 1360, 1225, 1186, 1120, 1045, 1016, 959, 877, 837, 783, 696.

HRMS (FAB, *m/z*): calc'd for $C_{17}H_{12}FNO_4$ $[M+H]^+$: 314.0823; found: 314.0859.

1,3-dioxoisoindolin-2-yl 2-(4-(dimethylamino)phenyl)propanoate (264)

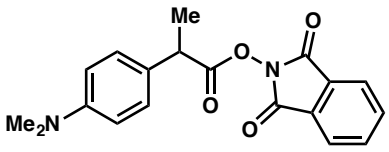

Prepared from 2-(4-(dimethylamino)phenyl)propanoic acid (392 mg, 2.02 mmol) according to General Procedure 1, with the exception of no DMAP. The crude residue was purified column chromatography (silica, 20 to 50% EtOAc/hexane) to yield 640 mg (94% yield) of **264** as a yellow solid.

R_f = 0.54 (silica gel, 50% EtOAc/hexane, UV).

m.p. = 106–108 °C

^{1}H NMR (400 MHz, $CDCl_3$): δ 7.85 (dd, *J* = 5.6, 3.1 Hz, 2H), 7.76 (dd, *J* = 5.5, 3.1 Hz, 2H), 7.27 (d, *J* = 8.8 Hz, 2H), 6.75 (d, *J* = 8.8 Hz, 2H), 4.04 (q, *J* = 7.2 Hz, 1H), 2.95 (s, 6H), 1.64 (d, *J* = 7.2 Hz, 3H).

^{13}C NMR (101 MHz, $CDCl_3$): δ 171.4, 162.1, 150.2, 134.8, 129.1, 128.3, 126.0, 124.0, 112.8, 42.1, 40.6, 19.2.

FTIR (NaCl, thin film, cm^{-1}): 1809, 1784, 1743, 1615, 1523, 1467, 1356, 1186, 1134, 1081, 1044, 878, 819, 697.

HRMS (FAB, *m/z*): calc'd for $C_{19}H_{18}N_2O_4$ $[M+\cdot]^+$: 338.1267; found: 338.1272.

1,3-dioxoisoindolin-2-yl 2-(3,4-dichlorophenyl)propanoate (265)

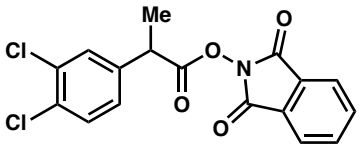

Prepared from 2-(3,4-dichlorophenyl)propanoic acid (231 mg, 1.05 mmol) according to General Procedure 1, with the exception of no DMAP. The crude residue was purified by column chromatography (silica, 0 to 15% EtOAc/hexane) to yield 241 mg (63% yield) of **265** as a white solid.

R_f = 0.35 (silica gel, 20% EtOAc/hexane, UV).

m.p. = 103–105 °C

^{1}H NMR (400 MHz, $CDCl_3$): δ 7.87 (dd, *J* = 5.5, 3.1 Hz, 2H), 7.79 (dd, *J* = 5.5, 3.1 Hz, 2H), 7.52 (d, *J* = 2.2 Hz, 1H), 7.47 (d, *J* = 8.3 Hz, 1H), 7.26 (dd, *J* = 8.3, 2.2 Hz, 1H), 4.08 (q, *J* = 7.2 Hz, 1H), 1.66 (d, *J* = 7.2 Hz, 3H).

^{13}C NMR (101 MHz, $CDCl_3$): δ 170.1, 161.9, 138.4, 135.0, 133.1, 132.2, 131.0, 129.9, 128.9, 127.1, 124.2, 42.3, 19.0.

FTIR (NaCl, thin film, cm^{-1}): 2341, 2359, 1785, 1743, 1426, 1186, 1135, 1049, 962, 878, 696.

HRMS (FAB, *m/z*): calc'd for $C_{17}H_{11}Cl_2NO_4$ $[M+H]^+$: 364.0143; found: 364.0131.

1,3-dioxoisoindolin-2-yl 2-phenylbutanoate (266)

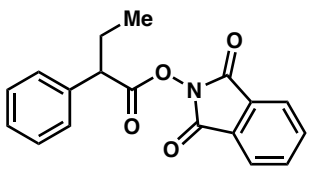

Prepared from 2-phenylbutanoic acid (5.0 g, 30.5 mmol) according to General Procedure 1. The crude residue was purified by column chromatography (silica, 20% EtOAc/hexane) to yield 8.1 g (86% yield) of **266** as a white solid.

R_f = 0.31 (silica gel, 20% EtOAc/hexane, UV).

m.p. = 61–64 °C

^{1}H NMR (400 MHz, $CDCl_3$): δ 7.85 (dd, *J* = 5.6, 3.1 Hz, 2H), 7.76 (dd, *J* = 5.5, 3.1 Hz, 2H), 7.42 – 7.29 (m, 5H), 3.86 (t, *J* = 7.6 Hz, 1H), 2.31 – 2.18 (m, 1H), 2.03 – 1.90 (m, 1H), 1.04 (t, *J* = 7.4 Hz, 3H).

^{13}C NMR (101 MHz, $CDCl_3$): δ 170.4, 162.0, 136.9, 134.8, 129.0, 128.9, 128.2, 128.0, 124.0, 50.5, 27.3, 12.0.

FTIR (NaCl, thin film, cm^{-1}): 1811, 1786, 1744, 1467, 1455, 1360, 1186, 1128, 1080, 1058, 969, 877, 656.

HRMS (ESI-TOF, *m/z*): calc'd for $C_{18}H_{15}NO_4$ $[M+H]^+$: 310.1079; found: 310.1061.

1,3-dioxoisoindolin-2-yl 2,3-diphenylpropanoate (267)

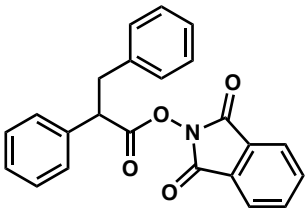

Prepared from 2,3-diphenylpropanoic acid (353 mg, 1.56 mmol) according to General Procedure 1. The crude residue was purified by column chromatography (silica, 20% EtOAc/hexane) to yield 542 mg (94% yield) of **267** as a white solid.

R_f = 0.28 (silica gel, 20% EtOAc/hexane, UV).

m.p. = 116–119 °C

^{1}H NMR (400 MHz, $CDCl_3$): δ 7.85 (dd, *J* = 5.5, 3.0 Hz, 2H), 7.76 (dd, *J* = 5.5, 3.1 Hz, 2H), 7.41 – 7.20 (m, 8H), 7.15 – 7.10 (m, 2H), 4.23 (t, *J* = 7.6 Hz, 1H), 3.56 (dd, *J* = 13.9, 7.5 Hz, 1H), 3.19 (dd, *J* = 13.9, 7.8 Hz, 1H).

^{13}C NMR (101 MHz, $CDCl_3$): δ 170.0, 161.8, 137.7, 136.4, 134.8, 129.2, 129.0, 128.9, 128.6, 128.3, 128.1, 126.9, 124.0, 50.9, 39.9.

FTIR (NaCl, thin film, cm^{-1}): 3030, 1810, 1784, 1744, 1496, 1467, 1454, 1359, 1186, 1134, 1080, 1068, 972, 877, 736, 695.

HRMS (ESI-TOF, *m/z*): calc'd for $C_{23}H_{17}NO_4$ $[M+H]^+$: 372.1236; found: 372.1236.

1,3-dioxoisoindolin-2-yl 3-methyl-2-phenylbutanoate (268)

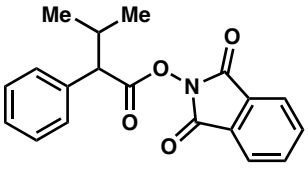

Prepared from 3-methyl-2-phenylbutanoic acid (300 mg, 1.68 mmol) according to General Procedure 1. The crude residue was purified by filtering through a plug of silica with 20%

EtOAc/hexane as the eluent to yield 509 mg (93% yield) of **268** as a white solid.

R_f = 0.34 (silica gel, 20% EtOAc/hexane, UV).

m.p. = 77–81 °C

^{1}H NMR (400 MHz, $CDCl_3$): δ 7.84 (dd, *J* = 5.6, 3.1 Hz, 2H), 7.76 (dd, *J* = 5.5, 3.1 Hz, 2H), 7.42 – 7.29 (m, 5H), 3.58 (d, *J* = 10.0 Hz, 1H), 2.51 – 2.37 (m, 1H), 1.23 (d, *J* = 6.6 Hz, 3H), 0.84 (d, *J* = 6.7 Hz, 3H).

^{13}C NMR (101 MHz, $CDCl_3$): δ 170.2, 162.0, 136.1, 134.8, 129.0, 128.8, 128.7, 128.0, 124.0, 56.7, 32.6, 21.3, 20.3.

FTIR (NaCl, thin film, cm^{-1}): 2966, 1811, 1786, 1745, 1468, 1455, 1375, 1311, 1186, 1132, 1080, 1060, 974, 889, 877, 786, 745, 696.

HRMS (ESI-TOF, *m/z*): calc'd for $C_{19}H_{17}NO_4$ $[M+H]^+$: 324.1236; found: 324.1227.

1,3-dioxoisoindolin-2-yl 3-((*tert*-butyldimethylsilyl)oxy)-2-phenylpropanoate (269)

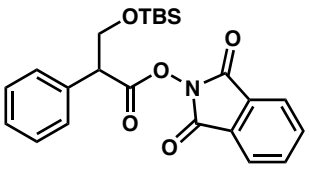

To a round bottom flask equipped with a stirring magnet was added tropic acid (830 mg, 5 mmol, 1 equiv), *tert*-butyldimethylsilyl chloride (1.1 g, 5.5 mmol, 1.1 equiv), dimethylaminopyridine (63 mg, 0.5 mmol, 0.1 equiv), and imidazole (682 mg, 10 mmol, 2 equiv). The reagents were dissolved in 15 mL of CH_2Cl_2 and stirred overnight at room temperature. The reaction was quenched with aq. NH_4Cl, extracted with Et_2O, dried with $MgSO_4$, filtered, and concentrated under reduced pressure to afford crude 3-((*tert*-butyldimethylsilyl)oxy)-2-phenylpropanoic acid. This crude material was used in the esterification step without purification, which was performed according to General Procedure 1. The crude residue was purified by column chromatography and dried under high vacuum (silica, 0 to 20% EtOAc/hexane) to yield 664 mg (31% yield) of **269** as a colorless oil.

R_f = 0.38 (silica gel, 20% EtOAc/hexane, UV).

^{1}H NMR (400 MHz, $CDCl_3$): δ 7.86 (dd, *J* = 5.6, 3.1 Hz, 2H), 7.77 (dd, *J* = 5.5, 3.1 Hz, 2H), 7.43 – 7.31 (m, 5H), 4.28 – 4.18 (m, 2H), 3.93 (dd, *J* = 8.6, 4.4 Hz, 1H), 0.89 (s, 9H), 0.05 (s, 3H), 0.03 (s, 3H).

^{13}C NMR (101 MHz, $CDCl_3$): δ 169.0, 161.8, 134.8, 134.1, 129.1, 129.0, 128.5, 128.3, 124.0, 65.3, 52.2, 25.9, 18.4, -5.4, -5.6.

FTIR (NaCl, thin film, cm^{-1}): 2953, 2929, 2856, 1814, 1788, 1747, 1468, 1361, 1256, 1186, 1113, 1049, 1023, 877, 836, 780, 696.

HRMS (ESI-TOF, *m/z*): calc'd for $C_{23}H_{27}NO_5Si$ $[M+H]^+$: 426.1737; found: 426.1708.

1,3-dioxoisoindolin-2-yl 2-phenylpent-4-enoate (270)

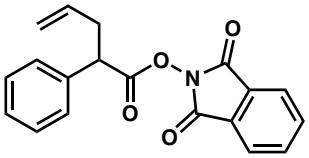

Prepared from 2-phenylpent-4-enoic acid (240 mg, 1.36 mmol) according to General Procedure 1. The crude residue was purified by column chromatography (silica, 0 to 20% EtOAc/hexane) to yield 295 mg (67% yield) of **270** as a white solid.

R$_f$ = 0.31 (silica gel, 20% EtOAc/hexane, UV).

m.p. = 68–69 °C

^{1}H NMR (400 MHz, CDCl$_3$): δ 7.85 (dd, *J* = 5.6, 3.1 Hz, 2H), 7.76 (dd, *J* = 5.5, 3.1 Hz, 2H), 7.42 – 7.31 (m, 5H), 5.81 (ddt, *J* = 17.1, 10.2, 6.9 Hz, 1H), 5.16 (dq, *J* = 17.1, 1.5 Hz, 1H), 5.14 – 5.09 (m, 1H), 4.04 (dd, *J* = 8.0, 7.2 Hz, 1H), 3.00 – 2.90 (m, 1H), 2.68 (dtt, *J* = 14.3, 7.1, 1.3 Hz, 1H).

^{13}C NMR (101 MHz, CDCl$_3$): δ 169.9, 161.9, 136.4, 134.9, 134.0, 129.02, 128.99, 128.2, 128.1, 124.0, 118.3, 48.8, 37.9.

FTIR (NaCl, thin film, cm^{-1}): 1811, 1785, 1743, 1467, 1359, 1186, 1133, 1080, 1068, 971, 877, 695.

HRMS (ESI-TOF, *m/z*): calc'd for $C_{19}H_{15}NO_4$ $[M+H]^+$: 322.1079; found: 322.1063.

1,3-dioxoisoindolin-2-yl 5-chloro-2-phenylpentanoate (271)

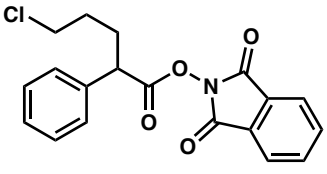

Prepared from 5-chloro-2-phenylpentanoic acid (1.01 g, 4.75 mmol) according to General Procedure 1. The crude residue was purified by filtering through a plug of silica with 20% EtOAc/hexane as the eluent to yield 977 mg (58% yield) of **271** as a white solid.

R$_f$ = 0.25 (silica gel, 20% EtOAc/hexane, UV).

m.p. = 96–99 °C

^{1}H NMR (400 MHz, CDCl$_3$): δ 7.85 (dd, *J* = 5.6, 3.1 Hz, 2H), 7.77 (dd, *J* = 5.5, 3.1 Hz, 2H), 7.42 – 7.31 (m, 5H), 3.97 (t, *J* = 7.7 Hz, 1H), 3.64 – 3.52 (m, 2H), 2.34 (dddd, *J* =

13.2, 10.4, 8.0, 5.1 Hz, 1H), 2.13 (dddd, *J* = 13.5, 10.3, 7.4, 5.5 Hz, 1H), 2.01 – 1.78 (m, 2H).

^{13}C NMR (101 MHz, $CDCl_3$): δ 170.1, 161.9, 136.4, 134.9, 129.1, 129.0, 128.2, 128.1, 124.1, 48.2, 44.4, 31.2, 30.1.

FTIR (NaCl, thin film, cm^{-1}): 2960, 1811, 1786, 1744, 1494, 1455, 1468, 1361, 1186, 1134, 1081, 1045, 965, 878, 697.

HRMS (FAB, *m/z*): calc'd for $C_{19}H_{16}NO_4Cl$ $[M+H]^+$: 358.0846; found: 358.0872.

1,3-dioxoisoindolin-2-yl 2-methoxy-2-phenylacetate (207)

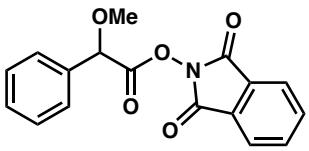

Prepared from 2-methoxy-2-phenylacetic acid (830 mg, 5.0 mmol) according to General Procedure 1. The crude residue was purified by column chromatography (silica, 10 to 30% EtOAc/hexane) to yield 1.16 g (74% yield) of **207** as a colorless oil. *Note: This compound will slowly decompose (solidifies/hydrolyzes) under ambient conditions over extended periods (~1 month).*

R_f = 0.22 (silica gel, 20% EtOAc/hexane, UV).

^{1}H NMR (400 MHz, $CDCl_3$): δ 7.83 (dd, *J* = 5.5, 3.1 Hz, 2H), 7.75 (dd, *J* = 5.5, 3.1 Hz, 2H), 7.60 – 7.52 (m, 2H), 7.50 – 7.37 (m, 3H), 5.19 (s, 1H), 3.56 (s, 3H).

^{13}C NMR (101 MHz, $CDCl_3$): δ 167.4, 161.6, 134.9, 134.4, 129.6, 129.0, 128.8, 127.6, 124.1, 81.0, 58.0.

FTIR (NaCl, thin film, cm^{-1}): 1818, 1789, 1745, 1468, 1359, 1186, 1079, 988, 969, 877, 696.

HRMS (ESI-TOF, *m/z*): calc'd for $C_{17}H_{13}NO_5$ $[M+H]^+$: 312.0872; found: 312.0846.

1,3-dioxoisoindolin-2-yl 2-cyclopropyl-2-phenylacetate (218)

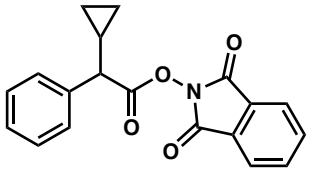

Prepared from 2-cyclopropyl-2-phenylacetic acid (50 mg, 0.28 mmol) according to General Procedure 1. The crude residue was purified by filtering through a plug of silica with 20% EtOAc/hexane as the eluent to yield 80 mg (89% yield) of **218** as a white solid.

R_f = 0.39 (silica gel, 50% EtOAc/hexane, UV).

m.p. = 92–93 °C

^{1}H NMR (400 MHz, $CDCl_3$): δ 7.87 (dd, *J* = 5.5, 3.0 Hz, 2H), 7.81 – 7.75 (m, 2H), 7.50 – 7.45 (m, 2H), 7.44 – 7.38 (m, 2H), 7.37 – 7.31 (m, 1H), 3.29 (d, *J* = 9.7 Hz, 1H), 1.53 (dtt, *J* = 9.7, 8.0, 4.9 Hz, 1H), 0.82 (dddd, *J* = 9.0, 8.1, 4.6, 2.9 Hz, 1H), 0.69 (dddd, *J* = 8.9, 8.0, 5.8, 4.8 Hz, 1H), 0.63 – 0.55 (m, 1H), 0.42 – 0.34 (m, 1H).

^{13}C NMR (101 MHz, $CDCl_3$): δ 170.0, 162.0, 136.8, 134.9, 129.1, 128.9, 128.1, 128.0, 124.1, 53.4, 14.6, 4.91, 4.90.

FTIR (NaCl, thin film, cm^{-1}): 1811, 1742, 1362, 1170, 1135, 1063, 974, 876.

HRMS (FAB, *m/z*): calc'd for $C_{19}H_{15}NO_4$ $[M+H]^+$: 322.1079; found: 322.1065.

4.7.3.2 *Alkenyl Bromide Synthesis*

General Procedure 2: Alkenyl Bromides from Aldehydes

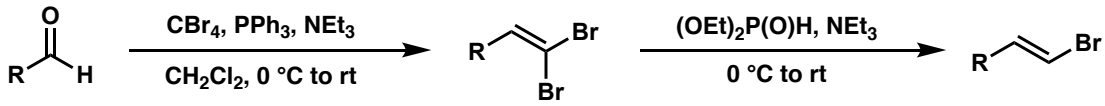

General Procedure 2, Part A: According to a procedure by Alexakis and coworkers, a flame dried round bottom flask equipped with a magnetic stir bar was put under an inert atmosphere (N_2) and charged with the tetrabromomethane (20 mmol, 2 equiv) and triphenylphosphine (40 mmol, 4 equiv). The flask was cooled to 0 °C and then CH_2Cl_2 (30 mL) was added, followed by the triethylamine (10 mmol, 1 equiv). The aldehyde (10 mmol, 1 equiv) was dissolved in CH_2Cl_2 (5 mL) and added dropwise to the reaction mixture. The reaction was allowed to warm to room temperature and continued to stir for 90 minutes. The reaction was removed from the stir plate and slowly added to a vigorously stirring solution of Et_2O (150 mL) and hexane (150 mL), filtered through a plug of silica gel, and concentrated under reduced pressure to afford the desired dibromoalkene.

4-(2,2-dibromovinyl)phenyl 4-methylbenzenesulfonate (272)

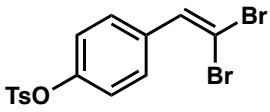

Prepared from 4-formylphenyl 4-methylbenzenesulfonate (5.14 g, 18.6 mmol) following General Procedure 2A. The crude residue was purified by filtering through a plug of silica to yield 6.2 g (77% yield) of **272** as a white solid.

R_f = 0.38 (silica gel, 10% EtOAc/hexane).

m.p. = 108–110 °C

^{1}H NMR (400 MHz, $CDCl_3$): δ 7.73 – 7.67 (m, 2H), 7.49 – 7.43 (m, 2H), 7.41 (s, 1H), 7.34 – 7.29 (m, 2H), 7.01 – 6.95 (m, 2H), 2.45 (s, 3H).

^{13}C NMR (101 MHz, $CDCl_3$): δ 149.3, 145.7, 135.6, 134.2, 132.3, 129.9, 129.8, 128.6, 122.5, 90.8, 21.9.

FTIR (NaCl, thin film, cm^{-1}): 3081, 3065, 1929, 1910, 1596, 1500, 1495, 1406, 1379, 1360, 1271, 1178, 1160, 1094, 1018, 877, 832, 914, 781, 732, 706, 698, 658.

HRMS (FAB, m/z): calc'd for $C_{15}H_{12}Br_2O_3S$ $[M+H]^+$: 432.8932; found: 432.8915.

5-(2,2-dibromovinyl)-2-methoxypyridine (273)

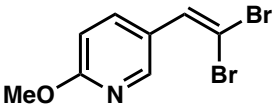

Prepared from 6-methoxynicotinaldehyde (1.36 g, 10 mmol) following General Procedure 2A. The crude residue was purified by column chromatography (silica, 1% Et_2O/hexane to 10% Et_2O/hexane) to yield 570 mg (20% yield) of **273** as a yellow oil.

R_f = 0.48 (silica gel, 10% EtOAc/hexane).

^{1}H NMR (500 MHz, $CDCl_3$): δ 8.25 (dt, *J* = 2.4, 0.6 Hz, 1H), 7.90 (ddd, *J* = 8.7, 2.5, 0.6 Hz, 1H), 7.37 (q, *J* = 0.6 Hz, 1H), 6.74 (dt, *J* = 8.7, 0.5 Hz, 2H), 3.94 (s, 3H).

^{13}C NMR (126 MHz, $CDCl_3$): δ 163.8, 147.6, 137.8, 133.5, 124.9, 110.7, 89.3, 53.8.

FTIR (NaCl, thin film, cm^{-1}): 2982, 2946, 1603 1595, 1561, 1491, 1381, 1309, 1289, 1254, 1132, 1024, 1014, 867, 819, 751.

HRMS (ESI-TOF, m/z): calc'd for $C_8H_7NOBr_2$ $[M+H]^+$: 291.8973; found: 291.8967.

General Procedure 2, Part B: The dibromoalkene (1.7 mmol, 1 equiv) and diethyl phosphite (5.1 mmol, 3 equiv) were added to a vial with a magnetic stirring rod and put under an inert atmosphere (N_2). The solution was cooled to 0 °C and the triethylamine (5.1 mmol, 3 equiv) was added dropwise. The reaction was warmed to room temperature and stirred overnight. The reaction was quenched with water (5 mL) and extracted with CH_2Cl_2 (20 mL). The organic layer was washed with brine (5 mL), dried with Na_2SO_4, filtered, and concentrated under reduced pressure. The crude residue was purified by column chromatography (silica, ether/hexanes) to afford the vinyl bromide.

(*E*)-4-(2-bromovinyl)phenyl 4-methylbenzenesulfonate (274)

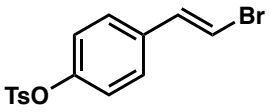

Prepared from **272** (4.32 g, 10 mmol) following General Procedure 2B. The crude residue was purified by column chromatography (silica, 5% EtOAc/hexane to 20% EtOAc/hexane) to yield 2.75 g (78% yield, 90:10 E:Z) of **274** as a white solid.

R_f = 0.34 (silica gel, 10% EtOAc/hexane).

m.p. = 90–93 °C

^{1}H NMR (400 MHz, $CDCl_3$): δ 7.72 – 7.67 (m, 2H), 7.34 – 7.28 (m, 2H), 7.23 – 7.17 (m, 2H), 7.03 (d, *J* = 14.0 Hz, 1H), 6.96 – 6.90 (m, 2H), 6.73 (d, *J* = 14.0 Hz, 1H), 2.44 (s, 3H).

^{13}C NMR (101 MHz, $CDCl_3$): δ 149.3, 145.6, 135.9, 134.9, 132.3, 129.9, 128.6, 127.3, 122.9, 107.7, 21.9.

HRMS (FAB, m/z): calc'd for $C_{15}H_{13}BrO_3S$ $[M+\cdot]^+$: 353.9748; found: 353.9733.

(*E*)-5-(2-bromovinyl)-2-methoxypyridine (275)

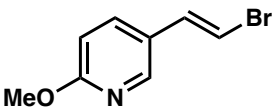

Prepared from **273** (500 mg, 1.7 mmol) following General Procedure 2B. The crude residue was purified by column chromatography (silica, 2% Et_2O/hexane to 5% Et_2O/hexane) to yield 314 mg (86% yield, 96:4 E:Z) of **275** as a white solid.

R_f = 0.46 (silica gel, 10% EtOAc/hexane).

m.p. = 53–56 °C

^{1}H NMR (500 MHz, $CDCl_3$): δ 8.05 (d, *J* = 2.5 Hz, 1H), 7.54 (ddd, *J* = 8.7, 2.5, 0.4 Hz, 1H), 7.02 (dq, *J* = 14.0, 0.5 Hz, 1H), 6.70 (dt, *J* = 8.7, 0.6 Hz, 1H), 6.65 (d, *J* = 14.0 Hz, 1H), 3.93 (s, 3H).

^{13}C NMR (126 MHz, $CDCl_3$): δ 164.0, 145.3, 135.3, 133.5, 125.5, 111.4, 105.5, 53.7.

FTIR (NaCl, thin film, cm^{-1}): 3061, 2943, 1613, 1598, 1562, 1490, 1385, 1303, 1285, 1258, 1238, 1026, 1015, 947, 837, 790.

HRMS (ESI-TOF, m/z): calc'd for C_8H_8NOBr $[M+H]^+$: 213.9868; found: 213.9858.

4.7.4 *Enantioselective Reductive Cross-Coupling*

4.7.4.1 *General Procedures for Enantioselective Cross-Coupling of N-Hydroxyphthalimide Esters with Alkenyl Bromides*

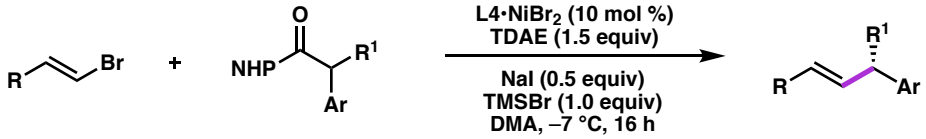

General Procedure 3: Cross-Coupling on 0.2 mmol scale

On a bench-top, a 1 dram vial equipped with a stir bar was charged with the vinyl bromide (if air stable, 0.2 mmol, 1 equiv), NHP ester (0.2 mmol, 1 equiv), **L4•NiBr$_2$** (11.5 mg, 0.02 mmol, 0.10 equiv), and sodium iodide (15.0 mg, 0.1 mmol, 0.5 equiv). The vial was then brought into the glovebox and charged with the vinyl bromide (if air sensitive, 0.2 mmol, 1 equiv) and DMA (0.2 mL, 1.0 M). The vial was then cooled to –7 °C and the reagents were stirred at 250 rpm until dissolved. *Note: The recirculating Julabo LH45 chiller was set to –10 °C however an external thermometer in the glovebox read the temperature as –7 °C.* The tetrakis(dimethyl-amino)ethylene (TDAE, 0.3 mmol, 70 μl, 1.5 equiv) was added and stirred for 10 minutes before the trimethylsilyl bromide (TMSBr, 0.2 mmol, 26 μL, 1 equiv) was added. The vial was sealed with a screw cap and stirred under nitrogen at –7 °C for 16 hours (overnight) in temperature controlled well plates in the glovebox. *Note: Monitoring the reaction kinetics for product **28** revealed that the reaction went to >90% conversion after 1 hour, however we choose to run these reactions overnight to ensure full conversion.* As the reaction proceeds, the TDAE salts begin to precipitate, forming an orange slurry. The crude reaction was quenched with 0.5 mL of 1 M HCl, diluted with water (5 mL), and extracted with diethyl ether (3 x 10 mL). *Note: In order to efficiently remove all of the viscous reaction contents from the vial, we*

found it useful to fill the vial ¾ full with an extraction solvent (2.5 mL each time: first HCl/water, then Et_2O, water, Et_2O 3x), screw on a Teflon cap, and shake the vial vigorously with the stir bar still inside. The contents could then be easily poured into a separatory funnel. The combined organic layers were washed with brine (5 mL), dried with $MgSO_4$, filtered, and concentrated under reduced pressure. The crude residue was purified by column chromatography.

Reaction Setup: (Left) The computer console sets the chiller to –10.0 °C, while actual temperature reading is –7.1 °C; stir plate set at 250 rpm and reads 255.7 rpm. **(Center)** Reactions conducted on 0.2 mmol scale and stirred in the temperature controlled glovebox stir plates. **(Right)** Conducting the reaction on the benchtop on a 5 mmol scale under a balloon of nitrogen; a cryocool is used to cool the reaction to –5 °C.

General Procedure 4: Cross-Coupling on 5.0 mmol scale

On a bench-top to a 25 mL round bottom flask equipped with a stir bar was added vinyl bromide **27** (1.065 g, 5 mmol, 1 equiv), NHP ester **31** (1.476 g, 5 mmol, 1 equiv), **L4•NiBr$_2$** (0.29 g, 0.5 mmol, 0.10 equiv), and sodium iodide (0.37 g, 2.5 mmol, 0.5 equiv). The flask was sealed with a rubber septum, purged with nitrogen, and the reagents

were dissolved in DMA (5.0 mL, 1.0 M). The flask was cooled to –5 °C by submerging it in an isopropanol bath cooled with a Thermo Scientific EK90 Immersion Cooler. *Note: We found that TDAE will begin to freeze at temperatures lower than –8 °C with this setup.* The tetrakis(dimethylamino)ethylene (TDAE, 1.74 mL, 7.5 mmol, 1.5 equiv) was added and stirred for 10 minutes before the trimethylsilyl bromide (TMSBr, 0.66 mL, 5.0 mmol, 1 equiv) was added. The flask was stirred under a balloon of nitrogen at –5 °C for 16 hours. As the reaction proceeds, the TDAE salts begin to precipitate, forming an orange slurry. The crude reaction was quenched with 1 M HCl (30 mL), and extracted with diethyl ether (3 x 20 mL). The combined organic layers were washed with water (2 x 20 mL) and brine (20 mL), dried with $MgSO_4$, filtered, and concentrated under reduced pressure. The crude residue was purified by column chromatography (silica gel, 10 to 20% toluene/hexane) to yield **28** (918 mg, 77% yield) in 91% ee as a colorless oil.

4.7.4.2 *Characterization of Reaction Products*

(*S*,*E*)-1-methoxy-4-(3-phenylbut-1-en-1-yl)benzene (28)

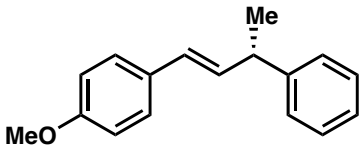

Prepared from (*E*)-1-(2-bromovinyl)-4-methoxybenzene (43 mg, 0.2 mmol) and 1,3-dioxoisoindolin-2-yl 2-phenylpropanoate (59 mg, 0.2 mmol) according to General Procedure 3. The crude residue was purified by column chromatography (silica gel, 10 to 20% toluene/hexane) to yield **28** (39 mg, 80% yield) in 96% ee as a colorless oil. Spectral data matched those reported in literature.

R_f = 0.59 (silica gel, 10% EtOAc/hexane, UV).

Chiral SFC: (OB-H, 2.5 mL/min, 20% IPA in CO_2, λ = 254 nm): t_R (major) = 7.1 min, t_R (minor) = 8.4 min.

$[\alpha]_D^{25}$ = –34° (c = 1.0, $CHCl_3$).

^{1}H NMR (400 MHz, $CDCl_3$): δ 7.37 – 7.27 (m, 6H), 7.25 – 7.20 (m, 1H), 6.85 (d, *J* = 8.8 Hz, 2H), 6.38 (d, *J* = 16.2 Hz, 1H), 6.27 (dd, *J* = 15.9, 6.7 Hz, 1H), 3.81 (s, 3H), 3.70 – 3.58 (m, 1H), 1.48 (d, *J* = 7.0 Hz, 3H).

^{13}C NMR (101 MHz, $CDCl_3$): δ 158.9, 146.0, 133.3, 130.5, 128.6, 128.0, 127.42, 127.36, 126.3, 114.0, 55.4, 42.7, 21.5.

(*S*,*E*)-1-methyl-4-(3-phenylbut-1-en-1-yl)benzene (180)

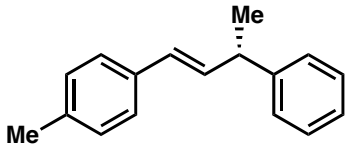

Prepared from (*E*)-1-(2-bromovinyl)-4-methylbenzene (39 mg, 0.2 mmol) and 1,3-dioxoisoindolin-2-yl 2-phenylpropanoate (59 mg, 0.2 mmol) according to General Procedure 3. The crude residue was purified by column chromatography (10% $AgNO_3$ silica gel, 0 to 2% Et_2O/hexane) to yield **180** (39 mg, 88% yield) in 95% ee as a colorless oil. Spectral data matched those reported in literature.

R_f = 0.26 (silica gel, hexane, UV).

Chiral SFC: (OJ-H, 2.5 mL/min, 7% IPA in CO_2, λ = 254 nm): t_R (minor) = 8.0 min, t_R (major) = 10.0 min.

$[\alpha]_D^{25}$ = –41° (c = 1.0, $CHCl_3$).

^{1}H NMR (400 MHz, $CDCl_3$): δ 7.41 – 7.30 (m, 6H), 7.30 – 7.24 (m, 1H), 7.16 (d, *J* = 8.0 Hz, 2H), 6.52 – 6.34 (m, 2H), 3.74 – 3.64 (m, 1H), 2.38 (s, 3H), 1.53 (d, *J* = 7.0 Hz, 3H).

^{13}C NMR (101 MHz, $CDCl_3$): δ 145.9, 136.9, 134.9, 134.3, 129.3, 128.6, 128.5, 127.5, 126.3, 126.2, 42.7, 21.5, 21.3.

(*S*,*E*)-*N*,*N*-dimethyl-4-(3-phenylbut-1-en-1-yl)aniline (181)

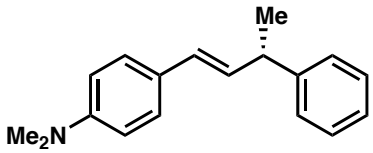

Prepared from (*E*)-4-(2-bromovinyl)-*N*,*N*-dimethylaniline (45 mg, 0.2 mmol) and 1,3-dioxoisoindolin-2-yl 2-phenylpropanoate (59 mg, 0.2 mmol) according to General Procedure 3. The crude residue was purified by column chromatography (silica gel, 5% Et_2O/hexane) to yield **181** (38 mg, 76% yield) in 97% ee as a white solid. Spectral data matched those reported in literature.

R_f = 0.21 (silica gel, 5% Et_2O/hexane, UV).

m.p. = 65–67 °C

Chiral SFC: (OB-H, 2.5 mL/min, 35% IPA in CO_2, λ = 254 nm): t_R (major) = 6.0 min, t_R (minor) = 9.0 min.

$[\alpha]_D^{25}$ = –56° (c = 1.0, $CHCl_3$).

^{1}H NMR (400 MHz, $CDCl_3$): δ 7.40 – 7.29 (m, 6H), 7.29 – 7.23 (m, 1H), 6.73 (d, *J* = 8.8 Hz, 2H), 6.40 (d, *J* = 15.9 Hz, 1H), 6.24 (dd, *J* = 15.8, 6.8 Hz, 1H), 3.72 – 3.62 (m, 1H), 3.00 (s, 6H), 1.51 (d, *J* = 7.0 Hz, 3H).

^{13}C NMR (101 MHz, $CDCl_3$): δ 149.9, 146.4, 131.2, 128.5, 128.4, 127.5, 127.1, 126.4, 126.1, 112.7, 42.7, 40.8, 21.6.

(*S*,*E*)-1-(3-phenylbut-1-en-1-yl)-4-(trifluoromethyl)benzene (182)

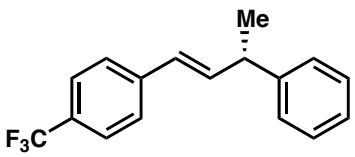

Prepared from (*E*)-1-(2-bromovinyl)-4-(trifluoromethyl)benzene (50 mg, 0.2 mmol) and 1,3-dioxoisoindolin-2-yl 2-phenylpropanoate (59 mg, 0.2 mmol) according to General Procedure 3. The crude residue was purified by column chromatography (silica gel, hexane) to yield **182** (48 mg, 87% yield) in 93% ee as a colorless oil. Spectral data matched those reported in literature.

R_f = 0.32 (silica gel, hexane, UV).

Chiral SFC: (OJ-H, 2.5 mL/min, 3% IPA in CO_2, λ = 254 nm): t_R (minor) = 6.3 min, t_R (major) = 7.3 min.

$[\alpha]_D^{25}$ = –27° (c = 1.0, $CHCl_3$).

^{1}H NMR (400 MHz, $CDCl_3$): δ 7.56 (d, *J* = 8.6 Hz, 2H), 7.46 (d, *J* = 8.2 Hz, 2H), 7.40 – 7.33 (m, 2H), 7.33 – 7.23 (m, 3H), 6.52 (dd, *J* = 15.9, 6.2 Hz, 1H), 6.45 (d, *J* = 16.0 Hz, 1H), 3.74 – 3.64 (m, 1H), 1.51 (d, *J* = 7.0 Hz, 3H).

^{13}C NMR (101 MHz, $CDCl_3$): δ 145.2, 141.2 (q, J_{C-F} = 1 Hz), 138.1, 129.0 (q, J_{C-F} = 32 Hz), 128.7, 127.5, 127.4, 126.6, 126.4, 125.6 (q, J_{C-F} = 4 Hz), 124.4 (q, J_{C-F} = 272 Hz), 42.8, 21.2.

^{19}F NMR (282 MHz, $CDCl_3$): δ –65.6.

(*S*,*E*)-4-(3-phenylbut-1-en-1-yl)benzonitrile (183)

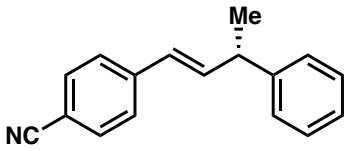

Prepared from methyl (*E*)-4-(2-bromovinyl)benzonitrile (42 mg, 0.2 mmol) and 1,3-dioxoisoindolin-2-yl 2-phenylpropanoate (59 mg, 0.2 mmol) according to General Procedure 3. The crude residue was purified by column chromatography (silica gel, 0 to 3% Et_2O/hexane) to yield **183** (42 mg, 91% yield) in 94% ee as a colorless oil.

R_f = 0.42 (silica gel, 10% EtOAc/hexane, UV).

Chiral SFC: (OB-H, 2.5 mL/min, 10% IPA in CO_2, λ = 254 nm): t_R (minor) = 9.5 min, t_R (major) = 10.1 min.

$[\alpha]_D^{25}$ = –51° (c = 1.0, $CHCl_3$).

^{1}H NMR (400 MHz, $CDCl_3$): δ 7.54 (d, *J* = 8.5 Hz, 2H), 7.40 (d, *J* = 8.3 Hz, 2H), 7.36 – 7.30 (m, 2H), 7.28 – 7.19 (m, 3H), 6.52 (dd, *J* = 15.9, 6.7 Hz, 1H), 6.40 (d, *J* = 16.0 Hz, 1H), 3.72 – 3.61 (m, 1H), 1.48 (d, *J* = 7.0 Hz, 3H).

^{13}C NMR (101 MHz, $CDCl_3$): δ 144.7, 142.1, 139.5, 132.4, 128.7, 127.3, 127.2, 126.7, 126.6, 119.2, 110.2, 42.8, 21.0.

FTIR (NaCl, thin film, cm^{-1}): 3027, 2967, 2872, 2225, 1646, 1604, 1504, 1493, 1452, 1412, 1176, 1013, 970, 866, 819, 763, 701.

HRMS (FAB, *m/z*): calc'd for $C_{17}H_{15}N$ $[M+H]^+$: 234.1283; found: 234.1265.

Methyl (*S*,*E*)-4-(3-phenylbut-1-en-1-yl)benzoate (184)

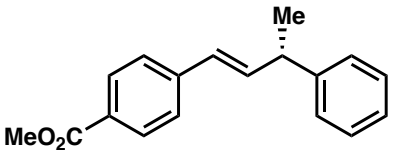

Prepared from methyl (*E*)-4-(2-bromovinyl)benzoate (48 mg, 0.2 mmol) and 1,3-dioxoisoindolin-2-yl 2-phenylpropanoate (59 mg, 0.2 mmol) according to General Procedure 3. The crude residue was purified by column chromatography (silica gel, 5% Et_2O/hexane) to yield **184** (46 mg, 87% yield) in 95% ee as a colorless oil.

R_f = 0.19 (silica gel, 5% Et_2O/hexane, UV).

Chiral SFC: (OB-H, 2.5 mL/min, 20% IPA in CO_2, λ = 254 nm): t_R (minor) = 8.2 min, t_R (major) = 11.6 min.

$[\alpha]_D^{25}$ = –44° (c = 1.0, $CHCl_3$).

^{1}H NMR (400 MHz, $CDCl_3$): δ 7.96 (d, *J* = 8.4 Hz, 2H), 7.41 (d, *J* = 8.3 Hz, 2H), 7.37 – 7.30 (m, 2H), 7.30 – 7.20 (m, 3H), 6.53 (dd, *J* = 15.9, 6.5 Hz, 1H), 6.44 (d, *J* = 16.1 Hz, 1H), 3.91 (s, 3H), 3.72 – 3.62 (m, 1H), 1.49 (d, *J* = 7.0 Hz, 3H).

^{13}C NMR (101 MHz, $CDCl_3$): δ 167.1, 145.2, 142.2, 138.2, 130.0, 128.7, 128.6, 127.9, 127.4, 126.5, 126.1, 52.2, 42.8, 21.2.

FTIR (NaCl, thin film, cm^{-1}): 3025, 2963, 1718, 1605, 1492, 1433, 1411, 1276, 1177, 1108, 1015, 968, 759, 698.

LRMS (GC-MS, *m/z*): calc'd for $C_{18}H_{18}O_2$ $[M]^+$: 266.1; found: 266.1.

(*S*,*E*)-4-(3-phenylbut-1-en-1-yl)phenyl 4-methylbenzenesulfonate (185)

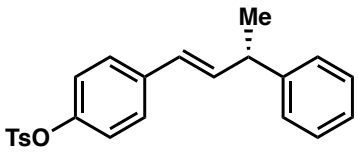

Prepared from (*E*)-4-(2-bromovinyl)phenyl 4-methylbenzenesulfonate (71 mg, 0.2 mmol) and 1,3-dioxoisoindolin-2-yl 2-phenylpropanoate (89 mg, 0.3 mmol) according to General Procedure 3 with the exception that 1.5 equiv NHP ester was used instead of 1.0 equiv. *Note: The addition of excess NHP ester ensured full consumption of the vinyl bromide, which we found to be inseparable from the product when it remained in the crude reaction.* The crude residue was purified by column chromatography (silica gel, hexane to 5% Et_2O/hexane) to yield **185** (61 mg, 80% yield) in 94% ee as a colorless oil.

R_f = 0.39 (silica gel, 10% EtOAc/hexane, UV).

Chiral SFC: (OJ-H, 2.5 mL/min, 15% IPA in CO_2, λ = 254 nm): t_R (minor) = 12.2 min,

t_R (major) = 13.7 min.

$[\alpha]_D^{25}$ = –24° (c = 1.0, $CHCl_3$).

^{1}H NMR (400 MHz, $CDCl_3$): δ 7.70 (d, *J* = 8.4 Hz, 2H), 7.36 – 7.28 (m, 4H), 7.28 – 7.20 (m, 5H), 6.90 (d, *J* = 8.7 Hz, 2H), 6.39 – 6.30 (m, 2H), 3.69 – 3.58 (m, 1H), 2.45 (s, 3H), 1.46 (d, *J* = 7.0 Hz, 3H).

^{13}C NMR (101 MHz, $CDCl_3$): δ 148.5, 145.4, 145.3, 136.7, 136.5, 132.4, 129.8, 128.6, 127.3, 127.2, 126.4, 122.5, 42.7, 21.8, 21.2.

FTIR (NaCl, thin film, cm^{-1}): 3061, 3028, 2966, 2928, 2872, 1647, 1599, 1504, 1453, 1372, 1307, 1296, 1198, 1176, 1152, 1093, 1016, 969, 867, 841, 815, 763, 735, 700, 661.

HRMS (FAB, *m/z*): calc'd for $C_{23}H_{22}O_3S$ $[M+\cdot]^+$: 378.1290; found: 378.1283.

(*S*,*E*)-but-1-ene-1,3-diyldibenzene (186)

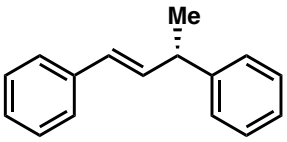

Prepared from (*E*)-(2-bromovinyl)benzene (37 mg, 0.2 mmol) and 1,3-dioxoisoindolin-2-yl 2-phenylpropanoate (59 mg, 0.2 mmol) according to General Procedure 3. The crude residue was purified by column chromatography (silica gel, hexane) to yield **186** (37 mg, 88% yield) in 96% ee as a colorless oil.

R_f = 0.48 (silica gel, hexane, UV).

Chiral SFC: (OJ-H, 2.5 mL/min, 5% IPA in CO_2, λ = 254 nm): t_R (minor) = 9.8 min, t_R (major) = 10.9 min.

$[\alpha]_D^{25}$ = –35° (c = 1.0, $CHCl_3$).

^{1}H NMR (400 MHz, $CDCl_3$): δ 7.43 – 7.29 (m, 8H), 7.29 – 7.21 (m, 2H), 6.51 – 6.38 (m, 2H), 3.73 – 3.65 (m, 1H), 1.52 (d, *J* = 7.0 Hz, 3H).

^{13}C NMR (101 MHz, $CDCl_3$): δ 145.7, 137.7, 135.3, 128.6 (3C), 127.4, 127.2, 126.35, 126.27, 42.7, 21.4.

FTIR (NaCl, thin film, cm^{-1}): 3080, 3058, 3024, 2964, 2928, 2871, 1599, 1492, 1448, 1371, 1010, 964, 742, 692.

HRMS (ESI-TOF, *m/z*): calc'd for $C_{16}H_{16}$ $[M–H_2+H]^+$: 207.1174; found: 207.1155.

(*S*,*E*)-2-methoxy-5-(3-phenylbut-1-en-1-yl)pyridine (187)

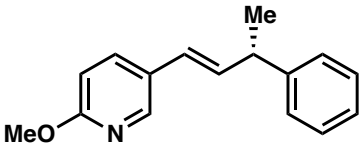

Prepared from (*E*)-5-(2-bromovinyl)-2-methoxypyridine (43 mg, 0.2 mmol) and 1,3-dioxoisoindolin-2-yl 2-phenylpropanoate (59 mg, 0.2 mmol) according to General Procedure 3. The crude residue was purified by column chromatography (silica gel, 5% Et_2O/hexane) to yield **187** (32 mg, 67% yield) in 95% ee as a colorless oil.

R_f = 0.53 (silica gel, 10% EtOAc/hexane, UV).

Chiral SFC: (OB-H, 2.5 mL/min, 15% IPA in CO_2, λ = 280 nm): t_R (major) = 5.0 min, t_R (minor) = 6.9 min.

$[\alpha]_D^{25}$ = –33° (c = 1.0, $CHCl_3$).

^{1}H NMR (400 MHz, $CDCl_3$): δ 8.06 (d, *J* = 2.4 Hz, 1H), 7.62 (dd, *J* = 8.7, 2.5 Hz, 1H), 7.35 – 7.28 (m, 2H), 7.28 – 7.18 (m, 3H), 6.67 (d, *J* = 8.6 Hz, 1H), 6.33 (d, *J* = 16.1 Hz, 1H), 6.26 (dd, *J* = 15.9, 6.3 Hz, 1H), 3.91 (s, 3H), 3.66 – 3.57 (m, 1H), 1.45 (d, *J* = 7.0 Hz, 3H).

^{13}C NMR (101 MHz, $CDCl_3$): δ 163.4, 145.6, 145.3, 135.5, 134.7, 128.7, 127.4, 126.8, 126.4, 124.7, 110.9, 53.6, 42.8, 21.3.

FTIR (NaCl, thin film, cm^{-1}): 2965, 1601, 1493, 1384, 1286, 1026, 962, 822, 762, 699.

HRMS (FAB, *m/z*): calc'd for $C_{16}H_{17}NO$ $[M+H]^+$: 240.1388; found: 240.1398.

(*S*,*E*)-5-phenylhex-3-en-1-yl benzoate (188)

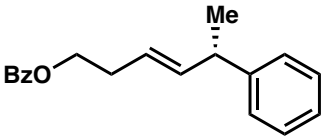

Prepared from (*E*)-4-bromobut-3-en-1-yl benzoate (51 mg, 0.2 mmol) and 1,3-dioxoisoindolin-2-yl 2-phenylpropanoate (59 mg, 0.2 mmol) according to General Procedure 3. The crude residue was purified by column chromatography (silica gel, 5% Et_2O/hexane) to yield **188** (49 mg, 88% yield) in 97% ee as a colorless oil. Spectral data matched those reported in literature.

R_f = 0.24 (silica gel, 5% Et_2O/hexane, UV).

Chiral SFC: (OJ-H, 2.5 mL/min, 10% IPA in CO_2, λ = 254 nm): t_R (major) = 5.2 min, t_R (minor) = 6.1 min.

$[\alpha]_D^{25}$ = +5° (c =1.0, $CHCl_3$).

^{1}H NMR (400 MHz, $CDCl_3$): δ 8.04 – 8.00 (m, 2H), 7.59 – 7.53 (m, 1H), 7.46 – 7.40 (m, 2H), 7.29 – 7.23 (m, 2H), 7.22 – 7.15 (m, 3H), 5.77 (ddt, *J* = 15.4, 6.8, 1.3 Hz, 1H), 5.52 (dtd, *J* = 15.2, 6.8, 1.3 Hz, 1H), 4.36 (td, *J* = 6.7, 1.4 Hz, 2H), 3.50 – 3.42 (m, 1H), 2.54 – 2.46 (m, 2H), 1.35 (d, *J* = 7.0 Hz, 3H).

^{13}C NMR (101 MHz, $CDCl_3$): δ 166.7, 146.0, 138.3, 133.0, 130.5, 129.7, 128.5, 128.4, 127.3, 126.2, 124.3, 64.4, 42.4, 32.2, 21.4.

(*S*,*E*)-(7-chlorohept-3-en-2-yl)benzene (189)

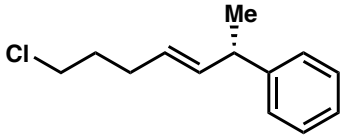

Prepared from (*E*)-1-bromo-5-chloropent-1-ene (37 mg, 0.2 mmol) and 1,3-dioxoisoindolin-2-yl 2-phenylpropanoate (59 mg, 0.2 mmol) according to General Procedure 3. The crude residue was purified by column chromatography (silica gel, hexane) to yield **189** (29 mg, 69% yield) in 91% ee as a colorless oil.

R_f = 0.29 (silica gel, hexane, UV/CAM).

Chiral SFC: (OD-H, 2.5 mL/min, 1% IPA in CO_2, λ = 210 nm): t_R (minor) = 5.4 min, t_R (major) = 6.0 min.

$[\alpha]_D^{25}$ = +9° (c =1.0, $CHCl_3$).

^{1}H NMR (400 MHz, $CDCl_3$): δ 7.35 – 7.29 (m, 2H), 7.25 – 7.18 (m, 3H), 5.69 (ddt, *J* = 15.3, 6.8, 1.4 Hz, 1H), 5.43 (dtd, *J* = 15.1, 6.8, 1.1 Hz, 1H), 3.54 (t, *J* = 6.7 Hz, 2H), 3.50 – 3.40 (m, 1H), 2.23 – 2.16 (m, 2H), 1.90 – 1.82 (m, 2H), 1.36 (d, *J* = 7.0 Hz, 3H).

^{13}C NMR (101 MHz, $CDCl_3$): δ 146.3, 136.7, 128.5, 127.24, 127.17, 126.1, 44.6, 42.4, 32.4, 29.7, 21.6.

FTIR (NaCl, thin film, cm^{-1}): 3025, 2962, 2929, 2871, 1601, 1492, 1450, 1371, 1297, 1017, 969, 759, 698.

HRMS (FAB, *m/z*): calc'd for $C_{13}H_{17}Cl$ $[M–H_2+H]^+$: 207.0940; found: 207.0910.

(*S*,*E*)-dec-3-en-2-ylbenzene (190)

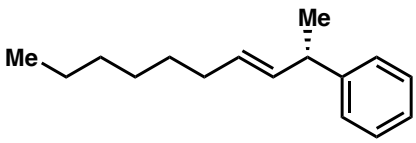

Prepared from (*E*)-1-bromooct-1-ene (38 mg, 0.2 mmol) and 1,3-dioxoisoindolin-2-yl 2-phenylpropanoate (59 mg, 0.2 mmol) according to

General Procedure 3. The crude residue was purified by column chromatography (silica gel, hexane) to yield **190** (31 mg, 72% yield) in 94% ee as a colorless oil.

R_f = 0.59 (silica gel, hexane, UV/CAM).

Chiral SFC: (OJ-H, 2.5 mL/min, 1% IPA in CO_2, λ = 210 nm): t_R (minor) = 3.9 min, t_R (major) = 4.5 min.

$[\alpha]_D^{25}$ = +4° (c = 0.9, $CHCl_3$).

^{1}H NMR (400 MHz, $CDCl_3$): δ 7.34 – 7.27 (m, 2H), 7.25 – 7.15 (m, 3H), 5.60 (ddt, *J* = 15.3, 6.6, 1.4 Hz, 1H), 5.46 (dtd, *J* = 15.1, 6.6, 1.2 Hz, 1H), 3.47 – 3.38 (m, 1H), 2.06 – 1.97 (m, 2H), 1.40 – 1.22 (m, 11H), 0.95 – 0.83 (m, 3H).

^{13}C NMR (101 MHz, $CDCl_3$): δ 146.7, 135.0, 129.5, 128.4, 127.3, 126.0, 42.4, 32.7, 31.9, 29.6, 29.0, 22.8, 21.7, 14.3.

FTIR (NaCl, thin film, cm^{-1}): 3025, 2959, 2925, 2854, 1492, 1451, 1371, 1016, 965, 758, 697.

LRMS (GC-MS, *m/z*): calc'd for $C_{16}H_{24}$ $[M]^+$: 216.2; found: 216.2.

(*S*,*E*)-trimethyl((5-phenylhex-3-en-1-yl)oxy)silane (191)

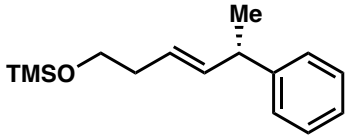

Prepared from (*E*)-4-bromobut-3-en-1-ol (30 mg, 0.2 mmol) and 1,3-dioxoisoindolin-2-yl 2-phenylpropanoate (59 mg, 0.2 mmol) according to General Procedure 3 with the exception that 2.0 equiv TMSBr was used instead of 1.0 equiv. The reaction was quenched with water instead of 1 M HCl to prevent decomposition of the primary silyl ether. *Note: An acidic workup yielded a mixture of the silyl ether and alcohol product, however the alcohol was inseparable from the phthalimide byproduct.* The crude residue was purified by column chromatography (florisil, hexane to 1% Et_2O/hexane) to yield **191** (33 mg, 66% yield) as a colorless oil. *Note: The two enantiomers of the racemic silyl ether were inseparable by chiral SFC.*

R_f = 0.67 (silica gel, 10% EtOAc/hexane, UV/CAM).

$[\alpha]_D^{25}$ = +6° (c = 1.0, $CHCl_3$).

^{1}H NMR (400 MHz, $CDCl_3$): δ 7.35 – 7.28 (m, 2H), 7.25 – 7.17 (m, 3H), 5.69 (ddt, *J* = 15.4, 6.7, 1.3 Hz, 1H), 5.47 (dtd, *J* = 15.3, 6.9, 1.4 Hz, 1H), 3.61 (t, *J* = 7.0 Hz, 2H), 3.49 – 3.40 (m, 1H), 2.28 (qt, *J* = 7.0, 1.1 Hz, 2H), 1.36 (d, *J* = 7.1 Hz, 3H), 0.13 (s, 9H).

^{13}C NMR (101 MHz, $CDCl_3$): δ 146.3, 137.3, 128.5, 127.3, 126.1, 125.4, 62.7, 42.5, 36.2, 21.5, -0.3.

FTIR (NaCl, thin film, cm^{-1}): 2961, 2930, 2902, 2863, 1602, 1493, 1452, 1382, 1251, 1094, 968, 940, 876, 841, 758, 748, 699.

HRMS (FAB, *m/z*): calc'd for $C_{15}H_{24}OSi$ $[M+H]^+$: 249.1675; found: 249.1684.

(*S*,*E*)-5-phenylhex-3-en-1-ol (276)

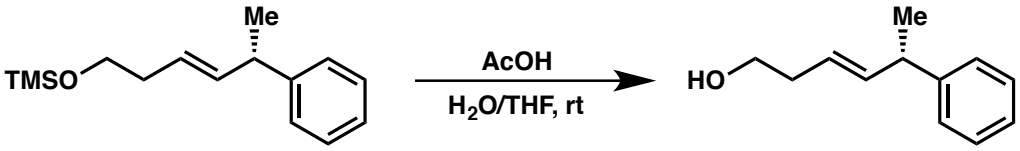

Deprotection of Silyl Ether: Silyl ether **191** (33.0 mg, 0.132 mmol, 1 equiv) was dissolved in a solution of acetic acid (0.5 mL), water (0.5 mL), and THF (2.5 mL) in a 20 mL vial equipped with a magnetic stir bar and stirred at room temperature for 15 min. The reaction was slowly quenched with a solution of saturated $NaHCO_3$ until the pH was slightly basic (approx. 15 mL), extracted with Et_2O (3 x 10 mL), dried with $MgSO_4$, filtered, and concentrated under reduced pressure to yield **276** (22.6 mg, 97% yield) in 89% ee as a colorless oil. Spectral data matched those reported in literature.

R_f = 0.11 (silica gel, 10% EtOAc/hexane, UV/CAM).

Chiral SFC: (OB-H, 2.5 mL/min, 3% IPA in CO_2, λ = 210 nm): t_R (minor) = 6.9 min, t_R (major) = 7.5 min.

$[\alpha]_D^{25}$ = +9° (c = 1.0, $CHCl_3$).

^{1}H NMR (400 MHz, $CDCl_3$): δ 7.34 – 7.27 (m, 2H), 7.25 – 7.16 (m, 3H), 5.76 (ddt, *J* = 15.4, 6.7, 1.4 Hz, 1H), 5.45 (dtd, *J* = 15.3, 7.0, 1.4 Hz, 1H), 3.65 (t, *J* = 6.3 Hz, 2H), 3.52 – 3.42 (m, 1H), 2.30 (q, *J* = 6.3 Hz, 2H), 1.54 (s, 1H), 1.37 (d, *J* = 7.1 Hz, 3H).

^{13}C NMR (101 MHz, $CDCl_3$): δ 146.1, 138.8, 128.6, 127.2, 126.2, 124.8, 62.2, 42.5, 36.0, 21.6.

(*S*,*E*)-6-methyl-2-(3-phenylbut-1-en-1-yl)-1,3,6,2-dioxazaborocane-4,8-dione (192)

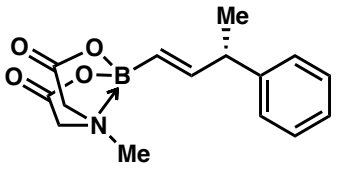

Prepared from *trans*-1-bromovinylboronic acid MIDA ester (52 mg, 0.2 mmol) and 1,3-dioxoisoindolin-2-yl 2-phenylpropanoate (59 mg, 0.2 mmol) according to General Procedure 3. The crude residue was purified by column chromatography (silica gel, 10% EtOAc/hexane to 100% EtOAc) to yield **192** (25 mg, 43% yield) in 97% ee as a yellow solid. *Note: The ^{1}H NMR contains two minor impurities that were identified as DMA and methyliminodiacetic acid.*

R_f = 0.35 (silica gel, EtOAc, UV/$KMnO_4$).

m.p. = 144–146 °C

Chiral SFC: (OJ-H, 2.5 mL/min, 30% IPA in CO_2, λ = 210 nm): t_R (major) = 5.5 min, t_R (minor) = 10.2 min.

$[\alpha]_D^{25}$ = +0.5° ± 1.1° (c = 1.0, $CHCl_3$). *Note*: *This compound shows low optical rotation*.

^{1}H NMR (400 MHz, $CDCl_3$): δ 7.32 – 7.23 (m, 2H), 7.21 – 7.13 (m, 3H), 6.32 (dd, *J* = 17.7, 6.4 Hz, 1H), 5.38 (dd, *J* = 17.7, 1.5 Hz, 1H), 3.92 (dd, *J* = 16.7, 4.5 Hz, 2H), 3.59 (dd, *J* = 16.8, 13.9 Hz, 2H), 3.54 – 3.46 (m, 1H), 2.69 (s, 3H), 1.36 (d, *J* = 7.0 Hz, 3H).

^{13}C NMR (101 MHz, $CDCl_3$): δ 168.34, 168.27, 151.7, 145.3, 128.6, 127.4, 126.3, 61.53, 61.49, 47.0, 44.8, 20.8.

FTIR (NaCl, thin film, cm^{-1}): 2963, 1762, 1636, 1492, 1338, 1290, 1246, 1193, 1154, 1126, 1090, 1025, 1007, 956, 867, 761, 702.

HRMS (FAB, *m/z*): calc'd for $C_{15}H_{18}BNO_4$ $[M+H]^+$: 288.1407; found: 288.1414.

(*S*,*E*)-trimethyl(3-phenylbut-1-en-1-yl)silane (193)

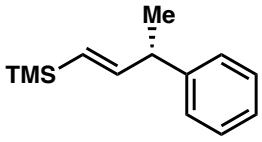

Prepared from (*E*)-(2-bromovinyl)trimethylsilane (36 mg, 0.2 mmol) and 1,3-dioxoisoindolin-2-yl 2-phenylpropanoate (59 mg, 0.2 mmol) according to General Procedure 3. Alkenyl bromide **206** is reported to be air sensitive, and was added to the reaction while inside the glovebox. The crude residue was purified by column chromatography (silica gel, hexane) to yield **193** (28 mg, 68% yield) in 97% ee as a colorless oil.

R_f = 0.65 (silica gel, hexane, UV/CAM).

Chiral SFC: (OJ-H, 2.5 mL/min, CO_2, λ = 210 nm): t_R (major) = 1.8 min, t_R (minor) = 2.0 min.

$[\alpha]_D^{25}$ = –2.4° ± 0.2° (c = 0.9, $CHCl_3$).

^{1}H NMR (400 MHz, $CDCl_3$): δ 7.35 – 7.28 (m, 2H), 7.24 – 7.18 (m, 3H), 6.19 (dd, *J* = 18.6, 5.9 Hz, 1H), 5.68 (dd, *J* = 18.6, 1.6 Hz, 1H), 3.52 – 3.44 (m, 1H), 1.36 (d, *J* = 7.0 Hz, 3H), 0.06 (s, 9H).

^{13}C NMR (101 MHz, $CDCl_3$): δ 150.8, 145.8, 128.5, 128.1, 127.5, 126.2, 45.6, 20.9, -1.0.

FTIR (NaCl, thin film, cm^{-1}): 3028, 2958, 1612, 1602, 1492, 1452, 1248, 1009, 987, 868, 837, 759, 698.

LRMS (GC-MS, *m/z*): calc'd for $C_{13}H_{20}Si$ $[M]^+$: 204.1; found: 204.1.

(*S*,*E*)-4,4'-(but-1-ene-1,3-diyl)bis(methoxybenzene) (194)

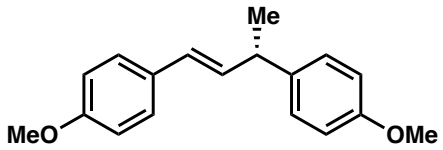

Prepared from (*E*)-1-(2-bromovinyl)-4-methoxybenzene (43 mg, 0.2 mmol) and 1,3-dioxoisoindolin-2-yl 2-(4-methoxyphenyl)-propanoate (65 mg, 0.2 mmol) according to General Procedure 3. The crude residue was purified by column chromatography (silica gel, 10% toluene/hexane then 10% Et_2O/hexane) to yield **194** (42 mg, 78% yield) in 93% ee as a white solid. Spectral data matched those reported in literature.

R_f = 0.45 (silica gel, 10% EtOAc/hexane, UV).

m.p. = 51–59 °C

Chiral SFC: (AD-H, 2.5 mL/min, 20% IPA in CO_2, λ = 235 nm): t_R (major) = 7.0 min, t_R (minor) = 8.5 min.

$[\alpha]_D^{25}$ = –34° (c = 1.0, $CHCl_3$).

^{1}H NMR (400 MHz, $CDCl_3$): δ 7.32 (d, *J* = 8.7 Hz, 2H), 7.22 (d, *J* = 8.5 Hz, 2H), 6.89 (d, *J* = 8.8 Hz, 2H), 6.86 (d, *J* = 8.8 Hz, 2H), 6.37 (d, *J* = 16.0 Hz, 1H), 6.25 (dd, *J* = 15.9, 6.6 Hz, 1H), 3.82 (s, 3H), 3.81 (s, 3H), 3.65 – 3.55 (m, 1H), 1.46 (d, *J* = 7.0 Hz, 3H).

^{13}C NMR (101 MHz, $CDCl_3$): δ 158.9, 158.0, 138.1, 133.6, 130.5, 128.3, 127.7, 127.3, 114.0, 113.9, 55.4 (2C), 41.8, 21.6.

(*S*,*E*)-1-methoxy-4-(3-(4-(trifluoromethyl)phenyl)but-1-en-1-yl)benzene (195)

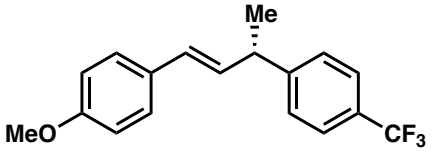

Prepared from (*E*)-1-(2-bromovinyl)-4-methoxybenzene (43 mg, 0.2 mmol) and 1,3-dioxoisoindolin-2-yl 2-(4-(trifluoromethyl)-phenyl)propanoate (73 mg, 0.2 mmol) according to General Procedure 3. The crude residue was purified by column chromatography (silica gel, 5% toluene/hexane) to yield **195** (40 mg, 65% yield) in 88% ee as a white solid.

R_f = 0.48 (silica gel, 10% EtOAc/hexane, UV).

m.p. = 67–70 °C

Chiral SFC: (OB-H, 2.5 mL/min, 5% IPA in CO_2, λ = 254 nm): t_R (major) = 6.5 min, t_R (minor) = 7.5 min.

$[\alpha]_D^{25}$ = –39° (c = 1.0, $CHCl_3$).

^{1}H NMR (400 MHz, $CDCl_3$): δ 7.58 (d, *J* = 8.1 Hz, 2H), 7.39 (d, *J* = 8.4 Hz, 2H), 7.30 (d, *J* = 8.7 Hz, 2H), 6.85 (d, *J* = 8.8 Hz, 2H), 6.38 (d, *J* = 16.0 Hz, 1H), 6.21 (dd, *J* = 15.9, 6.8 Hz, 1H), 3.81 (s, 3H), 3.73 – 3.64 (m, 1H), 1.48 (d, *J* = 7.0 Hz, 3H).

^{13}C NMR (101 MHz, $CDCl_3$): δ 159.1, 150.1 (q, $J_{C\text{-}F}$ = 1.4 Hz), 132.0, 130.1, 128.8, 128.6 (q, $J_{C\text{-}F}$ = 32.3 Hz), 127.8, 127.4, 125.5 (q, $J_{C\text{-}F}$ = 3.8 Hz), 124.5 (q, $J_{C\text{-}F}$ = 271.9 Hz), 114.1, 55.4, 42.6, 21.3.

^{19}F NMR (282 MHz, $CDCl_3$): δ –65.4.

FTIR (NaCl, thin film, cm^{-1}): 2965, 1608, 1512, 1252, 1174, 1164, 1122, 1069, 1036, 1016, 967, 840, 818.

HRMS (EI, *m/z*): calc'd for $C_{18}H_{17}F_3O$ $[M+\cdot]^+$: 306.1232; found: 306.1241.

(*S*,*E*)-1-bromo-4-(4-(4-methoxyphenyl)but-3-en-2-yl)benzene (196)

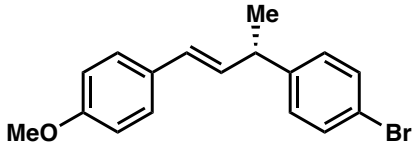

Prepared from (*E*)-1-(2-bromovinyl)-4-methoxybenzene (43 mg, 0.2 mmol) and 1,3-dioxoisoindolin-2-yl 2-(4-bromophenyl)-propanoate (75 mg, 0.2 mmol) according to General Procedure 3. The crude residue was purified by column chromatography (silica gel, 5 to 10% toluene/hexane) to yield **196** (51 mg, 80% yield) in 90% ee as a white solid. Spectral data matched those reported in literature.

R_f = 0.59 (silica gel, 10% EtOAc/hexane, UV).

m.p. = 74–76 °C

Chiral SFC: (OB-H, 2.5 mL/min, 35% IPA in CO_2, λ = 254 nm): t_R (major) = 5.3 min, t_R (minor) = 8.5 min.

$[\alpha]_D^{25}$ = –32° (c = 1.0, $CHCl_3$).

^{1}H NMR (400 MHz, $CDCl_3$): δ 7.45 (d, *J* = 8.5 Hz, 2H), 7.30 (d, *J* = 8.6 Hz, 2H), 7.16 (d, *J* = 8.3 Hz, 2H), 6.86 (d, *J* = 8.8 Hz, 2H), 6.36 (d, *J* = 16.0 Hz, 1H), 6.20 (dd, *J* = 15.9, 6.7 Hz, 1H), 3.81 (s, 3H), 3.64 – 3.55 (m, 1H), 1.45 (d, *J* = 7.0 Hz, 3H).

^{13}C NMR (101 MHz, $CDCl_3$): δ 159.0, 145.0, 132.5, 131.6, 130.2, 129.2, 128.4, 127.4, 120.0, 114.0, 55.4, 42.1, 21.3.

(*S*,*E*)-1-fluoro-4-(4-(4-methoxyphenyl)but-3-en-2-yl)benzene (197)

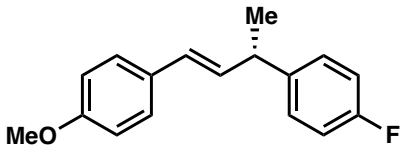

Prepared from (*E*)-1-(2-bromovinyl)-4-methoxybenzene (43 mg, 0.2 mmol) and 1,3-dioxoisoindolin-2-yl 2-(4-fluorophenyl)-propanoate (63 mg, 0.2 mmol) according to General Procedure 3. The crude residue was purified by column chromatography (silica gel, 5 to 30% toluene/hexane) to yield **197** (44 mg, 85% yield) in 92% ee as a colorless oil. Spectral data matched those reported in literature.

R_f = 0.70 (silica gel, 10% EtOAc/hexane, UV).

Chiral SFC: (OB-H, 2.5 mL/min, 15% IPA in CO_2, λ = 280 nm): t_R (major) = 5.9 min, t_R (minor) = 8.3 min.

$[\alpha]_D^{25}$ = –29° (c = 1.0, $CHCl_3$).

^{1}H NMR (400 MHz, $CDCl_3$): δ 7.34 – 7.28 (m, 2H), 7.28 – 7.20 (m, 2H), 7.06 – 6.98 (m, 2H), 6.89 – 6.83 (m, 2H), 6.40 – 6.32 (m, 1H), 6.23 (dd, *J* = 15.9, 6.7 Hz, 1H), 3.81 (s, 3H), 3.67 – 3.58 (m, 1H), 1.46 (d, *J* = 7.0 Hz, 3H).

^{13}C NMR (101 MHz, $CDCl_3$): δ 161.5 (d, $J_{C\text{-}F}$ = 243.7 Hz), 159.0, 141.6 (d, $J_{C\text{-}F}$ = 3.1 Hz), 133.0, 130.3, 128.8 (d, $J_{C\text{-}F}$ = 7.8 Hz), 128.1, 127.4, 115.3 (d, $J_{C\text{-}F}$ = 21.2 Hz), 114.1, 55.4, 41.9, 21.6.

^{19}F NMR (282 MHz, $CDCl_3$): δ -123.56 (tt, $J_{F\text{-}H}$ = 8.9, 5.4 Hz).

(*S*,*E*)-4-(4-(4-methoxyphenyl)but-3-en-2-yl)-*N*,*N*-dimethylaniline (198)

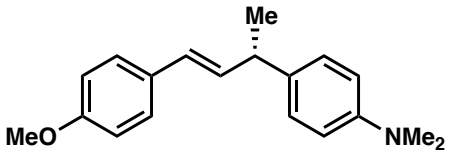

Prepared from (*E*)-1-(2-bromovinyl)-4-methoxybenzene (43 mg, 0.2 mmol) and 1,3-dioxoisoindolin-2-yl 2-(4-(dimethyl-amino)phenyl)propanoate (68 mg, 0.2 mmol) according to General Procedure 3. The reaction was quenched with water instead of 1 M HCl. The crude residue was purified by column chromatography (silica gel, hexane to 10% Et_2O/hexane) to yield **198** (37 mg, 66% yield) in 94% ee as a white solid.

R_f = 0.28 (silica gel, 10% EtOAc/hexane, UV).

m.p. = 72–75 °C

Chiral SFC: (AD-H, 2.5 mL/min, 20% IPA in CO_2, λ = 280 nm): t_R (major) = 8.2 min, t_R (minor) = 10.6 min.

$[\alpha]_D^{25}$ = –29° (c = 1.1, $CHCl_3$).

^{1}H NMR (400 MHz, $CDCl_3$): δ 7.29 (d, *J* = 8.7 Hz, 2H), 7.15 (d, *J* = 8.5 Hz, 2H), 6.83 (d, *J* = 8.8 Hz, 2H), 6.73 (d, *J* = 8.7 Hz, 2H), 6.34 (dd, *J* = 16.2, 0.8 Hz, 1H), 6.23 (dd, *J* = 15.9, 6.6 Hz, 1H), 3.80 (s, 3H), 3.58 – 3.50 (m, 1H), 2.93 (s, 6H), 1.42 (d, *J* = 7.1 Hz, 3H).

^{13}C NMR (101 MHz, $CDCl_3$): δ 158.8, 149.3, 134.1, 130.7, 128.0, 127.3, 114.0, 113.1, 55.4, 41.6, 41.0, 21.5.

FTIR (NaCl, thin film, cm^{-1}): 2958, 1608, 1518, 1509, 1456, 1341, 1249, 1173, 1034, 966, 948, 815.

HRMS (FAB, *m/z*): calc'd for $C_{19}H_{23}NO$ $[M+\cdot]^+$: 281.1780; found: 281.1774.

(*S*,*E*)-1,2-dichloro-4-(4-(4-methoxyphenyl)but-3-en-2-yl)benzene (199)

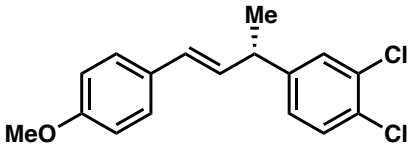

Prepared from (*E*)-1-(2-bromovinyl)-4-methoxybenzene (43 mg, 0.2 mmol) and 1,3-dioxoisoindolin-2-yl 2-(3,4-dichlorophenyl)-propanoate (73 mg, 0.2 mmol) according to General Procedure 3. The crude residue was purified by column chromatography (silica gel, hexane to 5% Et_2O/hexane) to yield **199** (48 mg, 77% yield) in 82% ee as a colorless oil.

R_f = 0.51 (silica gel, 10% EtOAc/hexane, UV).

Chiral SFC: (OB-H, 2.5 mL/min, 25% IPA in CO_2, λ = 280 nm): t_R (major) = 6.5 min, t_R (minor) = 9.0 min.

$[\alpha]_D^{25}$ = –26° (c = 1.1, $CHCl_3$).

^{1}H NMR (400 MHz, $CDCl_3$): δ 7.37 (d, *J* = 8.3 Hz, 1H), 7.35 (d, *J* = 2.1 Hz, 1H), 7.32 – 7.27 (m, 2H), 7.10 (ddd, *J* = 8.2, 2.1, 0.6 Hz, 1H), 6.87 – 6.82 (m, 2H), 6.35 (dd, *J* = 15.9, 1.3 Hz, 1H), 6.15 (dd, *J* = 15.9, 6.8 Hz, 1H), 3.81 (s, 3H), 3.62 – 3.53 (m, 1H), 1.43 (d, *J* = 7.0 Hz, 3H).

^{13}C NMR (101 MHz, $CDCl_3$): δ 159.2, 146.3, 132.4, 131.7, 130.5, 130.1, 130.0, 129.4, 128.9, 127.4, 127.0, 114.1, 55.4, 41.9, 21.2.

FTIR (NaCl, thin film, cm^{-1}): 2964, 1607, 1511, 1466, 1299, 1250, 1174, 1106, 1030, 967, 815.

HRMS (FAB, *m/z*): calc'd for $C_{17}H_{16}Cl_2O$ $[M+\cdot]^+$: 306.0578; found: 306.0582.

(*S*,*E*)-1-methoxy-4-(3-phenylpent-1-en-1-yl)benzene (200)

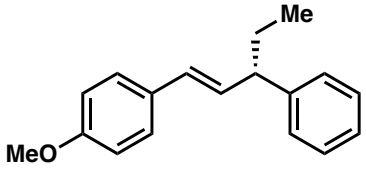

Prepared from (*E*)-1-(2-bromovinyl)-4-methoxybenzene (43 mg, 0.2 mmol) and 1,3-dioxoisoindolin-2-yl 2-phenylbutanoate (62 mg, 0.2 mmol) according to General Procedure 3. The crude residue was purified by column chromatography (silica gel, 10 to 20% toluene/hexane) to yield **200** (40 mg, 80% yield) in 97% ee as a colorless oil. Spectral data matched those reported in literature.

R_f = 0.59 (silica gel, 10% EtOAc/hexane, UV).

Chiral SFC: (OB-H, 2.5 mL/min, 15% IPA in CO_2, λ = 254 nm): t_R (minor) = 8.0 min, t_R (major) = 9.9 min.

$[\alpha]_D^{25}$ = –46° (c = 1.0, $CHCl_3$).

^{1}H NMR (400 MHz, $CDCl_3$): δ 7.37 – 7.19 (m, 7H), 6.84 (d, *J* = 8.8 Hz, 2H), 6.37 (d, *J* = 15.8 Hz, 1H), 6.21 (dd, *J* = 15.8, 7.8 Hz, 1H), 3.80 (s, 3H), 3.35 – 3.26 (m, 1H), 1.90 – 1.78 (m, 2H), 0.93 (t, *J* = 7.4 Hz, 3H).

^{13}C NMR (101 MHz, $CDCl_3$): δ 158.9, 144.9, 132.2, 130.6, 128.9, 128.6, 127.8, 127.3, 126.2, 114.0, 55.4, 51.1, 29.0, 12.5.

(*S*,*E*)-(4-(4-methoxyphenyl)but-3-ene-1,2-diyl)dibenzene (201)

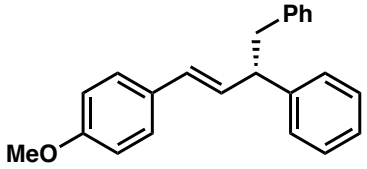

Prepared from (*E*)-1-(2-bromovinyl)-4-methoxybenzene (43 mg, 0.2 mmol) and 1,3-dioxoisoindolin-2-yl 2,3-diphenylpropanoate (74 mg, 0.2 mmol) according to General Procedure 3. The crude residue was purified by column chromatography (silica gel, 10% toluene/hexane then 10% Et_2O/hexane) to yield **201** (49 mg, 78% yield) in 95% ee as a white solid. Spectral data matched those reported in literature.

R_f = 0.48 (silica gel, 10% EtOAc/hexane, UV).

m.p. = 72–73 °C

Chiral SFC: (AS-H, 2.5 mL/min, 10% IPA in CO_2, λ = 254 nm): t_R (minor) = 6.0 min, t_R (major) = 6.5 min.

$[\alpha]_D^{25}$ = +19° (c = 1.0, $CHCl_3$).

^{1}H NMR (400 MHz, $CDCl_3$): δ 7.34 – 7.13 (m, 10H), 7.10 (d, *J* = 8.8 Hz, 2H), 6.83 (d, *J* = 8.8 Hz, 2H), 6.30 (dd, *J* = 15.9, 6.3 Hz, 1H), 6.25 (d, *J* = 15.9 Hz, 1H), 3.80 (s, 3H), 3.78 – 3.67 (m, 1H), 3.19 – 3.06 (m, 2H).

^{13}C NMR (101 MHz, $CDCl_3$): δ 158.9, 144.1, 140.2, 131.3, 130.4, 129.53, 129.49, 128.5, 128.2, 128.0, 127.4, 126.4, 126.0, 114.0, 55.4, 51.0, 42.9.

(*S*,*E*)-1-methoxy-4-(4-methyl-3-phenylpent-1-en-1-yl)benzene (202)

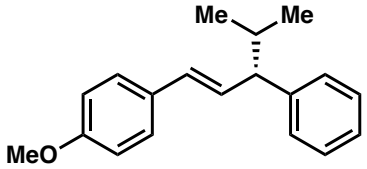

Prepared from (*E*)-1-(2-bromovinyl)-4-methoxybenzene (43 mg, 0.2 mmol) and 1,3-dioxoisoindolin-2-yl 3-methyl-2-phenylbutanoate (65 mg, 0.2 mmol) according to General Procedure 3. The crude residue was purified by column chromatography (silica gel, 10 to 20% toluene/hexane) to yield **202** (25 mg, 47% yield) in 97% ee as a white solid.

R_f = 0.58 (silica gel, 10% EtOAc/hexane, UV).

m.p. = 67–68 °C

Chiral SFC: (AS-H, 2.5 mL/min, 10% IPA in CO_2, λ = 254 nm): t_R (minor) = 4.8 min, t_R (major) = 6.1 min.

$[\alpha]_D^{25}$ = –39° (c = 1.0, $CHCl_3$).

^{1}H NMR (400 MHz, $CDCl_3$): δ 7.34 – 7.28 (m, 4H), 7.26 – 7.17 (m, 3H), 6.84 (d, *J* = 8.8 Hz, 2H), 6.36 (d, *J* = 15.7 Hz, 1H), 6.26 (dd, *J* = 15.7, 8.8 Hz, 1H), 3.80 (s, 3H), 3.04 (t, *J* = 8.8 Hz, 1H), 2.14 – 1.96 (m, 1H), 1.02 (d, *J* = 6.7 Hz, 3H), 0.82 (d, *J* = 6.6 Hz, 3H).

^{13}C NMR (101 MHz, $CDCl_3$): δ 158.9, 144.7, 131.2, 130.6, 129.8, 128.5, 128.1, 127.3, 126.1, 114.0, 57.8, 55.4, 33.4, 21.3, 21.1.

FTIR (NaCl, thin film, cm^{-1}): 2953, 1600, 1509, 1450, 1251, 1027, 966, 838, 701.

LRMS (GC-MS, *m/z*): calc'd for $C_{19}H_{22}O$ $[M]^+$: 266.2; found: 266.1.

(*S*,*E*)-*tert*-butyl((4-(4-methoxyphenyl)-2-phenylbut-3-en-1-yl)oxy)dimethylsilane (203)

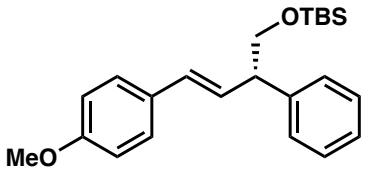

Prepared from (*E*)-1-(2-bromovinyl)-4-methoxybenzene (43 mg, 0.2 mmol) and 1,3-dioxoisoindolin-2-yl 3-((*tert*-butyldimethylsilyl)oxy)-2-phenylpropanoate (74 mg, 0.2 mmol) according to General Procedure 3. The crude residue was purified by column chromatography (silica gel, 10% toluene/hexane then 10% Et_2O/hexane) to yield **203** (43 mg, 58% yield) in 98% ee as a colorless oil.

R_f = 0.55 (silica gel, 10% EtOAc/hexane, UV).

Chiral SFC: (OJ-H, 2.5 mL/min, 10% IPA in CO_2, λ = 254 nm): t_R (major) = 3.4 min, t_R (minor) = 5.8 min.

$[\alpha]_D^{25}$ = –14° (c = 1.0, $CHCl_3$).

^{1}H NMR (400 MHz, $CDCl_3$): δ 7.39 – 7.29 (m, 6H), 7.28 – 7.23 (m, 1H), 6.87 (d, *J* = 8.8 Hz, 2H), 6.44 (d, *J* = 16.0 Hz, 1H), 6.34 (dd, *J* = 15.9, 7.2 Hz, 1H), 3.98 – 3.89 (m, 2H), 3.83 (s, 3H), 3.70 – 3.63 (m, 1H), 0.89 (s, 9H), 0.02 (s, 3H), 0.01 (s, 3H).

^{13}C NMR (101 MHz, $CDCl_3$): δ 159.0, 142.3, 130.7, 130.5, 128.8, 128.45, 128.42, 127.4, 126.6, 114.0, 67.5, 55.4, 51.8, 26.0, 18.4, -5.2, -5.3.

FTIR (NaCl, thin film, cm^{-1}): 2953, 2928, 2892, 2855, 1607, 1511, 1463, 1250, 1174, 1106, 1036, 836, 775, 699.

HRMS (FAB, *m/z*): calc'd for $C_{23}H_{32}O_2Si$ $[M–H_2+H]^+$: 367.2093; found: 367.2081.

(*S*,*E*)-1-methoxy-4-(3-phenylhexa-1,5-dien-1-yl)benzene (204)

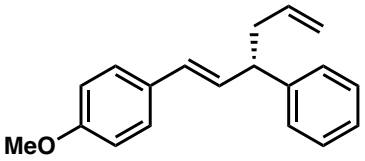

Prepared from (*E*)-1-(2-bromovinyl)-4-methoxybenzene (43 mg, 0.2 mmol) and 1,3-dioxoisoindolin-2-yl 2-phenylpent-4-enoate (53 mg, 0.2 mmol) according to General Procedure 3. The crude residue was purified by column chromatography (silica gel, 5 to 20% toluene/hexane) to yield **204** (42 mg, 79% yield) in 96% ee as a colorless oil.

R_f = 0.55 (silica gel, 10% EtOAc/hexane, UV).

Chiral SFC: (OJ-H, 2.5 mL/min, 10% IPA in CO_2, λ = 254 nm): t_R (minor) = 7.8 min, t_R (major) = 8.5 min.

$[\alpha]_D^{25}$ = –19° (c =1.0, $CHCl_3$).

^{1}H NMR (400 MHz, $CDCl_3$): δ 7.31 – 7.14 (m, 7H), 6.78 (d, *J* = 8.8 Hz, 2H), 6.30 (d, *J* = 15.9 Hz, 1H), 6.18 (dd, *J* = 15.8, 7.5 Hz, 1H), 5.73 (ddt, *J* = 17.1, 10.2, 6.9 Hz, 1H), 5.01 (ddt, *J* = 17.0, 2.0, 1.5 Hz, 1H), 4.95 (ddt, *J* = 10.2, 2.1, 1.0 Hz, 1H), 3.74 (s, 3H), 3.50 – 3.42 (m, 1H), 2.57 – 2.51 (m, 2H).

^{13}C NMR (101 MHz, $CDCl_3$): δ 159.0, 144.2, 136.8, 131.5, 130.4, 129.2, 128.6, 127.8, 127.4, 126.4, 116.4, 114.0, 55.4, 49.1, 40.4.

FTIR (NaCl, thin film, cm^{-1}): 3025, 2913, 2834, 1606, 1509, 1246, 1173, 1032, 963, 911, 756, 698.

HRMS (EI, *m/z*): calc'd for $C_{19}H_{20}O$ $[M+\cdot]^+$: 264.1514; found: 264.1521.

(*S*,*E*)-1-(6-chloro-3-phenylhex-1-en-1-yl)-4-methoxybenzene (205)

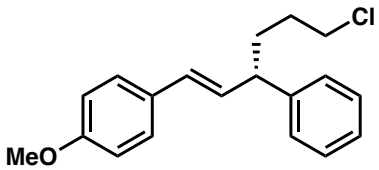

Prepared from (*E*)-1-(2-bromovinyl)-4-methoxybenzene (43 mg, 0.2 mmol) and 1,3-dioxoisoindolin-2-yl 5-chloro-2-phenylpentanoate (72 mg, 0.2 mmol) according to General Procedure 3. The crude residue was purified by column chromatography (silica gel, 5% Et_2O/hexane) to yield **205** (52 mg, 87% yield) in 93% ee as a colorless oil.

R_f = 0.53 (silica gel, 10% EtOAc/hexane, UV).

Chiral SFC: (AS-H, 2.5 mL/min, 15% IPA in CO_2, λ = 254 nm): t_R (minor) = 3.7 min, t_R

(major) = 4.7 min.

$[\alpha]_D^{25}$ = –21° (c = 1.0, $CHCl_3$).

^{1}H NMR (400 MHz, $CDCl_3$): δ 7.37 – 7.21 (m, 7H), 6.85 (d, *J* = 8.8 Hz, 2H), 6.38 (d, *J* = 15.8 Hz, 1H), 6.20 (dd, *J* = 15.8, 7.9 Hz, 1H), 3.81 (s, 3H), 3.56 (t, *J* = 6.5 Hz, 2H), 3.46 – 3.38 (m, 1H), 2.02 – 1.92 (m, 2H), 1.92 – 1.69 (m, 2H).

^{13}C NMR (101 MHz, $CDCl_3$): δ 159.0, 144.2, 131.5, 130.2, 129.2, 128.7, 127.7, 127.4, 126.5, 114.0, 55.4, 48.7, 45.2, 33.2, 30.8.

FTIR (NaCl, thin film, cm^{-1}): 2915, 1605, 1491, 1438, 1509, 1246, 1173, 1031, 964.

HRMS (FAB, *m/z*): calc'd for $C_{19}H_{21}ClO$ $[M+\cdot]^+$: 300.1281; found: 300.1274.

(*S*,*E*)-(3-methoxy-3-phenylprop-1-en-1-yl)trimethylsilane (208)

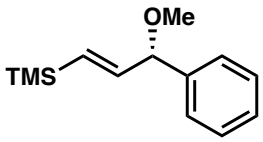

Prepared from (*E*)-(2-bromovinyl)trimethylsilane (36 mg, 0.2 mmol) and 1,3-dioxoisoindolin-2-yl 2-methoxy-2-phenylacetate (62 mg, 0.2 mmol) according to General Procedure 3. The crude residue was purified by column chromatography (silica gel, 0 to 3% Et_2O/hexane) to yield **208** (26 mg, 59% yield) in 91% ee as a colorless oil.

R_f = 0.62 (silica gel, 10% EtOAc/hexane, UV/CAM).

Chiral SFC: (OD-H, 2.5 mL/min, 1% IPA in CO_2, λ = 210 nm): t_R (minor) = 2.6 min, t_R (major) = 5.9 min.

$[\alpha]_D^{25}$ = +8° (c = 0.6, $CHCl_3$).

^{1}H NMR (400 MHz, $CDCl_3$): δ 7.40 – 7.27 (m, 5H), 6.10 (dd, *J* = 18.6, 5.9 Hz, 1H), 5.93 (dd, *J* = 18.6, 1.2 Hz, 1H), 4.61 (d, *J* = 5.8 Hz, 1H), 3.32 (s, 3H), 0.07 (s, 9H).

^{13}C NMR (101 MHz, $CDCl_3$): δ 145.7, 140.9, 131.9, 128.6, 127.7, 127.1, 86.6, 56.6, -1.2.

FTIR (NaCl, thin film, cm^{-1}): 2955, 2820, 1453, 1248, 1100, 990, 863, 838, 760, 699.

HRMS (FAB, *m/z*): calc'd for $C_{13}H_{20}OSi$ $[M–H_2+H]^+$: 219.1205; found: 219.1191.

4.7.5 Radical Clock Investigation

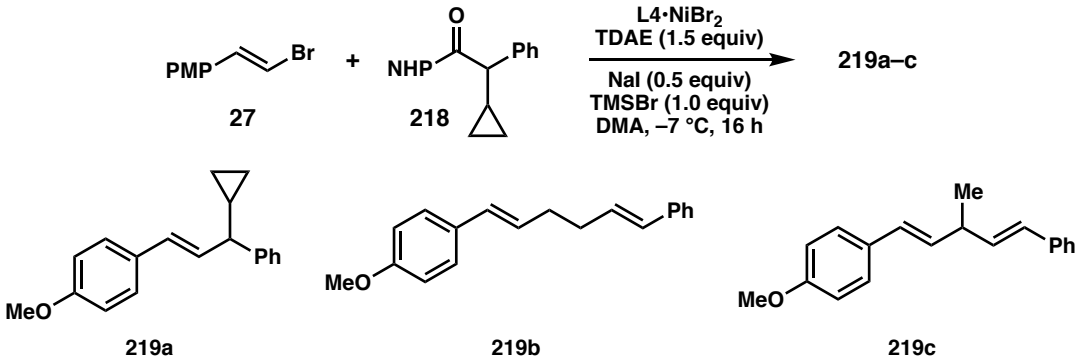

Prepared from (*E*)-1-(2-bromovinyl)-4-methoxybenzene (**27**, 43 mg, 0.2 mmol) and 1,3-dioxoisoindolin-2-yl 2-cyclopropyl-2-phenylacetate (**218**, 64 mg, 0.2 mmol) according to General Procedure 3. The crude residue was purified by column chromatography (silica gel, hexane to 30% toluene/hexane) to yield a mixture of **219a–c** (22 mg, 42% yield) as a colorless oil. The reaction was repeated with 5 mol % and 20 mol % of **L4•NiBr$_2$**, yielding a mixture of **219a–c** in 44% and 49% yield, respectively. Three products are confirmed by GC-MS (extract ion *m/z* = 264). Distinct ^{1}H/^{13}C signals and coupling correlations are confirmed by ^{1}H, ^{13}C, COSY, HSQC, and HMBC NMR spectroscopy.

NMR data for **219a–c** with 20 mol % **L4•NiBr$_2$**:

^{1}H NMR (400 MHz, CDCl$_3$): δ 7.42 – 7.18 (m, 7H), 6.86 (dq, *J* = 8.9, 2.5 Hz, 2H), 6.49 – 6.36 (m, 1.8H), 6.34 – 6.08 (m, 1.82H), 3.81 (s, 3H), 3.20 (qt, *J* = 6.9, 1.3 Hz, 0.1H, *11c*), 2.76 (ddd, *J* = 8.6, 6.9, 1.2 Hz, 0.2H, *11a*), 2.49 – 2.31 (m, 2.8H, *11b*), 1.31 (d, *J* = 6.9 Hz, 0.3H, *11c*), 1.23 – 1.13 (m, 0.2H, *11a*), 0.68 (dddd, *J* = 9.1, 8.0, 5.3, 4.1 Hz, 0.2H, *11a*), 0.56 (dddd, *J* = 9.4, 8.0, 5.2, 4.1 Hz, 0.2H, *11a*), 0.40 – 0.31 (m, 0.2H, *11a*), 0.28 (dtd, *J* = 9.3, 5.2, 4.2 Hz, 0.2H, *11a*).

^{13}C NMR (101 MHz, CDCl$_3$): δ 158.9, 158.8, 144.6, 137.9, 137.8, 134.7, 132.2, 131.2, 130.7, 130.5, 130.4, 130.3, 129.8, 129.0, 128.7, 128.6, 128.5, 128.3, 128.0, 127.9, 127.4, 127.3, 127.2, 127.1, 127.0, 126.4, 126.2, 126.1, 114.03, 114.02, 55.4, 53.2, 40.2, 33.2, 33.0, 20.5, 16.4, 4.9, 4.4.

FTIR (NaCl, thin film, cm^{-1}): 3026, 2931, 2837, 1607, 1511, 1252, 1176, 1034, 966, 800, 692.

LRMS (GC-MS, *m/z*): calc'd for $C_{19}H_{20}O$ $[M]^+$: 264.2; found: 3 products, 264.1, 264.1, 264.2.

Ratios of **219a–c** were determined by ^{1}H NMR analysis:

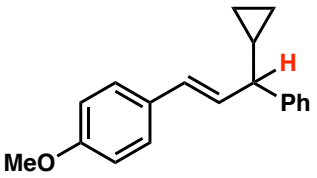

219a

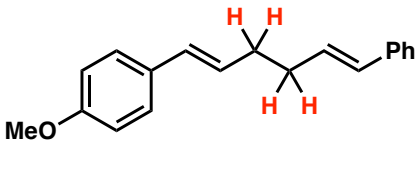

219b

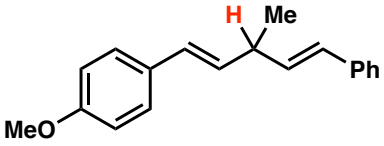

219c

5 mol % **L4•NiBr$_2$**:

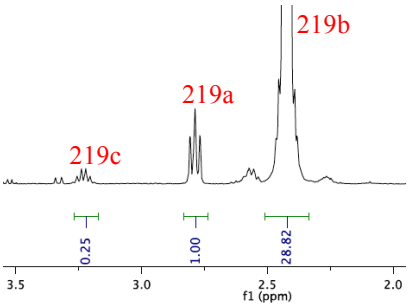

10 mol % **L4•NiBr$_2$**:

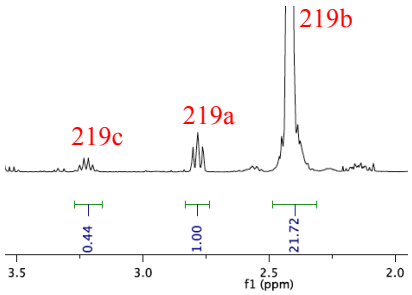

20 mol % **L4•NiBr$_2$**:

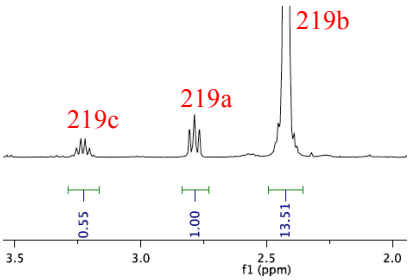

Integration of **219b** was divided by four to account for the contribution of four protons in the multiplet

NMR Integrations

Nickel Catalyst	Cyclopropane (219a)	Linear (219b)	Branched (219c)	Ring Closed Total	Ring Open Total
5%	1.00	7.21	0.25	1.00	7.46
10%	1.00	5.43	0.44	1.00	5.87
20%	1.00	3.38	0.55	1.00	3.93

4.7.6 *SFC Traces of Racemic and Enantioenriched Products*

28 (Table 4.3): racemic

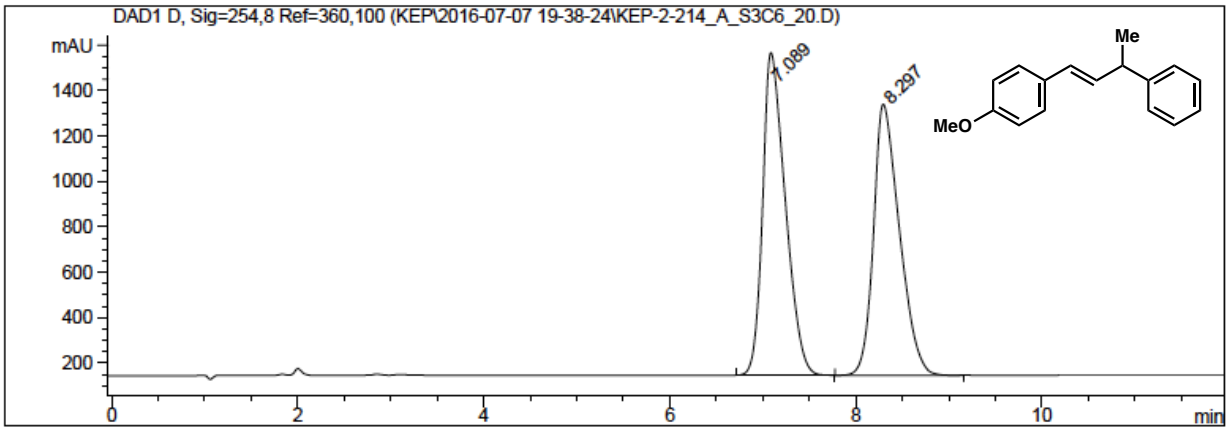

Peak #	RetTime [min]	Type	Width [min]	Area [mAU*s]	Height [mAU]	Area %
1	7.089	BV	0.2581	2.40965e4	1419.46216	50.9929
2	8.297	VB	0.2903	2.31582e4	1193.77161	49.0071

28 (Table 4.3): enantioenriched, 96% ee

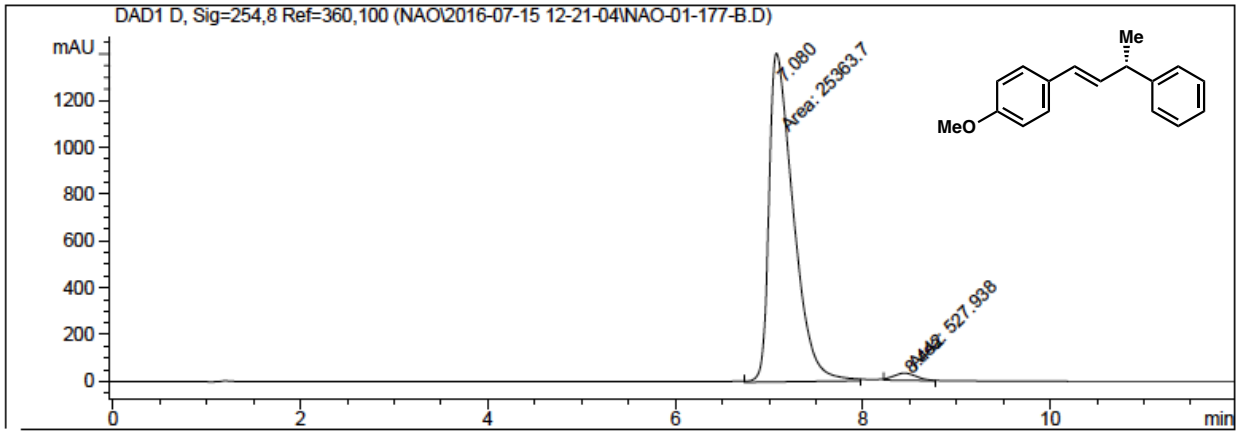

Peak #	RetTime [min]	Type	Width [min]	Area [mAU*s]	Height [mAU]	Area %
1	7.080	MM	0.3005	2.53637e4	1406.71533	97.9610
2	8.442	MM	0.2816	527.93842	31.25150	2.0390

180 (Table 4.3): racemic

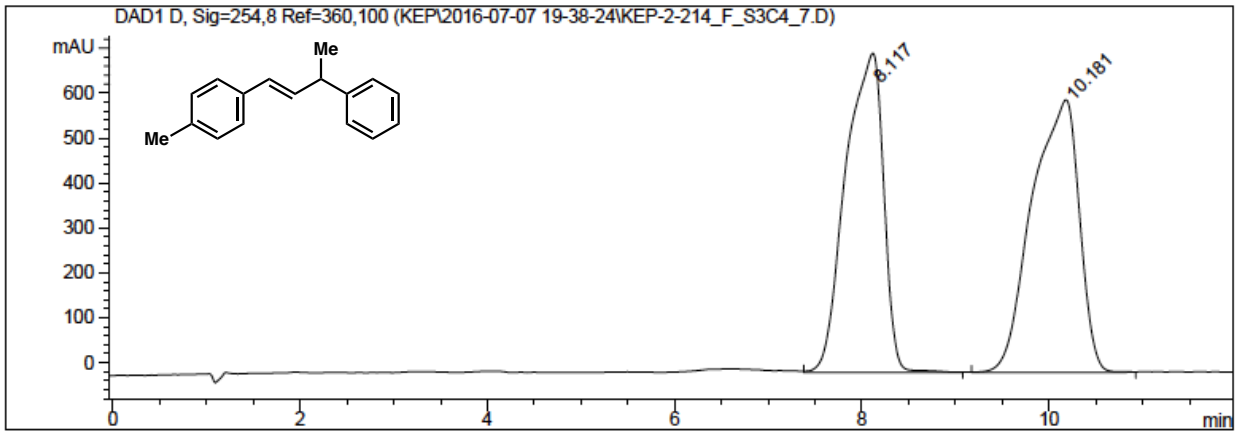

Peak #	RetTime [min]	Type	Width [min]	Area [mAU*s]	Height [mAU]	Area %
1	8.117	VB	0.3807	2.00095e4	710.31079	48.4555
2	10.181	BV	0.4692	2.12851e4	606.82129	51.5445

180 (Table 4.3): enantioenriched, 95% ee

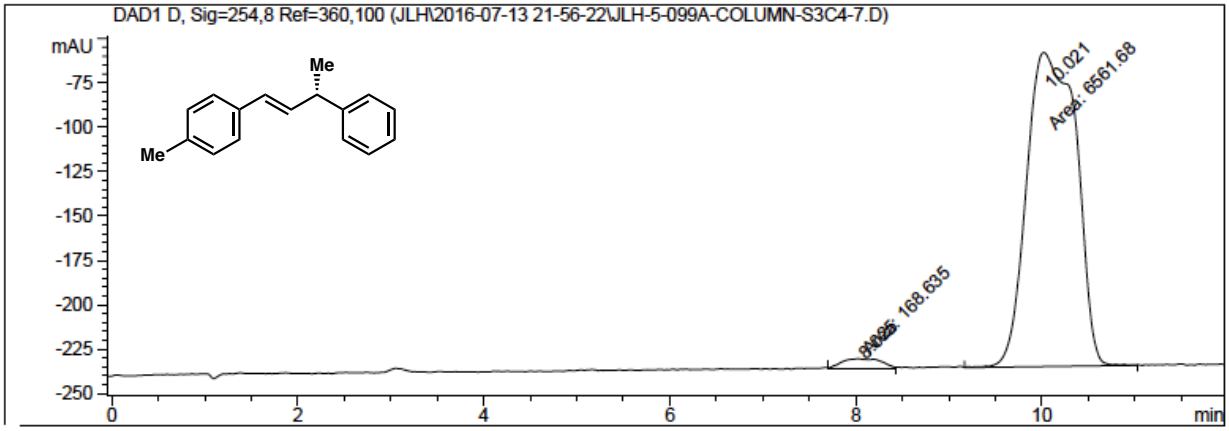

Peak #	RetTime [min]	Type	Width [min]	Area [mAU*s]	Height [mAU]	Area %
1	8.025	MM	0.4882	168.63531	5.75649	2.5056
2	10.021	MM	0.6182	6561.67920	176.91377	97.4944

181 (Table 4.3): racemic

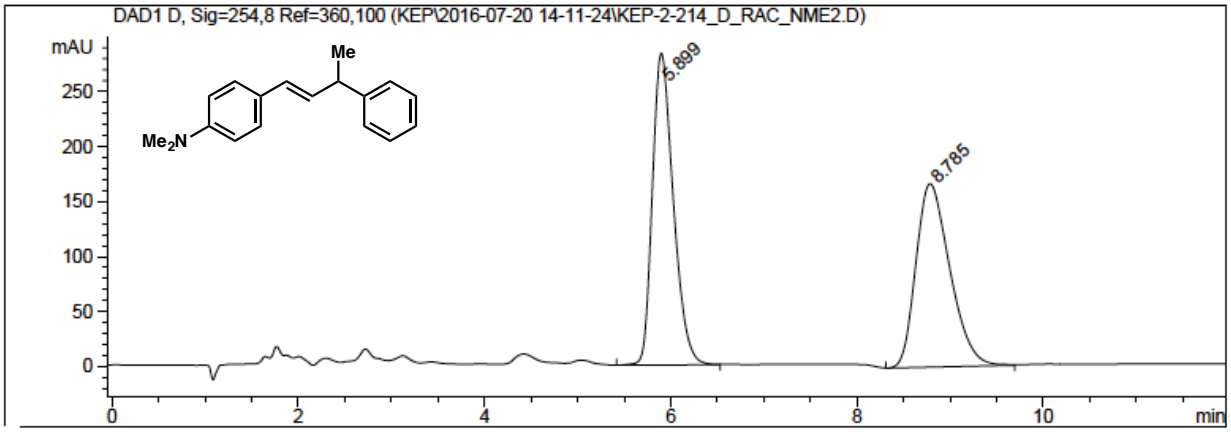

Peak #	RetTime [min]	Type	Width [min]	Area [mAU*s]	Height [mAU]	Area %
1	5.899	VB	0.2423	4429.97607	283.53226	51.2284
2	8.785	BB	0.3949	4217.52539	166.83267	48.7716

181 (Table 4.3): enantioenriched, 97% ee

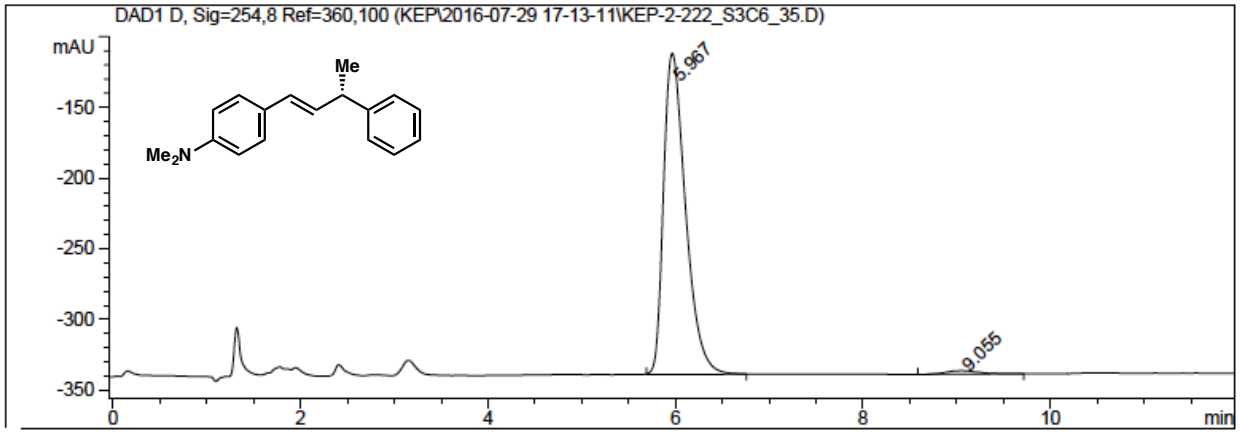

Peak #	RetTime [min]	Type	Width [min]	Area [mAU*s]	Height [mAU]	Area %
1	5.967	BB	0.2505	3707.96924	227.13380	98.4506
2	9.055	BB	0.2926	58.35402	2.46108	1.5494

182 (Table 4.3): racemic

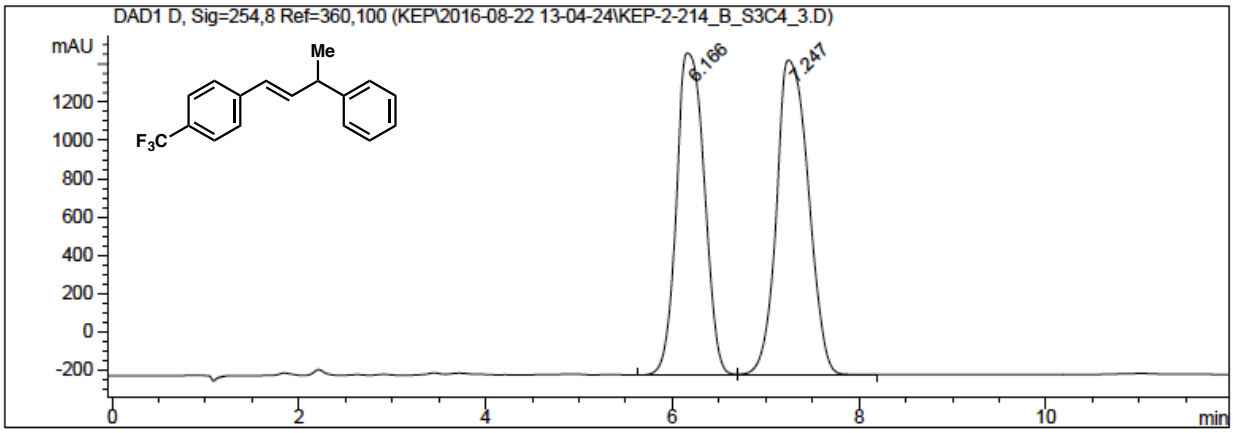

Peak #	RetTime [min]	Type	Width [min]	Area [mAU*s]	Height [mAU]	Area %
1	6.166	VV	0.3308	3.50747e4	1685.07422	47.1051
2	7.247	VB	0.3749	3.93858e4	1647.52795	52.8949

182 (Table 4.3): enantioenriched, 93% ee

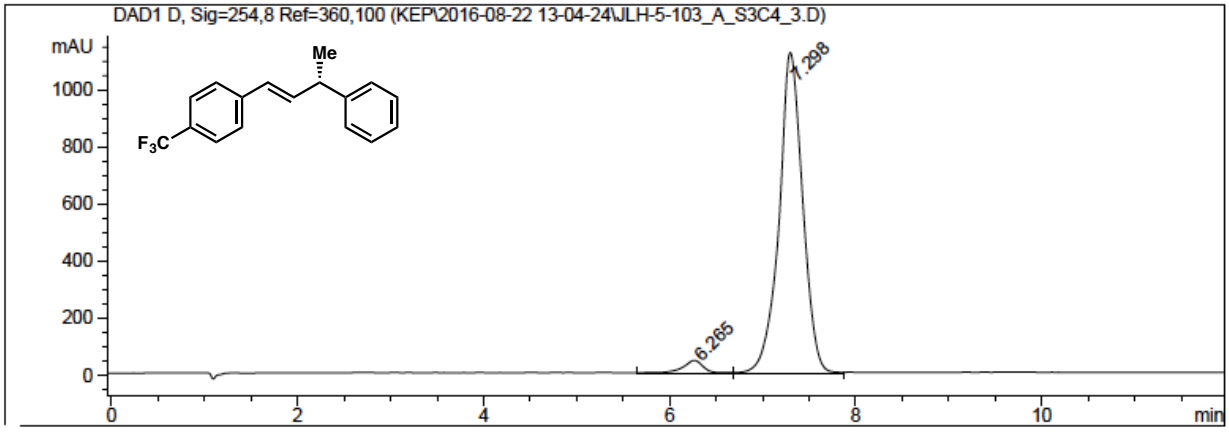

Peak #	RetTime [min]	Type	Width [min]	Area [mAU*s]	Height [mAU]	Area %
1	6.265	VV	0.2265	687.93018	43.98362	3.3472
2	7.298	VV	0.2624	1.98645e4	1122.81396	96.6528

183 (Table 4.3): racemic

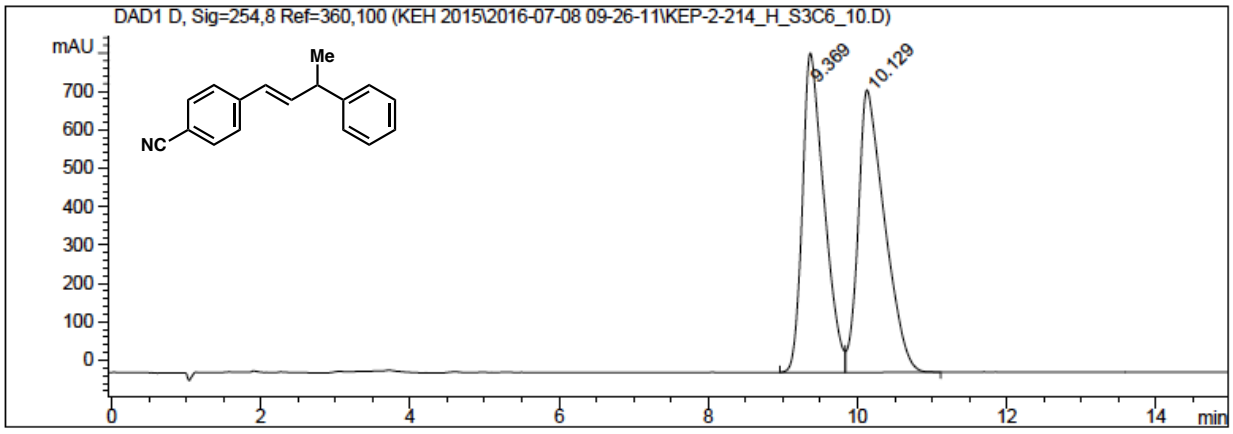

Peak #	RetTime [min]	Type	Width [min]	Area [mAU*s]	Height [mAU]	Area %
1	9.369	BV	0.2960	1.68057e4	830.62769	48.1897
2	10.129	VB	0.3508	1.80684e4	734.99915	51.8103

183 (Table 4.3): enantioenriched, 94% ee

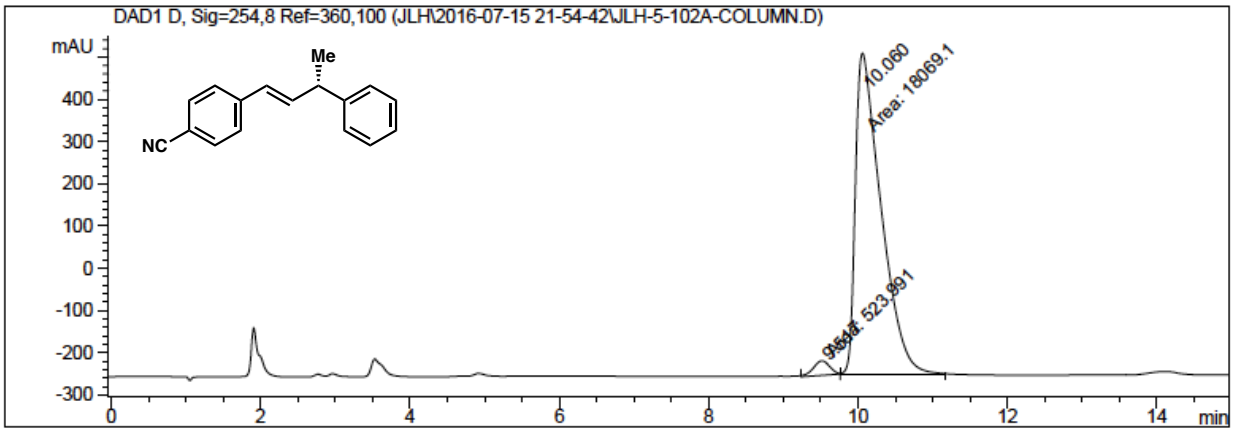

Peak #	RetTime [min]	Type	Width [min]	Area [mAU*s]	Height [mAU]	Area %
1	9.517	MM	0.2532	523.99091	34.49692	2.8182
2	10.060	MM	0.3962	1.80691e4	760.05249	97.1818

184 (Table 4.3): racemic

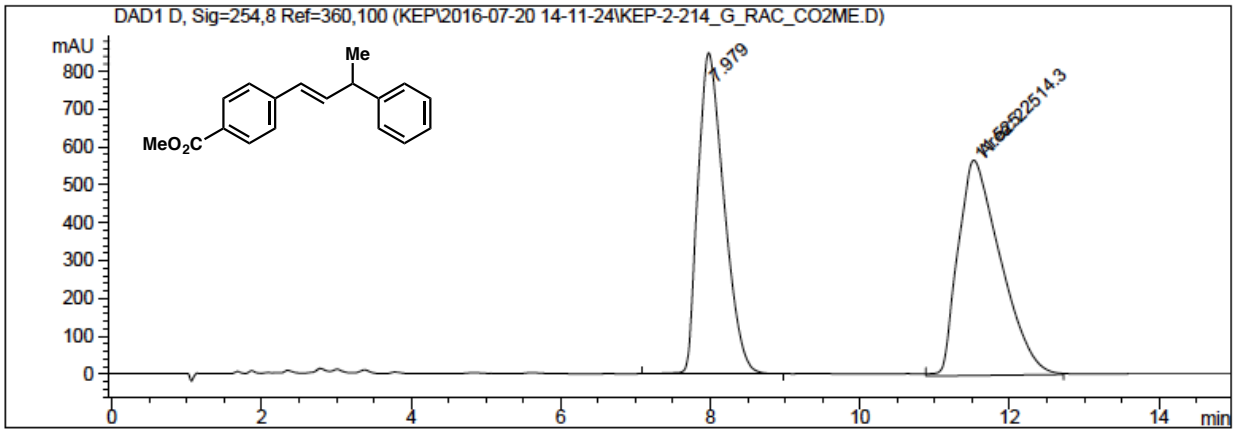

Peak #	RetTime [min]	Type	Width [min]	Area [mAU*s]	Height [mAU]	Area %
1	7.979	BB	0.3869	2.05724e4	848.34802	47.7466
2	11.525	MM	0.6592	2.25143e4	569.27423	52.2534

184 (Table 4.3): enantioenriched, 95% ee

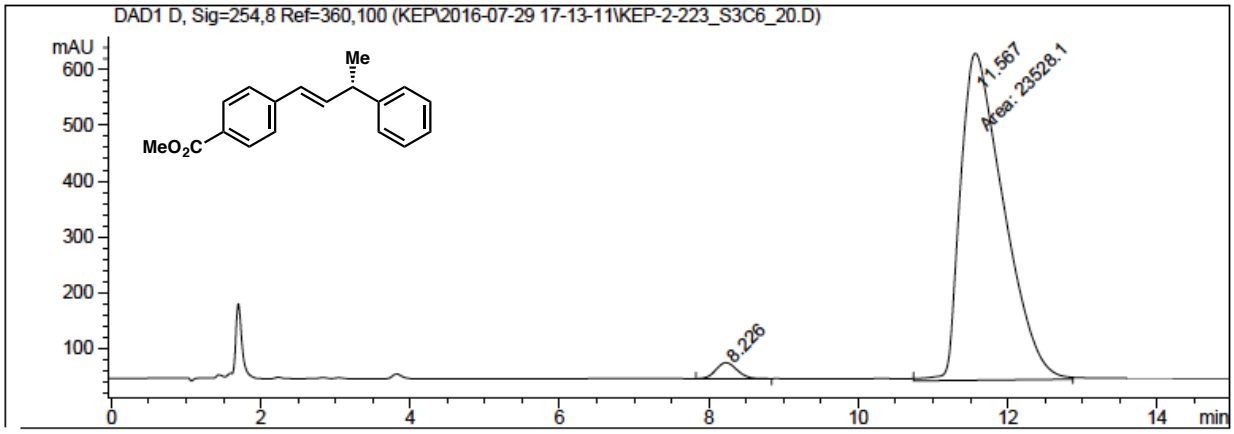

Peak #	RetTime [min]	Type	Width [min]	Area [mAU*s]	Height [mAU]	Area %
1	8.226	BB	0.3069	568.03058	28.69778	2.3574
2	11.567	MM	0.6679	2.35281e4	587.09686	97.6426

185 (Table 4.3): racemic

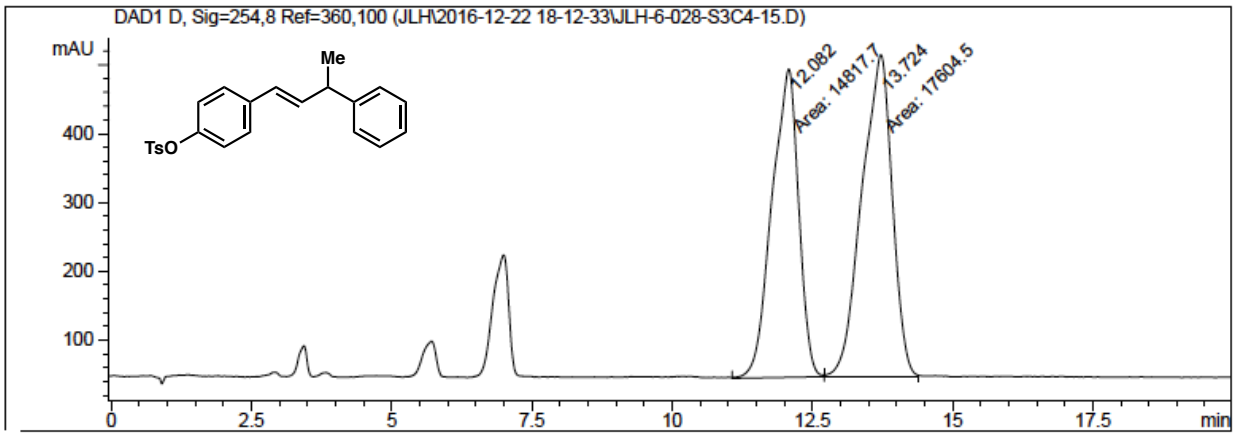

Peak #	RetTime [min]	Type	Width [min]	Area [mAU*s]	Height [mAU]	Area %
1	12.082	MM	0.5513	1.48177e4	447.97232	45.7023
2	13.724	MM	0.6275	1.76045e4	467.56030	54.2977

185 (Table 4.3): enantioenriched, 94% ee

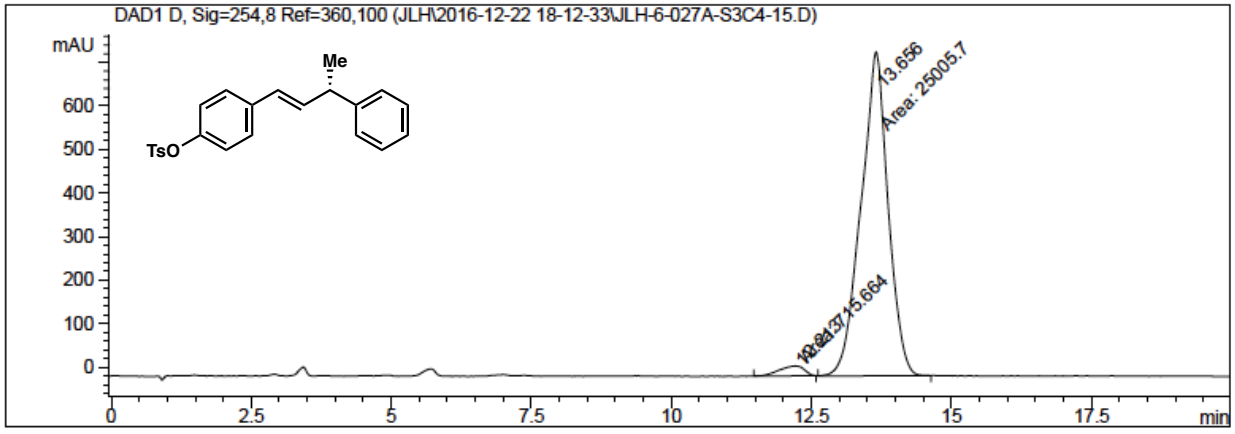

Peak #	RetTime [min]	Type	Width [min]	Area [mAU*s]	Height [mAU]	Area %
1	12.213	MM	0.5201	715.66412	22.93249	2.7824
2	13.656	MM	0.5598	2.50057e4	744.50916	97.2176

186 (Table 4.3): racemic

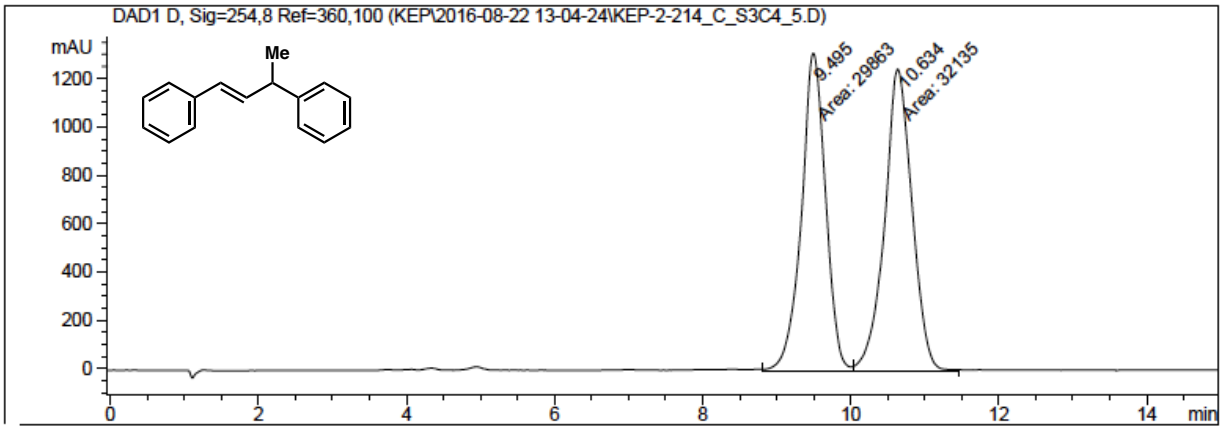

Peak #	RetTime [min]	Type	Width [min]	Area [mAU*s]	Height [mAU]	Area %
1	9.495	MM	0.3786	2.98630e4	1314.49744	48.1677
2	10.634	MM	0.4290	3.21350e4	1248.56421	51.8323

186 (Table 4.3): enantioenriched, 96% ee

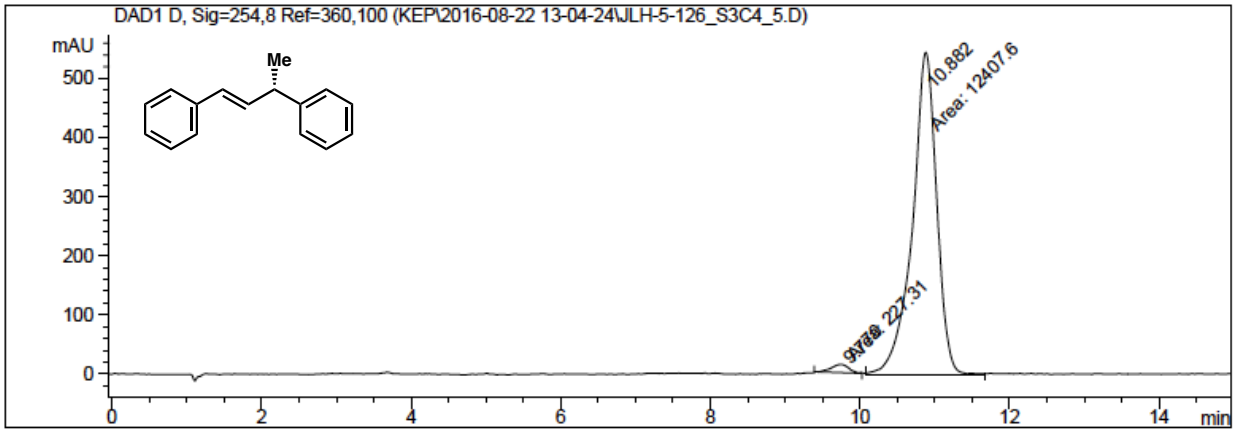

Peak #	RetTime [min]	Type	Width [min]	Area [mAU*s]	Height [mAU]	Area %
1	9.770	MM	0.2725	227.31046	13.90100	1.7991
2	10.882	MM	0.3782	1.24076e4	546.85577	98.2009

187 (Table 4.3): racemic

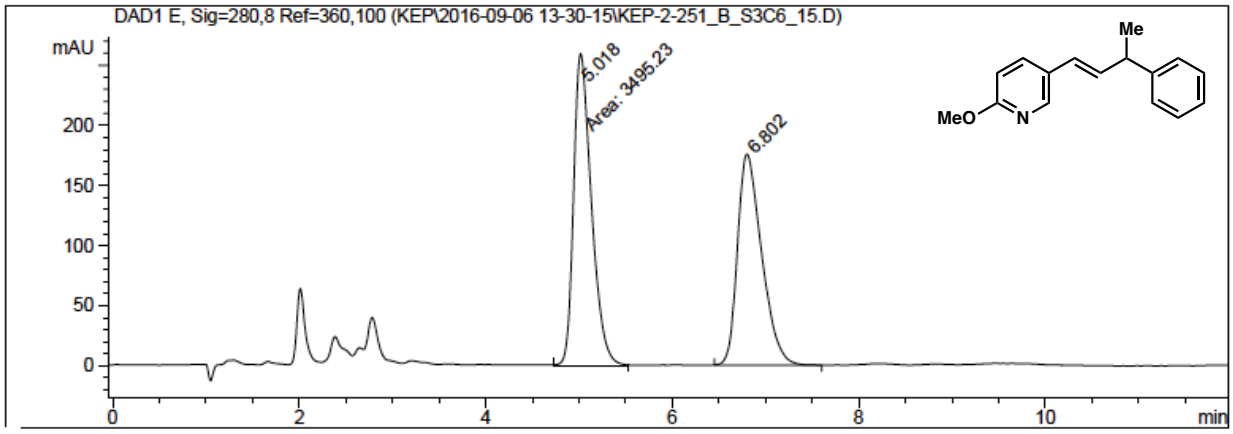

Peak #	RetTime [min]	Type	Width [min]	Area [mAU*s]	Height [mAU]	Area %
1	5.018	MM	0.2233	3495.22925	260.81982	52.4318
2	6.802	BB	0.2747	3171.01147	175.57878	47.5682

187 (Table 4.3): enantioenriched, 95% ee

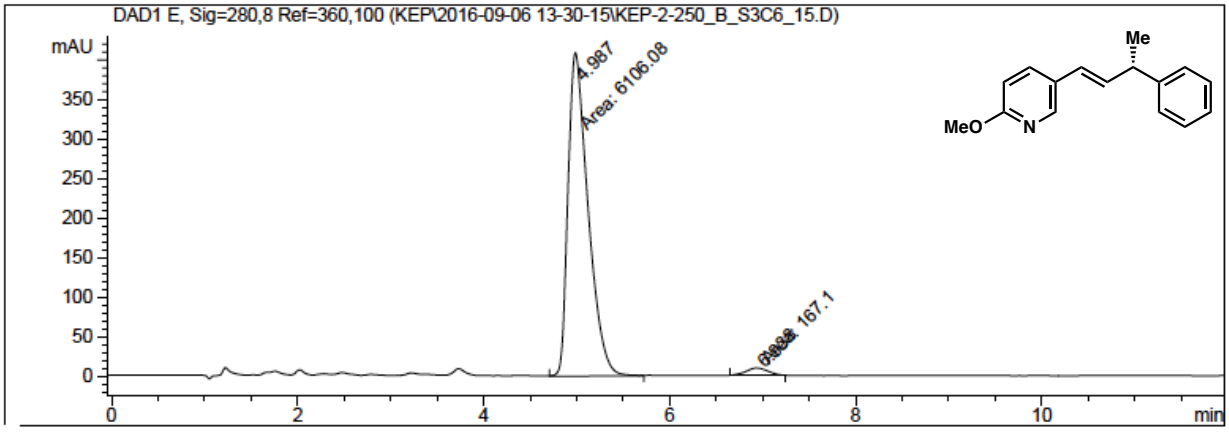

Peak #	RetTime [min]	Type	Width [min]	Area [mAU*s]	Height [mAU]	Area %
1	4.987	MM	0.2488	6106.07617	408.96854	97.3363
2	6.938	MM	0.2866	167.10007	9.71596	2.6637

188 (Table 4.3): racemic

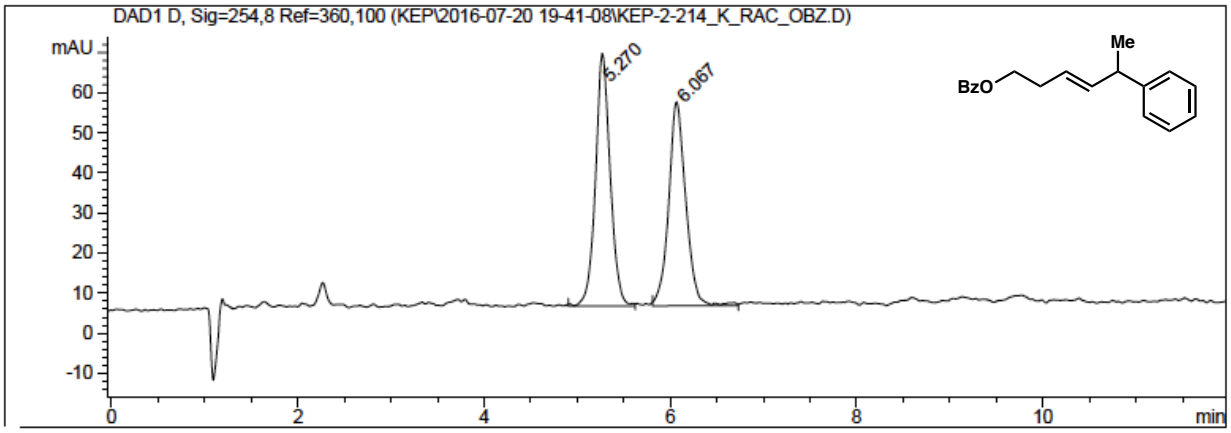

Peak #	RetTime [min]	Type	Width [min]	Area [mAU*s]	Height [mAU]	Area %
1	5.270	BB	0.1643	692.65100	62.99958	51.5795
2	6.067	BB	0.1892	650.22839	50.83070	48.4205

188 (Table 4.3): enantioenriched, 97% ee

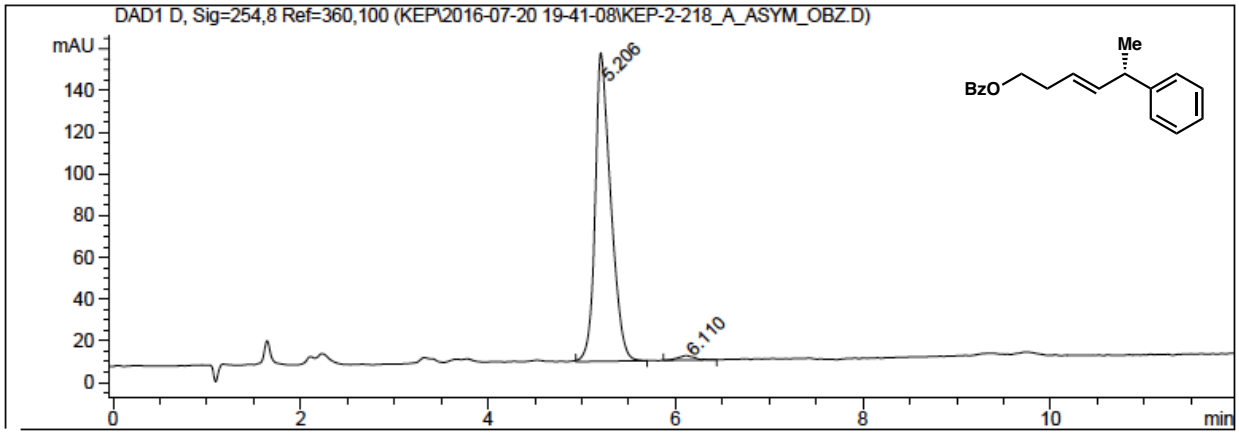

Peak #	RetTime [min]	Type	Width [min]	Area [mAU*s]	Height [mAU]	Area %
1	5.206	BB	0.1708	1710.15393	148.02460	98.4760
2	6.110	BB	0.1607	26.46575	2.19494	1.5240

189 (Table 4.3): racemic

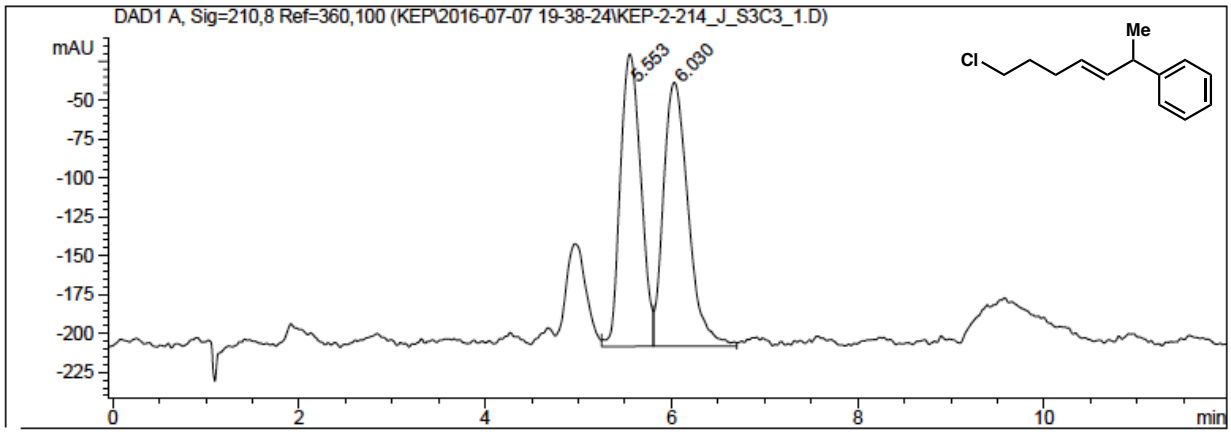

Peak #	RetTime [min]	Type	Width [min]	Area [mAU*s]	Height [mAU]	Area %
1	5.553	VV	0.2466	2879.10791	188.09062	47.7991
2	6.030	VV	0.2922	3144.24927	169.66949	52.2009

189 (Table 4.3): enantioenriched, 91% ee

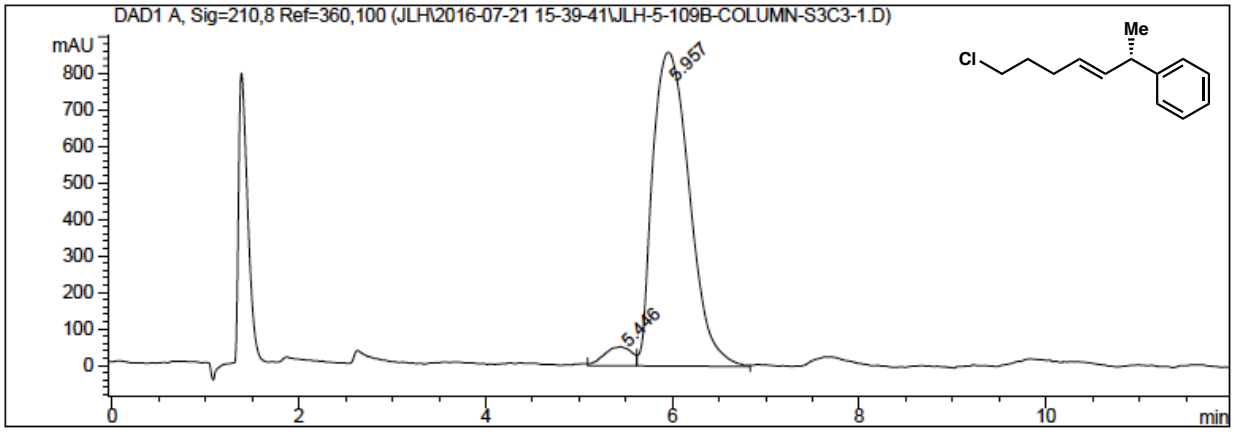

Peak #	RetTime [min]	Type	Width [min]	Area [mAU*s]	Height [mAU]	Area %
1	5.446	VV	0.2528	1053.08008	51.88251	4.2859
2	5.957	VV	0.4514	2.35179e4	858.91888	95.7141

190 (Table 4.3): racemic

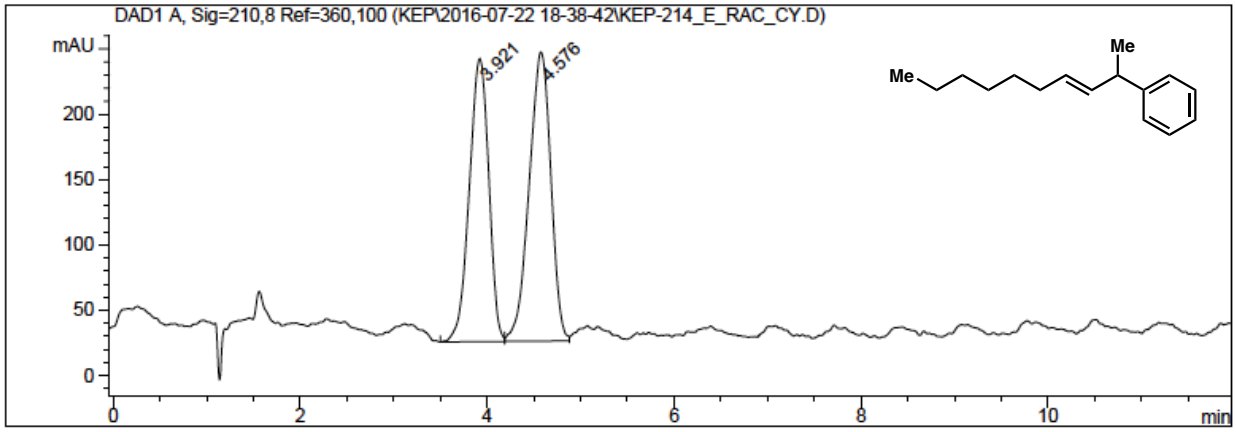

Peak #	RetTime [min]	Type	Width [min]	Area [mAU*s]	Height [mAU]	Area %
1	3.921	VV	0.2294	3145.27051	216.62386	46.8268
2	4.576	VV	0.2603	3571.54810	221.25337	53.1732

190 (Table 4.3): enantioenriched, 94% ee

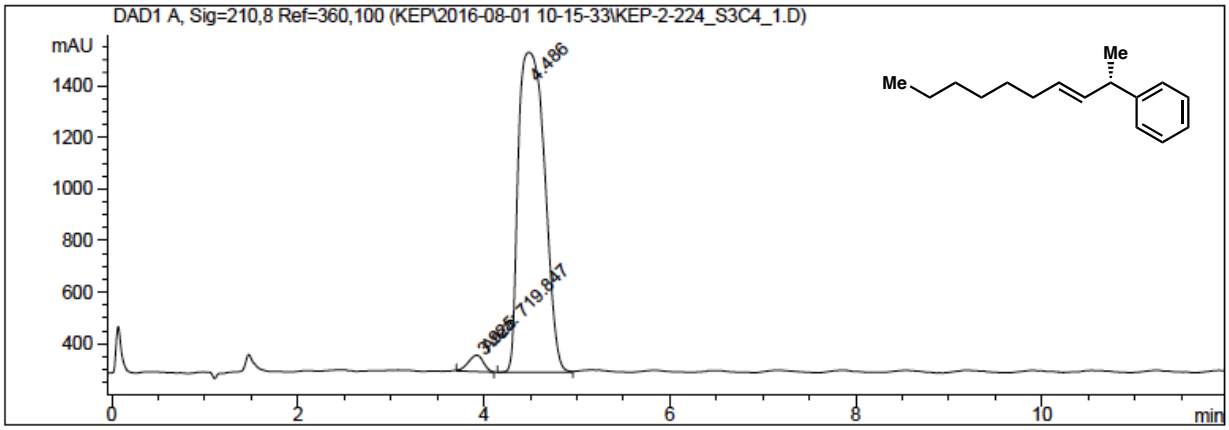

Peak #	RetTime [min]	Type	Width [min]	Area [mAU*s]	Height [mAU]	Area %
1	3.925	MM	0.1890	719.84717	63.47777	2.8630
2	4.486	VV	0.3261	2.44231e4	1238.09705	97.1370

276 (de-silylated 191, Table 4.3): racemic

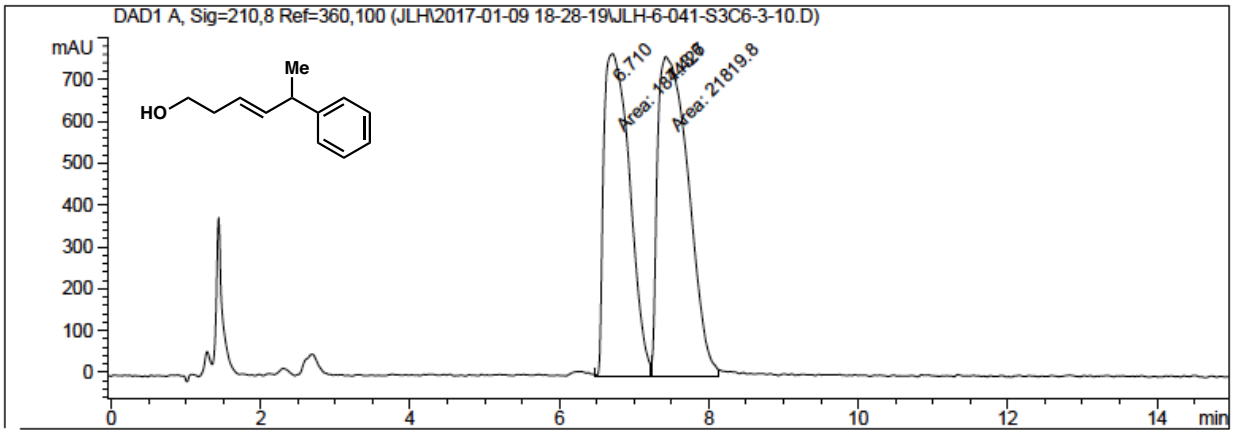

Peak #	RetTime [min]	Type	Width [min]	Area [mAU*s]	Height [mAU]	Area %
1	6.710	MM	0.3992	1.84436e4	770.06226	45.8074
2	7.427	MM	0.4761	2.18198e4	763.80591	54.1926

276 (de-silylated 191, Table 4.3): enantioenriched, 89% ee

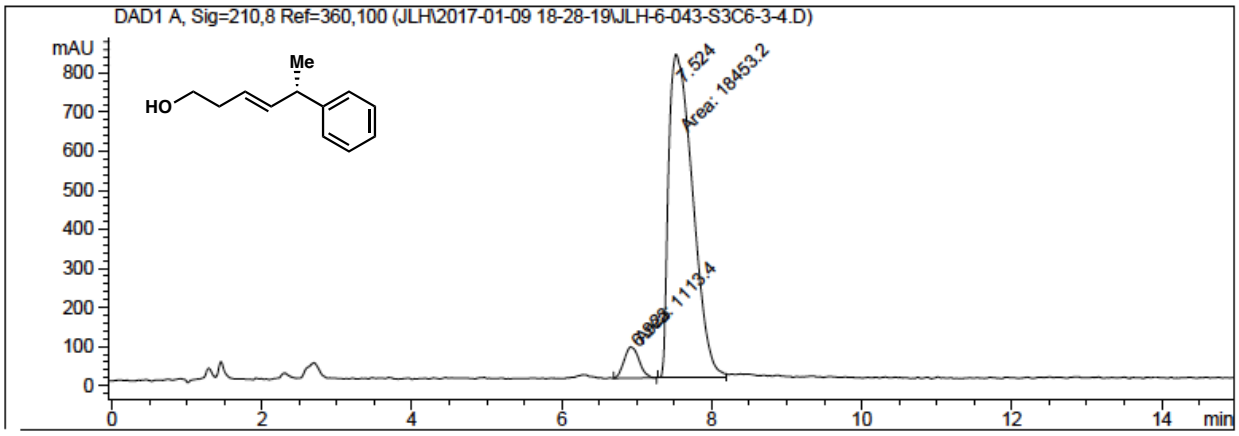

Peak #	RetTime [min]	Type	Width [min]	Area [mAU*s]	Height [mAU]	Area %
1	6.923	MM	0.2309	1113.40063	80.37251	5.6903
2	7.524	MM	0.3711	1.84532e4	828.86755	94.3097

192 (Table 4.3): racemic

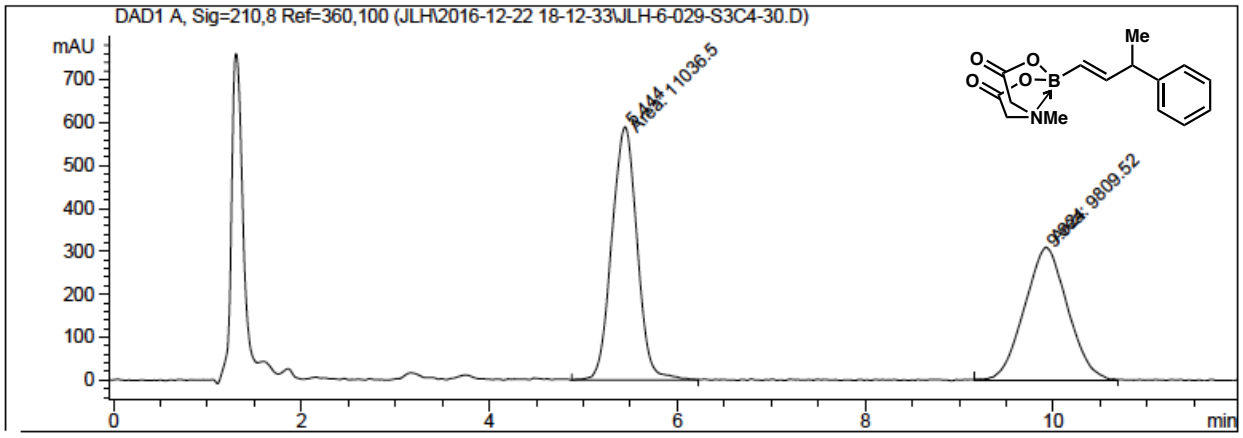

Peak #	RetTime [min]	Type	Width [min]	Area [mAU*s]	Height [mAU]	Area %
1	5.444	MM	0.3119	1.10365e4	589.78003	52.9429
2	9.924	MM	0.5290	9809.52246	309.03564	47.0571

192 (Table 4.3): enantioenriched, 97% ee

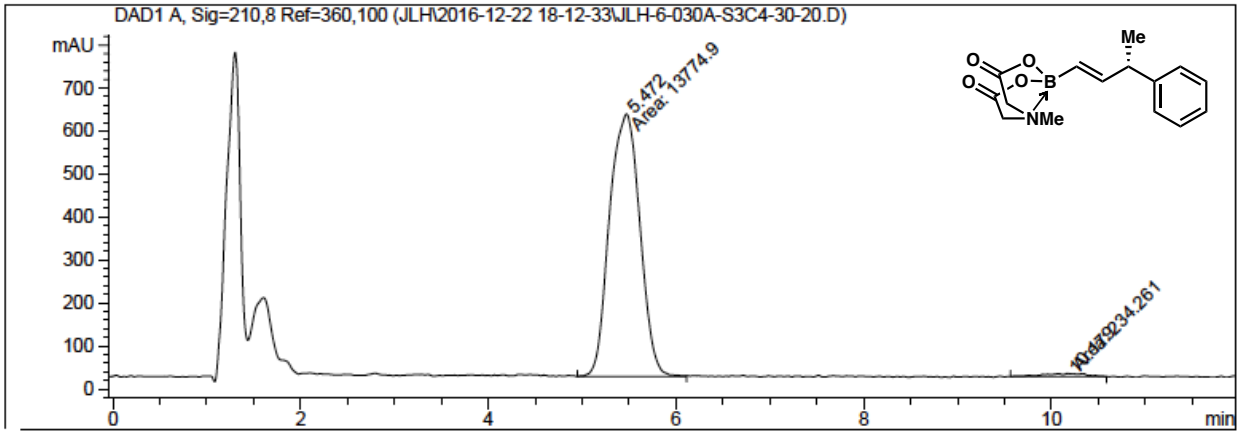

Peak #	RetTime [min]	Type	Width [min]	Area [mAU*s]	Height [mAU]	Area %
1	5.472	MM	0.3758	1.37749e4	610.96771	98.3278
2	10.179	MM	0.5146	234.26103	7.58734	1.6722

193 (Table 4.3): racemic

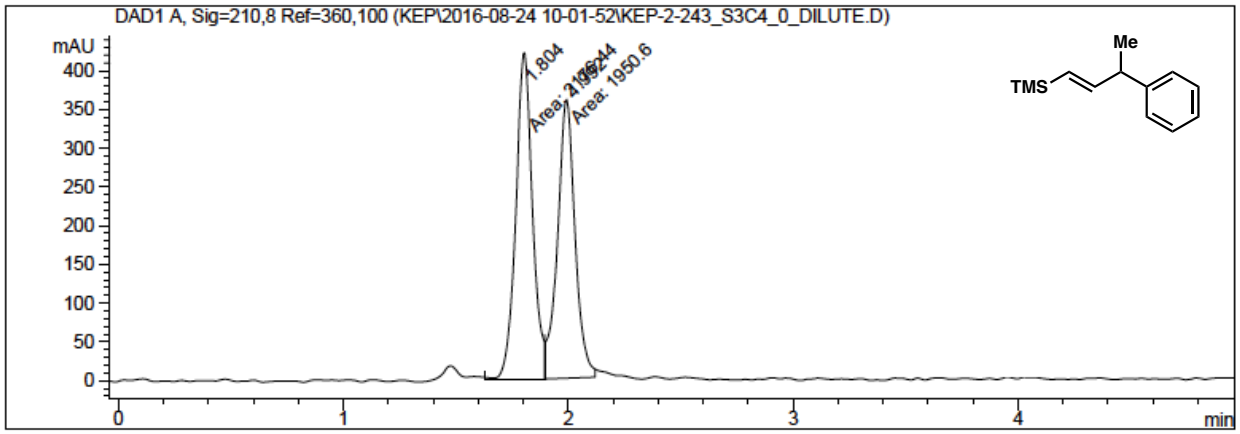

Peak #	RetTime [min]	Type	Width [min]	Area [mAU*s]	Height [mAU]	Area %
1	1.804	MM	0.0852	2176.43945	425.78909	52.7360
2	1.992	MM	0.0896	1950.60413	362.93353	47.2640

193 (Table 4.3): enantioenriched, 97% ee

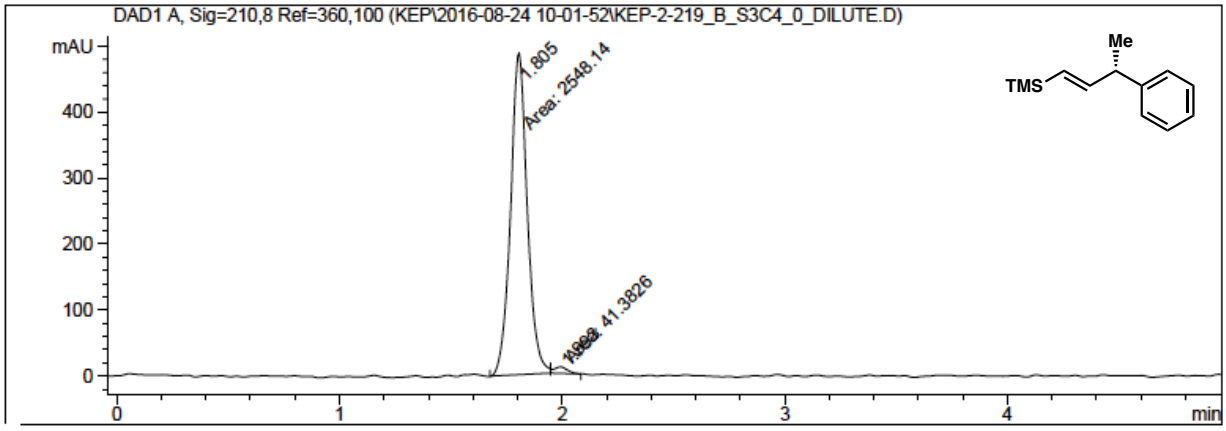

Peak #	RetTime [min]	Type	Width [min]	Area [mAU*s]	Height [mAU]	Area %
1	1.805	MM	0.0863	2548.14233	492.12225	98.4019
2	1.993	MM	0.0681	41.38256	10.12810	1.5981

194 (Table 4.4): racemic

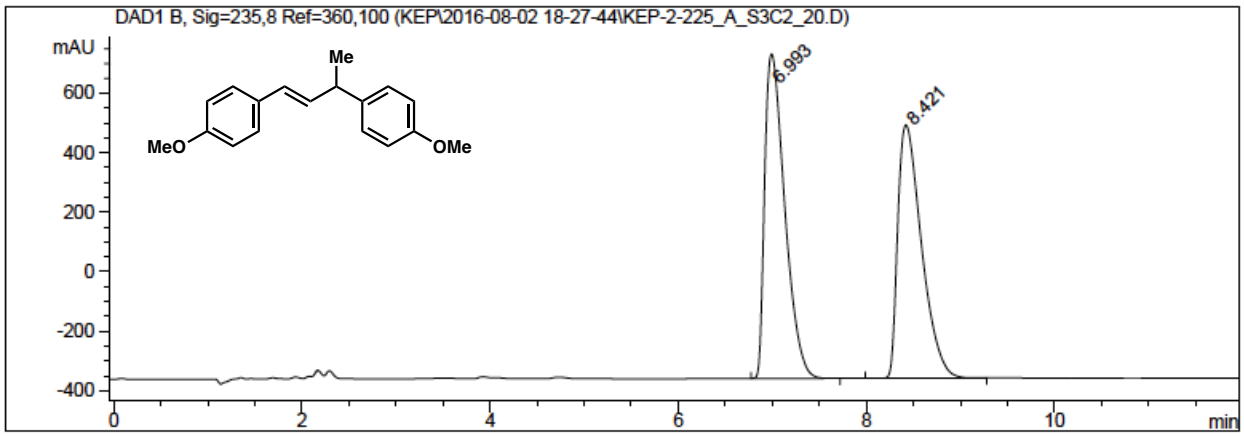

Peak #	RetTime [min]	Type	Width [min]	Area [mAU*s]	Height [mAU]	Area %
1	6.993	BB	0.2288	1.61745e4	1091.89661	51.9859
2	8.421	BB	0.2727	1.49387e4	851.43549	48.0141

194 (Table 4.4): enantioenriched, 93% ee

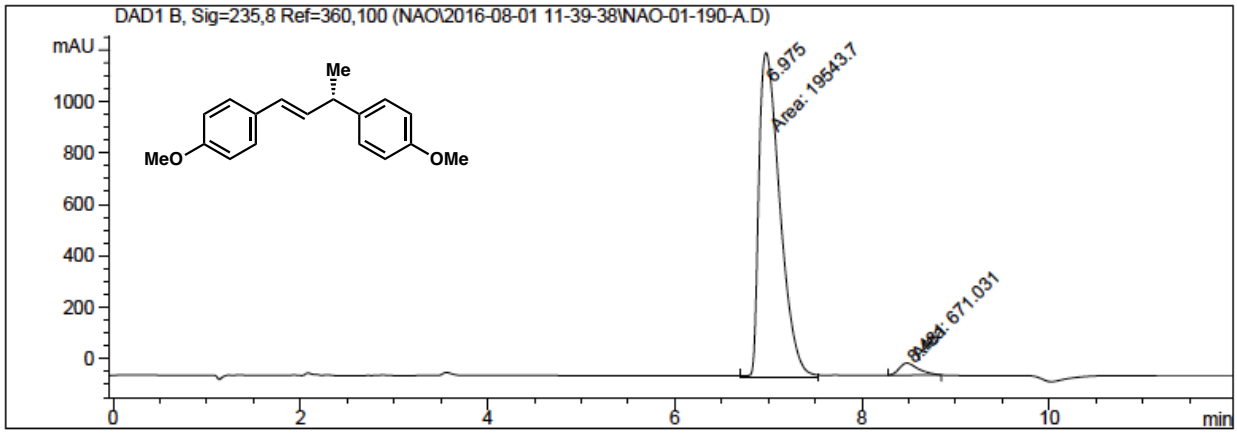

Peak #	RetTime [min]	Type	Width [min]	Area [mAU*s]	Height [mAU]	Area %
1	6.975	MM	0.2585	1.95437e4	1260.21631	96.6805
2	8.481	MM	0.2361	671.03094	47.35995	3.3195

195 (Table 4.4): racemic

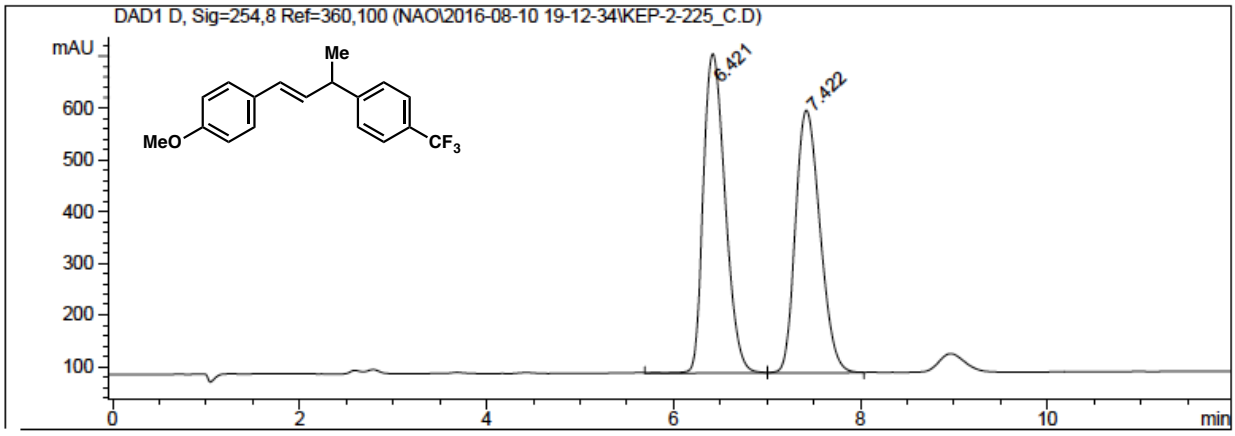

Peak #	RetTime [min]	Type	Width [min]	Area [mAU*s]	Height [mAU]	Area %
1	6.421	VV	0.2579	1.00441e4	616.96472	51.9654
2	7.422	VV	0.2894	9284.33398	507.48148	48.0346

195 (Table 4.4): enantioenriched, 88% ee

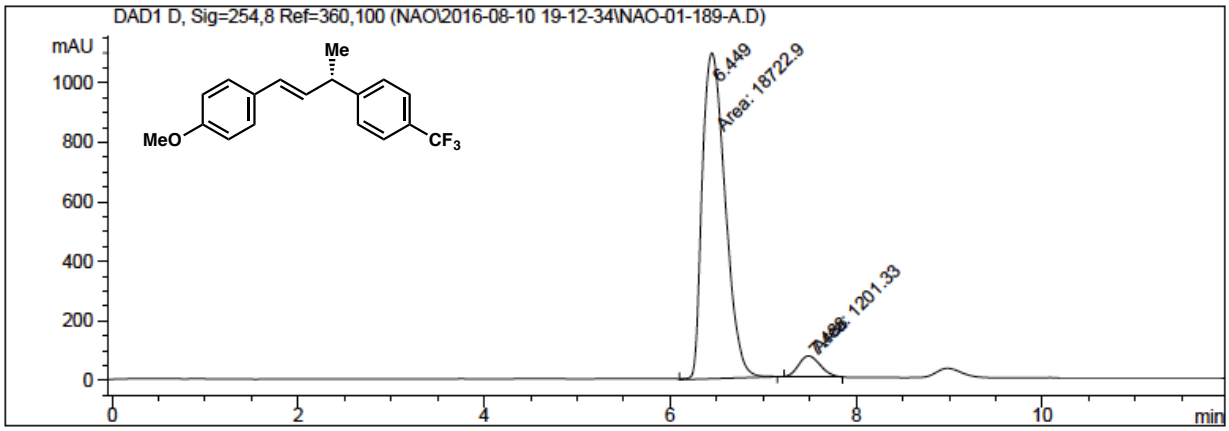

Peak #	RetTime [min]	Type	Width [min]	Area [mAU*s]	Height [mAU]	Area %
1	6.449	MM	0.2851	1.87229e4	1094.68372	93.9705
2	7.488	MM	0.2774	1201.33252	72.18948	6.0295

196 (Table 4.4): racemic

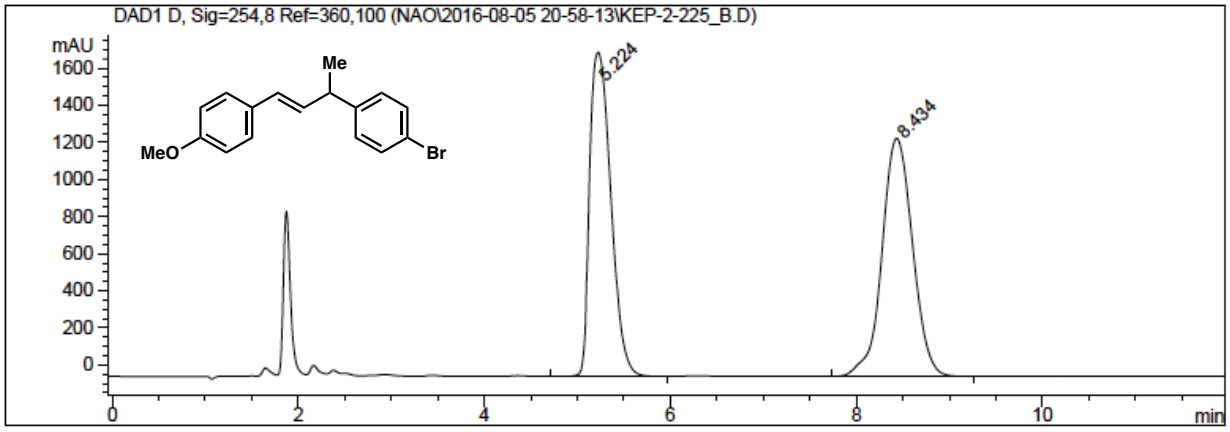

Peak #	RetTime [min]	Type	Width [min]	Area [mAU*s]	Height [mAU]	Area %
1	5.224	VV	0.2570	2.77188e4	1747.68750	48.5460
2	8.434	BB	0.3592	2.93793e4	1282.85803	51.4540

196 (Table 4.4): enantioenriched, 90% ee

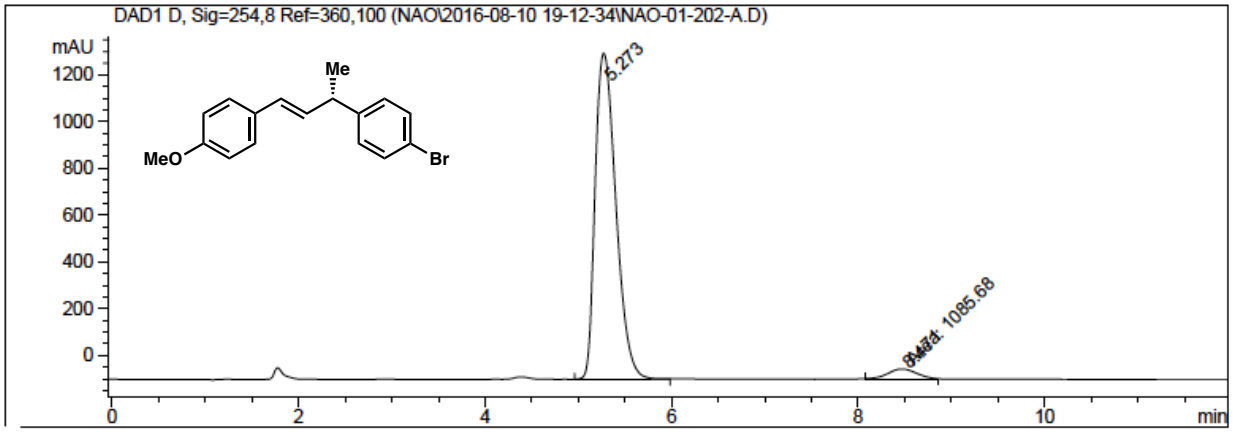

Peak #	RetTime [min]	Type	Width [min]	Area [mAU*s]	Height [mAU]	Area %
1	5.273	BB	0.2445	2.15843e4	1395.44788	95.2109
2	8.471	MM	0.3931	1085.67932	46.02574	4.7891

197 (Table 4.4): racemic

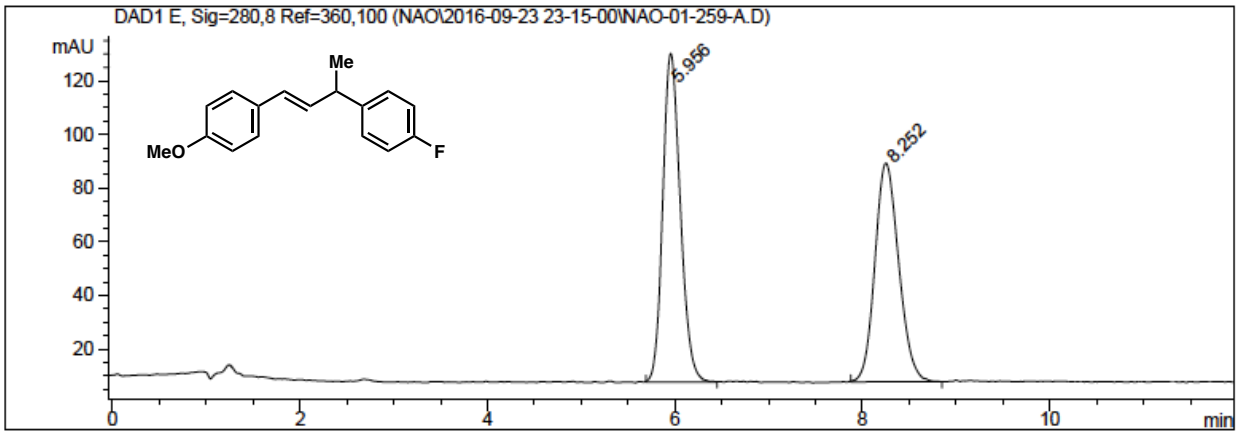

Peak #	RetTime [min]	Type	Width [min]	Area [mAU*s]	Height [mAU]	Area %
1	5.956	BB	0.2041	1597.30237	122.49622	52.5502
2	8.252	BB	0.2744	1442.27039	81.53059	47.4498

197 (Table 4.4): enantioenriched, 92% ee

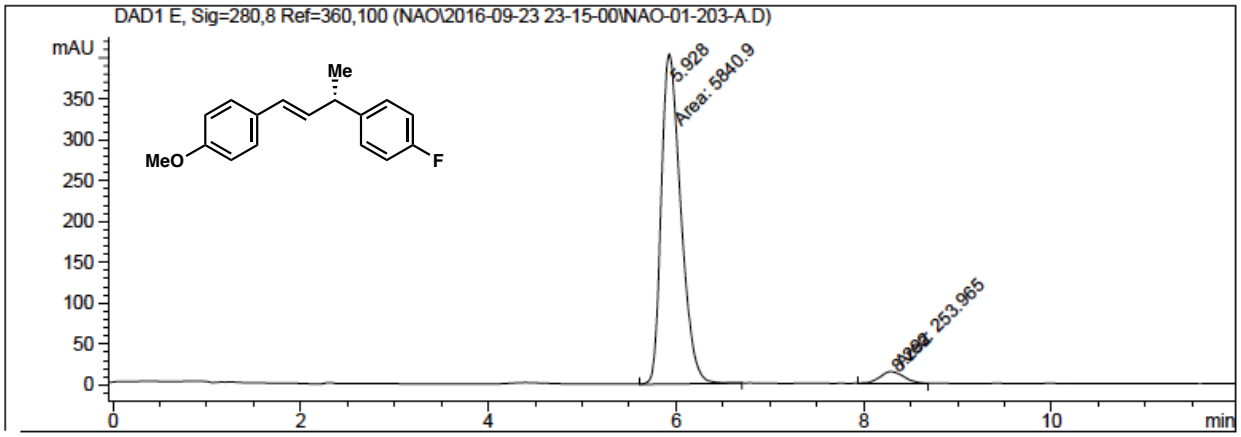

Peak #	RetTime [min]	Type	Width [min]	Area [mAU*s]	Height [mAU]	Area %
1	5.928	MM	0.2410	5840.89600	403.93130	95.8331
2	8.292	MM	0.2929	253.96486	14.45295	4.1669

198 (Table 4.4): racemic

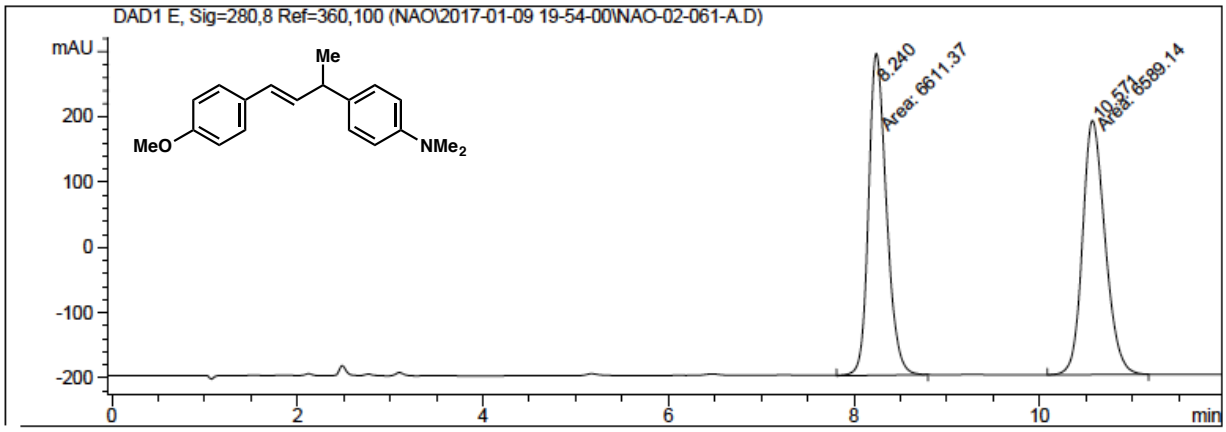

Peak #	RetTime [min]	Type	Width [min]	Area [mAU*s]	Height [mAU]	Area %
1	8.240	MM	0.2233	6611.36621	493.52872	50.0842
2	10.571	MM	0.2819	6589.13770	389.54446	49.9158

198 (Table 4.4): enantioenriched, 94% ee

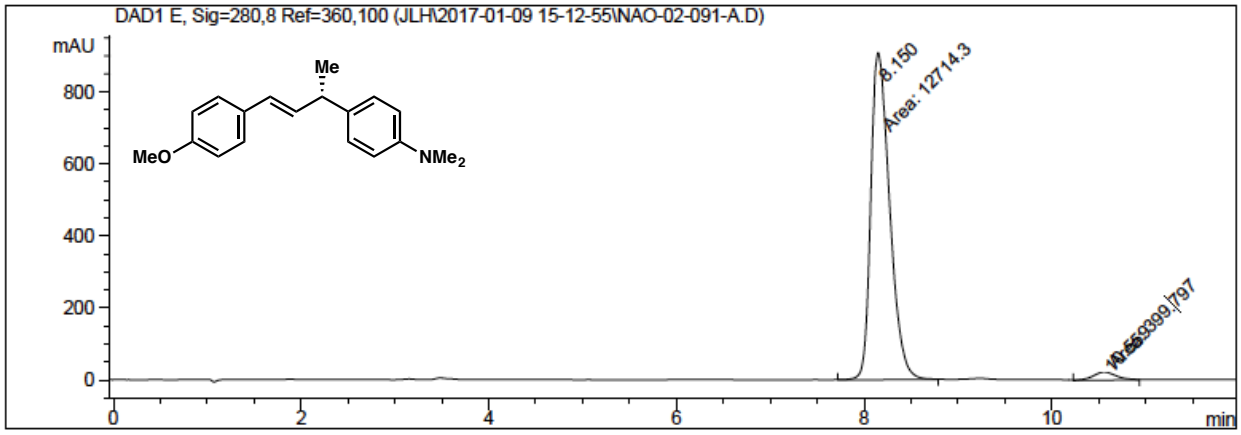

Peak #	RetTime [min]	Type	Width [min]	Area [mAU*s]	Height [mAU]	Area %
1	8.150	MM	0.2330	1.27143e4	909.57269	96.9514
2	10.559	MM	0.2917	399.79657	22.84231	3.0486

199 (Table 4.4): racemic

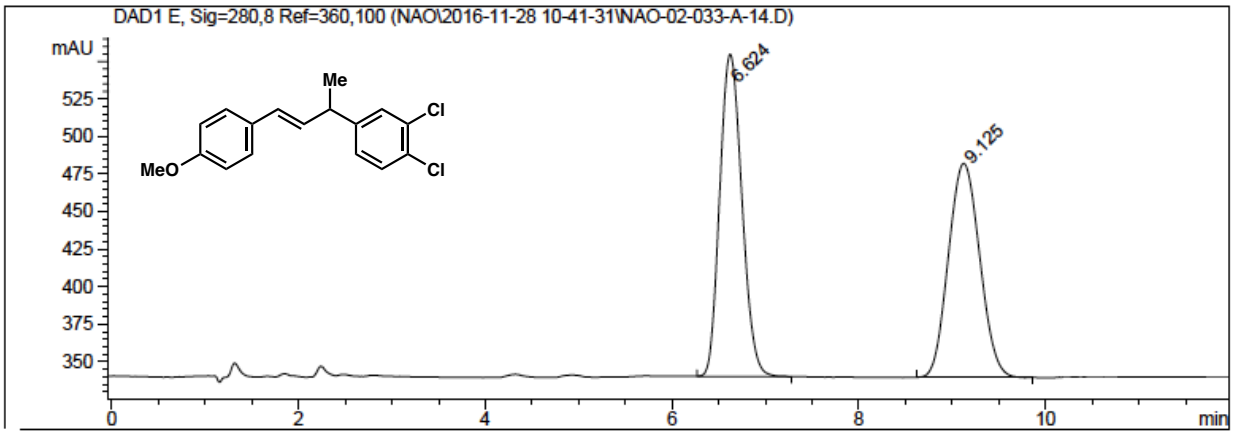

Peak #	RetTime [min]	Type	Width [min]	Area [mAU*s]	Height [mAU]	Area %
1	6.624	BB	0.2651	3551.33887	214.60269	51.6981
2	9.125	BB	0.3717	3318.03833	142.47495	48.3019

199 (Table 4.4): enantioenriched, 82% ee

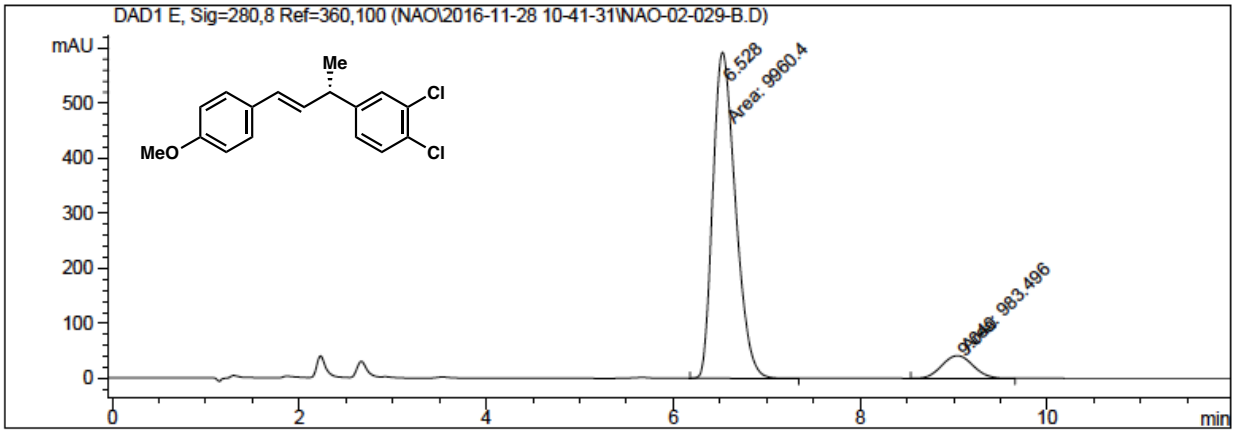

Peak #	RetTime [min]	Type	Width [min]	Area [mAU*s]	Height [mAU]	Area %
1	6.528	MM	0.2800	9960.39941	592.94763	91.0133
2	9.040	MM	0.3921	983.49628	41.80441	8.9867

200 (Table 4.4): racemic

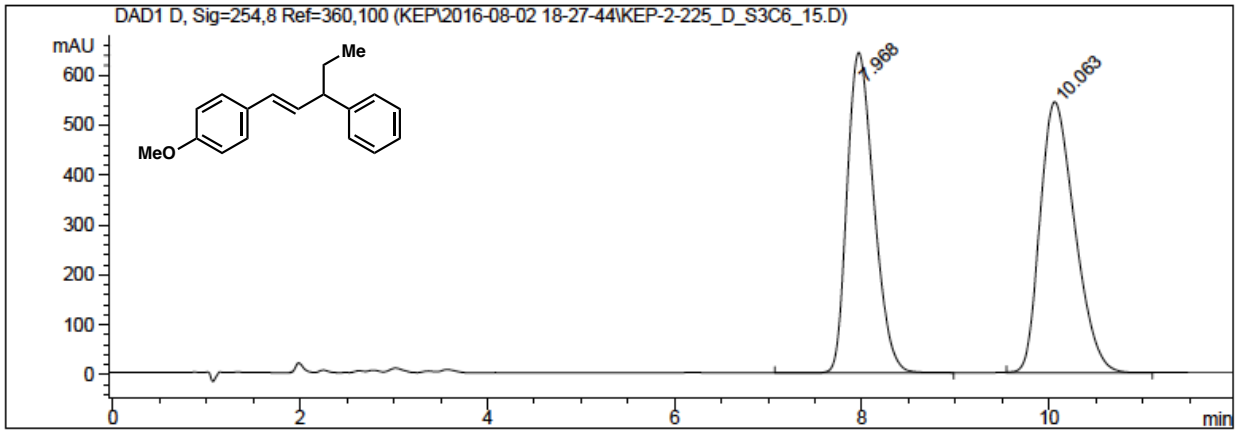

Peak #	RetTime [min]	Type	Width [min]	Area [mAU*s]	Height [mAU]	Area %
1	7.968	VB	0.3120	1.27647e4	642.02454	47.6750
2	10.063	BB	0.4049	1.40097e4	543.13721	52.3250

200 (Table 4.4): enantioenriched, 97% ee

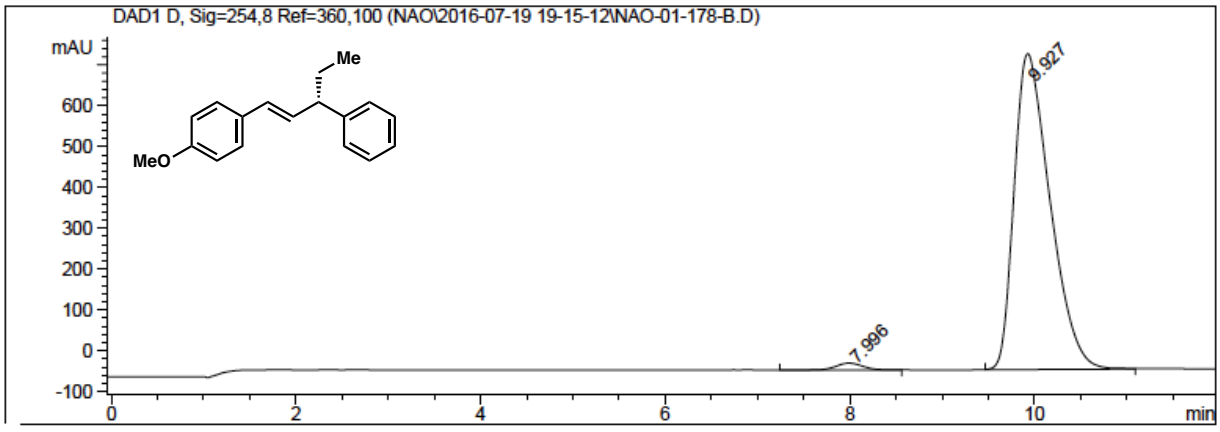

Peak #	RetTime [min]	Type	Width [min]	Area [mAU*s]	Height [mAU]	Area %
1	7.996	VB	0.3205	362.21658	17.28073	1.7024
2	9.927	BB	0.4153	2.09143e4	773.92688	98.2976

201 (Table 4.4): racemic

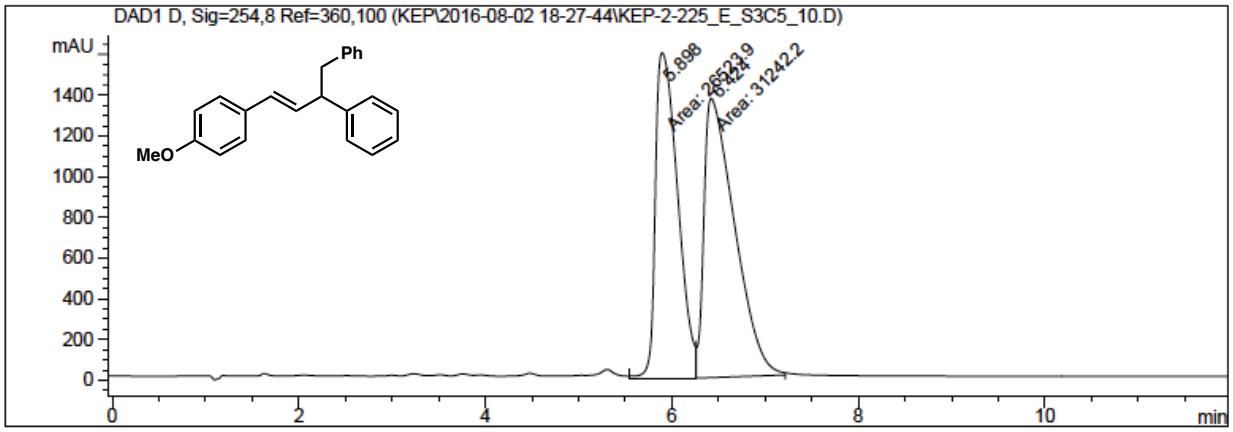

Peak #	RetTime [min]	Type	Width [min]	Area [mAU*s]	Height [mAU]	Area %
1	5.898	MM	0.2764	2.65239e4	1599.41284	45.9160
2	6.424	MM	0.3797	3.12422e4	1371.19714	54.0840

201 (Table 4.4): enantioenriched, 95% ee

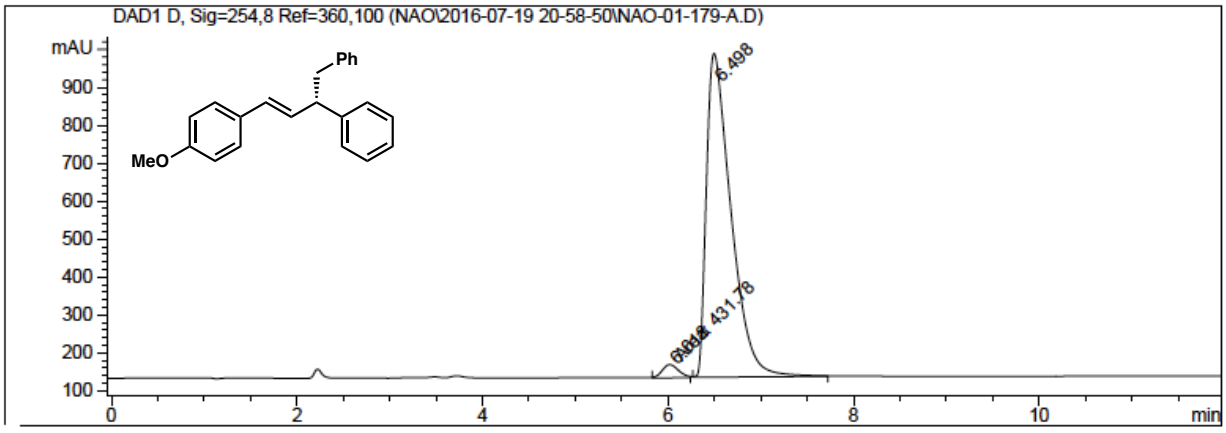

Peak #	RetTime [min]	Type	Width [min]	Area [mAU*s]	Height [mAU]	Area %
1	6.018	MM	0.2059	431.78006	34.94782	2.6714
2	6.498	VB	0.2791	1.57314e4	853.40881	97.3286

202 (Table 4.4): racemic

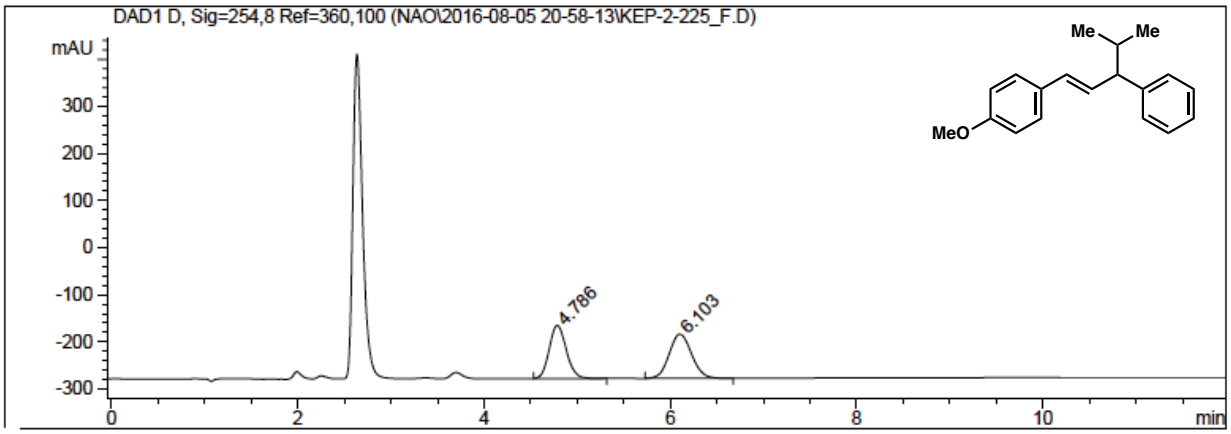

Peak #	RetTime [min]	Type	Width [min]	Area [mAU*s]	Height [mAU]	Area %
1	4.786	BB	0.2004	1430.79492	112.47615	47.8299
2	6.103	BB	0.2619	1560.63074	93.89527	52.1701

202 (Table 4.4): enantioenriched, 97% ee

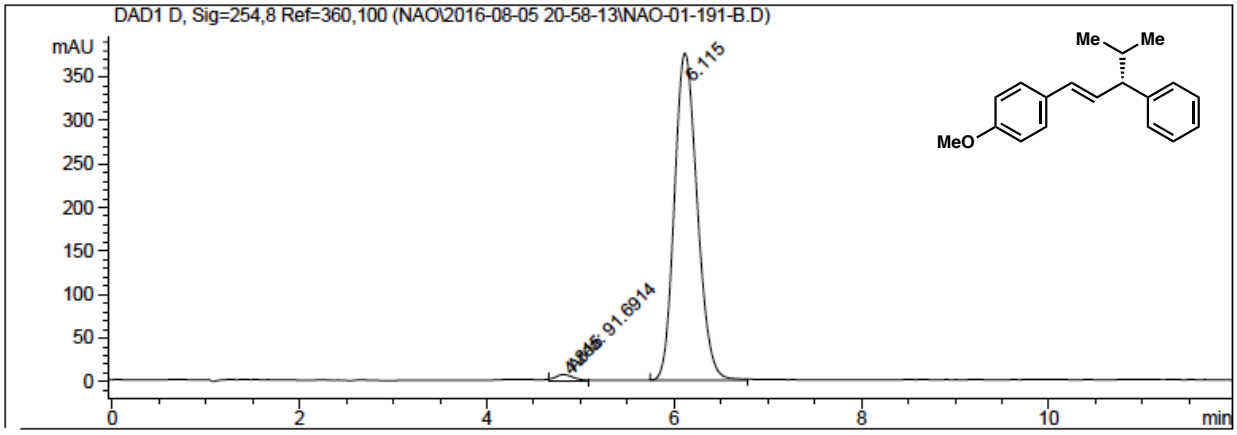

Peak #	RetTime [min]	Type	Width [min]	Area [mAU*s]	Height [mAU]	Area %
1	4.815	MM	0.2214	91.69138	6.90323	1.4194
2	6.115	BB	0.2659	6368.25781	375.46719	98.5806

203 (Table 4.4): racemic

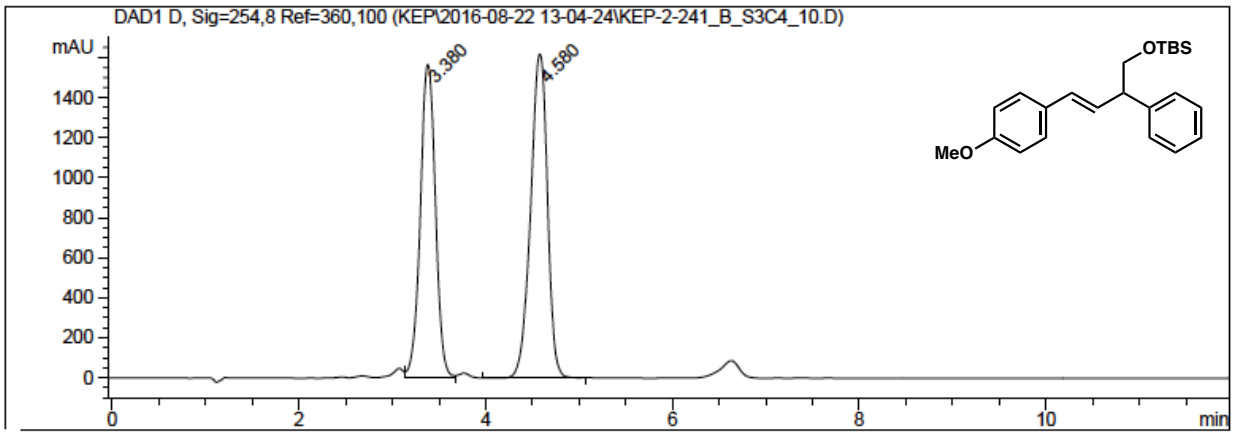

Peak #	RetTime [min]	Type	Width [min]	Area [mAU*s]	Height [mAU]	Area %
1	3.380	VV	0.1763	1.77440e4	1565.27930	46.6268
2	4.580	VB	0.1945	2.03113e4	1617.50305	53.3732

203 (Table 4.4): enantioenriched, 98% ee

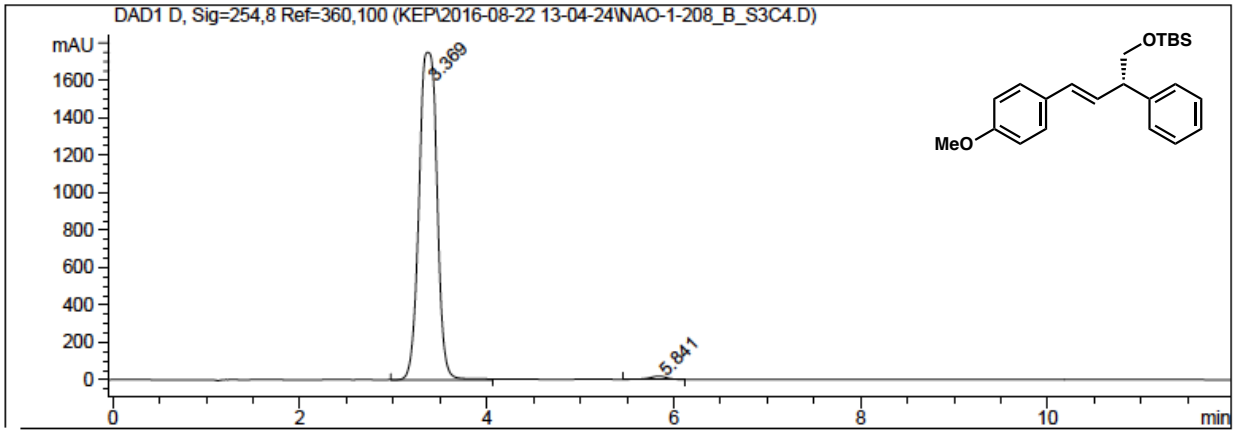

Peak #	RetTime [min]	Type	Width [min]	Area [mAU*s]	Height [mAU]	Area %
1	3.369	VV	0.2126	2.34730e4	1748.39075	98.8511
2	5.841	BV	0.2029	272.82288	19.07364	1.1489

204 (Table 4.4): racemic

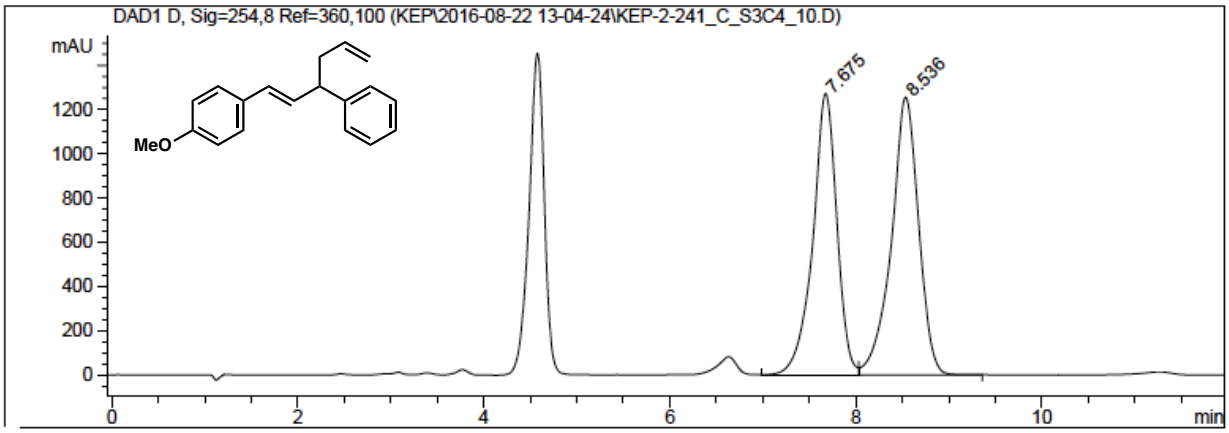

Peak #	RetTime [min]	Type	Width [min]	Area [mAU*s]	Height [mAU]	Area %
1	7.675	VV	0.2662	2.29359e4	1273.26990	47.2708
2	8.536	VB	0.3014	2.55844e4	1257.12512	52.7292

204 (Table 4.4): enantioenriched, 96% ee

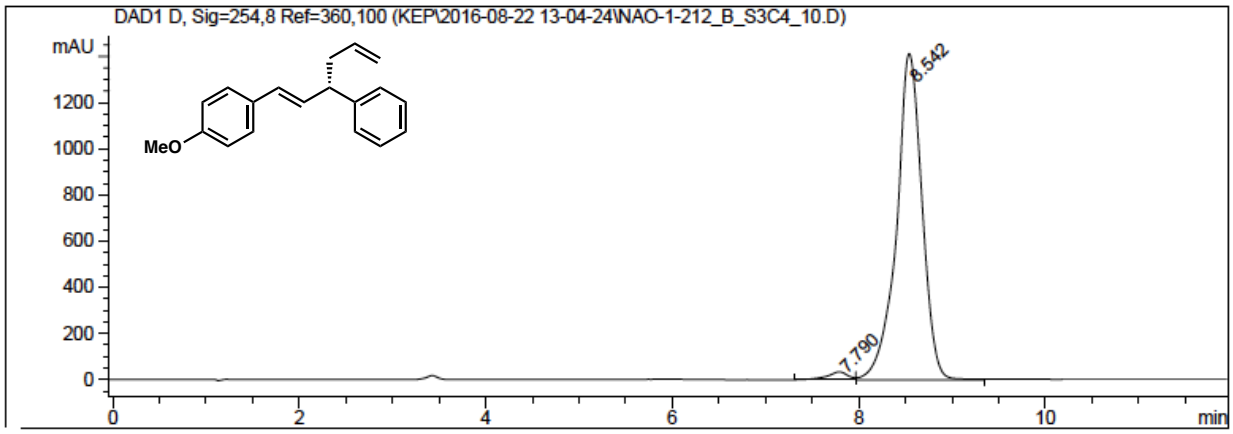

Peak #	RetTime [min]	Type	Width [min]	Area [mAU*s]	Height [mAU]	Area %
1	7.790	BV	0.2268	537.98590	34.33280	1.9596
2	8.542	VB	0.2824	2.69158e4	1411.98352	98.0404

205 (Table 4.4): racemic

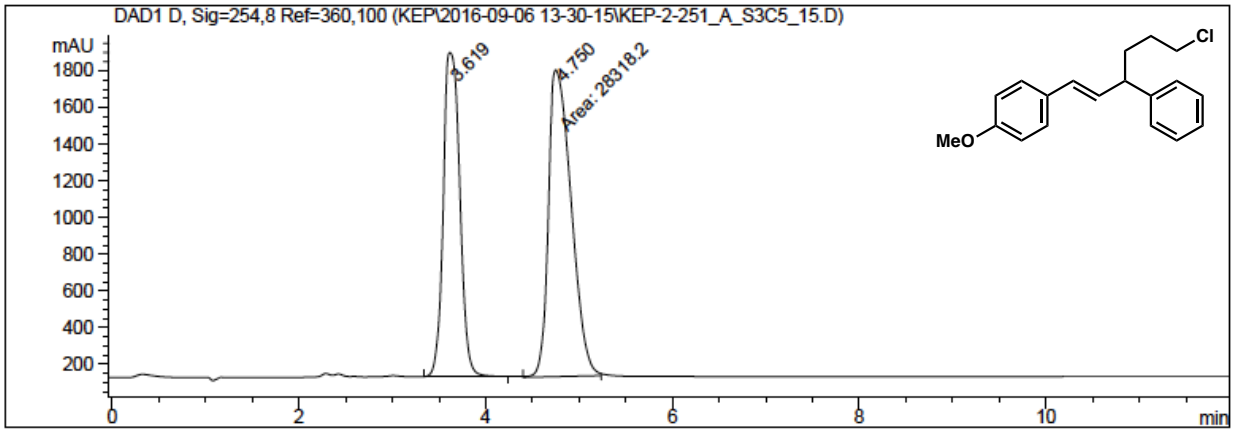

Peak #	RetTime [min]	Type	Width [min]	Area [mAU*s]	Height [mAU]	Area %
1	3.619	BV	0.1967	2.19414e4	1769.60486	43.6562
2	4.750	MM	0.2819	2.83182e4	1673.98267	56.3438

205 (Table 4.4): enantioenriched, 93% ee

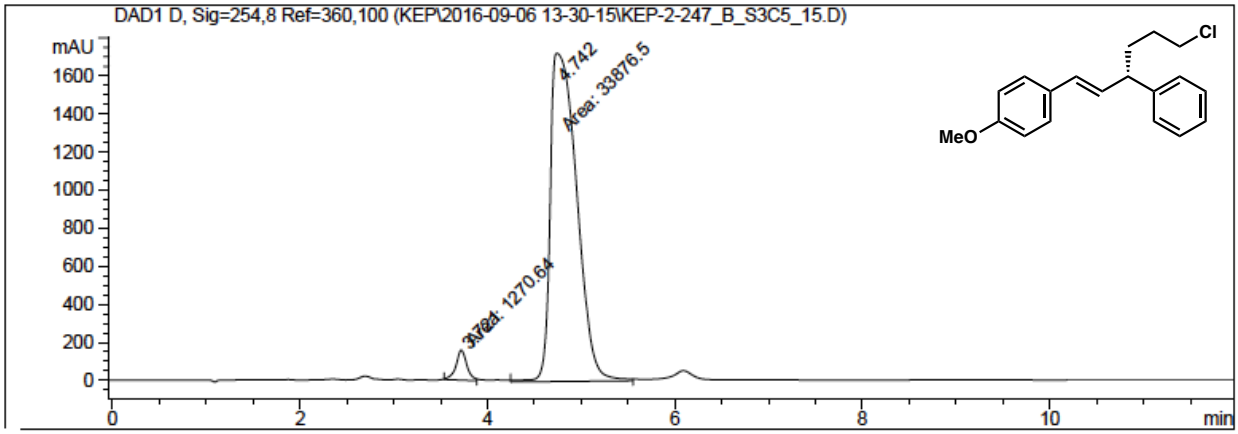

Peak #	RetTime [min]	Type	Width [min]	Area [mAU*s]	Height [mAU]	Area %
1	3.721	MM	0.1339	1270.64075	158.21689	3.6152
2	4.742	MM	0.3274	3.38765e4	1724.49841	96.3848

208 (Scheme 4.2): racemic

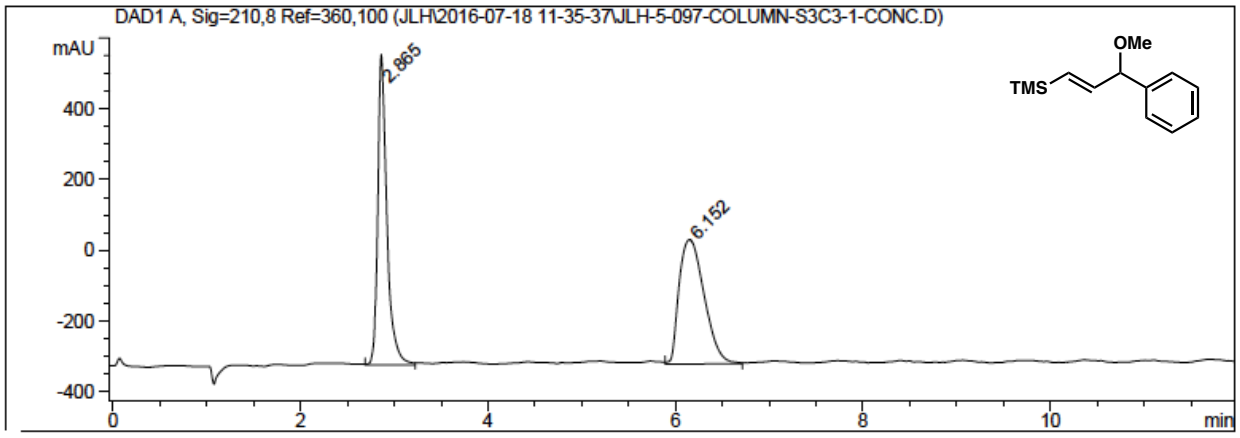

Peak #	RetTime [min]	Type	Width [min]	Area [mAU*s]	Height [mAU]	Area %
1	2.865	VV	0.1036	5942.20703	870.57599	47.5931
2	6.152	VV	0.2969	6543.22803	351.95050	52.4069

208 (Scheme 4.2): enantioenriched, 91% ee

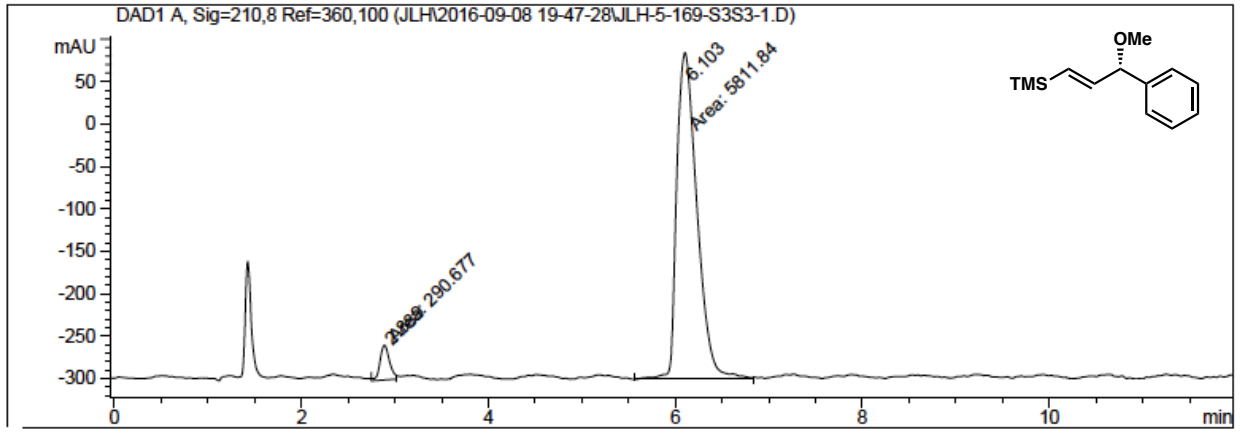

Peak #	RetTime [min]	Type	Width [min]	Area [mAU*s]	Height [mAU]	Area %
1	2.889	MM	0.1180	290.67731	41.05857	4.7632
2	6.103	MM	0.2515	5811.83789	385.08493	95.2368

4.8 NOTES AND REFERENCES

(1) Okada, K.; Okamoto, K.; Oda, M. *J. Am. Chem. Soc.* **1988**, *110*, 8736.

(2) Okada, K.; Okamoto, K.; Morita, N.; Okubo, K.; Oda, M. *J. Am. Chem. Soc.* **1991**, *113*, 9401.

(3) Qin, T.; Cornella, J.; Li, C.; Malins, L. R.; Edwards, J. T.; Kawamura, S.; Maxwell, B. D.; Eastgate, M. D.; Baran, P. S. *Science* **2016**, *352*, 801.

(4) Cornella, J.; Edwards, J. T.; Qin, T.; Kawamura, S.; Wang, J.; Pan, C.-M.; Gianatassio, R.; Schmidt, M.; Eastgate, M. D.; Baran, P. S. *J. Am. Chem. Soc.* **2016**, *138*, 2174.

(5) Wang, J.; Qin, T.; Chen, T.-G.; Wimmer, L.; Edwards, J. T.; Cornella, J.; Vokits, B.; Shaw, S. A.; Baran, P. S. *Angew. Chemie Int. Ed.* **2016**, *55*, 9676.

(6) Huihui, K. M. M.; Caputo, J. A.; Melchor, Z.; Olivares, A. M.; Spiewak, A. M.; Johnson, K. A.; Dibenedetto, T. A.; Kim, S.; Ackerman, L. K. G.; Weix, D. J. *J. Am. Chem. Soc.* **2016**, *138*, 5016.

(7) Konev, M. O.; Jarvo, E. R. *Angew. Chemie - Int. Ed.* **2016**, *55*, 11340.

(8) Lu, X.; Xiao, B.; Liu, L.; Fu, Y. *Chem. - A Eur. J.* **2016**, *22*, 11161.

(9) Cherney, A. H.; Reisman, S. E. *J. Am. Chem. Soc.* **2014**, *136*, 14365.

(10) Anka-Lufford, L. L.; Huihui, K. M. M.; Gower, N. J.; Ackerman, L. K. G.; Weix, D. J. *Chem. - A Eur. J.* **2016**, *22*, 11564.

(11) Takagi, K.; Hayama, N.; Inokawa, S. *Chem. Lett.* **1978**, *7*, 1435.

(12) Tsou, T. T.; Kochi, J. K. *J. Org. Chem.* **1980**, *45*, 1930.

(13) Everson, D. A.; Jones, B. A.; Weix, D. J. *J. Am. Chem. Soc.* **2012**, *134*, 6146.

(14) Johnson, K. A.; Biswas, S.; Weix, D. J. *Chem. - A Eur. J.* **2016**, *22*, 7399.

(15) Beckwith, A. L. J.; Bowry, V. W. *J. Am. Chem. Soc.* **1994**, *116*, 2710.

(16) Halgren, T. A.; Roberts, J. D.; Horner, J. H.; Martinez, F. N.; Tronche, C.; Newcomb, M. *J. Am. Chem. Soc.* **2000**, *122*, 2988.

(17) Biswas, S.; Weix, D. J. *J. Am. Chem. Soc.* **2013**, *135*, 16192.

(18) Gutierrez, O.; Tellis, J. C.; Primer, D. N.; Molander, G. A.; Kozlowski, M. C. *J. Am. Chem. Soc.* **2015**, *137*, 4896.

(19) Moore, B. S.; Chen, J.; Patterson, G. M. L.; Moore, R. E. *Tetrahedron* **1992**, *48*, 3001.

(20) Moore, B. S.; Chen, J. L.; Patterson, G. M. L.; Moore, R. E.; Brinen, L. S.; Kato, Y.;

Clardy, J. *J. Am. Chem. Soc.* **1990**, *112*, 4061.

(21) May, D. S.; Chen, W.-L.; Lantvit, D. D.; Zhang, X.; Krunic, A.; Burdette, J. E.; Eustaquio, A.; Orjala, J. *J. Nat. Prod.* **2017**, *80*, 1073.

(22) Nakamura, H.; Hamer, H. A.; Sirasani, G.; Balskus, E. P. *J. Am. Chem. Soc.* **2012**, *134*, 18518.

(23) Nakamura, H.; Wang, J. X.; Balskus, E. P. *Chem. Sci.* **2015**, *6*, 3816.

(24) Nakamura, H.; Schultz, E. E.; Balskus, E. P. *Nat. Chem. Biol.* **2017**, *13*, 916.

(25) Chlipala, G. E.; Sturdy, M.; Krunic, A.; Lantvit, D. D.; Shen, Q.; Porter, K.; Swanson, S. M.; Orjala, J. *J. Nat. Prod.* **2010**, *73*, 1529.

(26) Smith, A. B.; Kozmin, S. A.; Adams, C. M.; Paone, D. V. *J. Am. Chem. Soc.* **2000**, *122*, 4984.

(27) Smith, A. B.; Adams, C. M.; Kozmin, S. A.; Paone, D. V. *J. Am. Chem. Soc.* **2001**, *123*, 5925.

(28) Hoye, T. R.; Humpal, P. E.; Moon, B. *J. Am. Chem. Soc.* **2000**, *122*, 4982.

(29) Nicolaou, K. C.; Sun, Y.-P.; Korman, H.; Sarlah, D. *Angew. Chemie Int. Ed.* **2010**, *49*, 5875.

(30) Suzuki, N.; Hofstra, J. L.; Poremba, K. E.; Reisman, S. E. *Org. Lett.* **2017**, *19*, 2150.

(31) This work was conducted in collaboration with Cedric Lozano, an undergraduate summer researcher in the Reisman lab.

(32) Poremba, K. E.; Kadunce, N. T.; Suzuki, N.; Cherney, A. H.; Reisman, S. E. *J. Am. Chem. Soc.* **2017**, *139*, 5684.

(33) Hama, T.; Ge, S.; Hartwig, J. F. *J. Org. Chem.* **2013**, *78*, 8250.

(34) Murphy, J. M.; Tzschucke, C. C.; Hartwig, J. F. *Org. Lett.* **2007**, *9*, 757.

(35) Ishiyama, T.; Takagi, J.; Hartwig, J. F.; Miyaura, N. *Angew Chem Int Ed* **2002**, *41*, 3056.

(36) Cho, J.-Y.; Tse, M. K.; Holmes, D.; Jr., R. E. M.; III, M. R. S. *Science* **2002**, *295*, 305.

(37) Zhou, J.; Fu, G. C. *J. Am. Chem. Soc.* **2004**, *126*, 1340.

(38) González-Bobes, F.; Fu, G. C. *J. Am. Chem. Soc.* **2006**, *128*, 5360.

(39) Paquette, L. A.; Duan, M.; Konetzki, I.; Kempmann, C. *J. Am. Chem. Soc.* **2002**, *124*, 4257.

(40) This work was conducted in collaboration with Dr. Chris Lavoie, a postdoctoral scholar, and Sara Dibrell, a graduate student in the Reisman lab.